



Available online at www.sciencedirect.com



Prog. Polym. Sci. 29 (2004) 635–698

PROGRESS IN
POLYMER SCIENCE

www.elsevier.com/locate/ppolysci

Adaptive and responsive surfaces through controlled reorganization of interfacial polymer layers

Igor Luzinov^{a,*}, Sergiy Minko^{b,*}, Vladimir V. Tsukruk^{c,*}

^a*School of Materials Science and Engineering, Clemson University, Clemson, SC 29634, USA*

^b*Department of Chemistry, Clarkson University, Potsdam, NY 13699, USA*

^c*Department of Materials Science and Engineering, Iowa State University, Ames, IA 50011, USA*

Received 25 September 2003; revised 10 February 2004; accepted 3 March 2004

Available online 6 May 2004

Abstract

The present manuscript offers an overview of the current state of affairs within the research field of adaptive and environmentally sensitive polymer surfaces designed to respond to external stimuli in a controlled and predictable manner. Intensive study in the field of the adaptive/responsive surfaces began several decades ago in an attempt to understand relationships between bulk properties/composition of pristine polymeric materials and their surface characteristics. With time, the focus of the research has moved to the design of materials with ‘smart’ or ‘intelligent’ surface behavior. This review describes a number of approaches that has been employed to fabricate such materials, which include but not limited to (a) synthesis of functional polymers with specific composition and architecture; (b) blending of a virgin polymer material with small amounts of (macro)molecular additive; (c) surface modification by various chemical/physical treatment.

© 2004 Elsevier Ltd. All rights reserved.

Keywords: Adaptive materials; Responsive materials; Smart materials; Intelligent materials; Switchable materials; Polymer surface; Polymer interface; Polymer brush

Contents

1. Introduction	636
2. Pristine polymer materials.	637
2.1. Functionalized polymers.	637
2.2. Random copolymers.	638
2.3. Segmented polymers	639
2.4. Block and graft copolymers	640
2.5. Liquid crystalline polymers	644
3. Modified polymer materials	645
3.1. Modification of polymer surface behavior by blending.	646
3.2. Modification of polymer surface behavior by chemical/physical treatment	651
4. Grafted layers with adaptive/responsive behavior.	656
4.1. Photoresponsive surface layers	657

* Corresponding authors.

E-mail addresses: luzinov@clemson.edu (I. Luzinov); sminko@clarkson.edu (S. Minko); vladimir@iastate.edu (V.V. Tsukruk).

4.2. Thermally responsive surface layers	659
4.3. Responsive surface layers from dendritic polymers	660
4.4. Responsive surface layers from polyelectrolytes	665
5. Block-copolymer brushes	667
5.1. Self-assembly of block-copolymer brushes	668
5.2. Synthesis of block-copolymer brushes	671
5.3. Y-shaped copolymer brushes	672
6. Mixed brushes	673
6.1. Mechanism of phase segregation in mixed brushes	674
6.2. Responsive/switching/adaptive behavior	677
6.3. Polyelectrolyte mixed brushes	681
6.4. Synthesis of mixed brushes	683
6.5. Methods to study responsive behavior	685
7. Prospective applications of responsive brushes	687
8. Conclusions	691
Acknowledgements	691
References	692

1. Introduction

There is a general agreement that the ultimate performance of materials in many traditional and modern applications depends not only on their bulk properties, but also relies heavily on their surface microstructure and interfacial behavior. Indeed, many applications involve friction, shearing, lubrication, abrasion, wetting, adhesion, adsorption, and indentation [1–4]. This importance is becoming paramount in the age of shrinking operational dimensions in micro- and nanodevices, and the demand on materials with extreme properties [5–7]. In many studies, special attention is devoted to tuning the interface for specific applications, and careful design of the topmost surface layer incorporating all of the necessary elements controlling a predictable surface response, or a variable surface response under different conditions [8–14]. For this reason, the structure and characteristics of the phase boundaries are of the utmost importance for an understanding of the materials properties in processing and use. Moreover, further advances in materials science imposes requirements for dual surface properties that frequently are in conflict: a given material, depending on the conditions under which it is utilized, has to be hydrophobic and hydrophilic, acidic and basic, conductive or non-conductive, adhesive or repellent, and be able to release or adsorb some species. With the increasing demand for more sophisticated surfaces,

one current approach is to fabricate and understand materials with interfacial properties capable of undergoing reversible changes according to outside conditions or stimuli.

Intensive study in the field of the adaptive/responsive surfaces began several decades ago in an attempt to understand the relationships between bulk properties/composition of pristine polymeric materials and their surface characteristics. With time, the focus of research has moved to the design of materials with ‘smart’ or ‘intelligent’ surface behavior. A number of approaches have been employed to reach this goal, including, but not limited to (a) synthesis of functional polymers with specific composition and architecture; (b) blending of a virgin polymer material with small amounts of (macro)molecular additive; (c) surface modification by various chemical/physical treatment. Significant efforts have also been made to prepare, characterize, and understand the structure/properties relationships of adaptive/responsive surface layers attached to or deposited on the materials surface.

This review offers a broad overview of the current state of affairs in research on adaptive and environmentally sensitive polymer surfaces designed to respond to external stimuli in a controlled and predictable manner. Emphasis is placed on recent results available, with reference to several excellent reviews focused on prior developments in relevant fields.

2. Pristine polymer materials

From the standpoint of the classical definition of solids, the surface of a polymer material cannot be considered as rigid and unchangeable [15]. Polymer chains always respond to some extent to their environment or applied stimuli by changing the conformation and location of backbone, side chains, segments, pendant groups, or end groups. Thus, synthetic polymers offer a wealth of opportunities to design sophisticated materials with responsive surfaces by variation of the length, chemical composition, architecture, and topology of the chains [8]. The major response mechanisms are based on surface energies, entropy of the polymer chains, and variable specific segmental interactions. In particular, the surface energy has a great potential to govern the surface responsive/adaptive reorientation because of the fundamental tendency of a system to minimize the interfacial energy between the polymer surface and its environment. Theoretical models that provided favorable agreement with measured surface tension values have been developed to evaluate the surface tension of polymers possessing different chemical structures [16–18].

Experimentally, the effect of the surface composition adjustment can be observed for some homopolymers. Holly and Refojo [19] studied the wetting of poly(2-hydroxyethyl methacrylate) (PHEMA) with respect to water and air. Water did not spread spontaneously on a PHEMA gel, and large hysteresis was observed. It was suggested that this hydrogel surface was capable of changing its free energy through gradual reorientation of the polymer side chains and chain segments depending on the nature of the adjacent phase. The water content of this gel did not appear to have an effect on the surface wettability in the hydration range investigated. Ruckenstein and Lee [20–22] studied the surface restructuring of hydrophobic (polysiloxane) and hydrophilic (PHEMA) homopolymers in great detail. It was reported that these polymeric materials could adopt different surface configurations, depending upon whether they were equilibrated in polar or non-polar liquids. Correspondingly, their wetting properties were quite different in different environments. For instance, the equilibration of the hydrophilic polymer in a strong polar environment induced an increase in

the polarity of the surface; subsequent exposure of the restructured solid to a non-polar environment decreased the polarity of the surface.

2.1. Functionalized polymers

Multicomponent polymers, possessing more complex structures than homopolymers, naturally have a higher tendency for surface/interface reorientation, caused by additional segregation effects. In recent years, the modification of polymer end groups has emerged as a practical means of controlling the polymer surface properties [23–27]. The surface energy and the surface composition of various end-fluorinated polymers have been extensively studied to this end [23,28,29]. A strong segregation of the low-surface energy end groups to the polymer/air interface was demonstrated. For example, the end fluorinated polymer system demonstrated some surface rearrangement on the change of the interfacing surface environment from air (hydrophobic) to saturated water vapor (hydrophilic) [29].

Elman et al. [26] investigated the distribution of polymer terminal groups at surfaces and interfaces of end-functionalized polystyrenes (PS) using NR and X-ray photoelectron spectroscopy (XPS). Three cases of end group surface segregation were examined: a ‘neutral’ control specimen prepared by proton termination, a ‘repulsive’ end group system terminated with high-surface energy carboxylic acid end groups, and an ‘attractive’ end group system containing low-surface energy fluorocarbon chain ends. The surface structure of the ‘control’ sample was dominated by a sec-Bu initiator fragment located at one end of the chain. On the other hand, for the fluorosilane-terminated material, the low-energy fluorinated end groups were depleted from the silicon oxide substrate interface, but were found in excess at the air–film interface. As demonstrated, in the carboxyl-terminated material, the high-energy carboxyl end groups segregated preferentially to the silicon oxide overlayer on the substrate, and were depleted at the air surface.

In fact, the ability of the functional groups to segregate to certain boundaries can be readily utilized for the synthesis of homogeneous polymeric materials with smart/adaptive surfaces, where a distinct polymer possesses one, two or more different functional

groups. Then, the surface properties of the material will vary in response to environment variation. The location of functionalities on the polymer backbone, which have to migrate to the surface, may be of particular importance. O'Rourke-Muisener et al. [30] applied the Scheutjens–Fleer self-consistent mean-field (SCF) theory to evaluate the surface segregation of various groups bonded to functionalized polymers. Lattice calculations were employed to explore the effectiveness of a variety of functional polymer architectures to produce surfaces with either repellent or adhesive properties. The results obtained demonstrated the importance of the number and location of functional groups, and their surface preference relative to polymer backbone segments in determining surface segregation. In general, it was concluded that the adjacency of similar functional groups is the most effective means to enhance surface segregation of functional groups. Moreover, having two functional groups of similar character in macromolecular chains was always preferable to having two functional groups of opposite character.

The calculations revealed that the optimal architecture for producing a low-energy release surface is a functional polymer with adjacent low-energy functional groups located at one chain end. In this situation, both enthalpic and entropic factors serve to drive chain ends to the surface. In contrast, high-energy adhesive surfaces are best obtained by placing adjacent high-energy functional groups at the center of the polymer chain. The high-energy groups situated at the middle of the chain favor the sub-surface layer, from which they can migrate readily to the surface when it is contacted with any other high-surface energy medium.

2.2. Random copolymers

Random or statistical copolymers possessing monomers of different nature can be certainly considered for building the adaptive/responsive surfaces, since the different units of the copolymer macromolecule may segregate to the surface in response to some stimuli. Lukaš et al. [15] conducted an XPS study of the surface reorientation of statistical methacrylate copolymers, poly(2-hydroxyethyl methacrylate-*co*-butyl methacrylate) and poly{2-[2-(2-ethoxy)ethoxy]ethyl methacrylate-*co*-butyl

methacrylate}. The surface of the copolymers in both hydrated and dry states was investigated. Differences in the surface composition obtained for the different states characterized the chain reorientation process occurring in the surface layer in response to environmental changes.

Results obtained by Höpken and Möller [31] for styrene-based copolymers containing monomer with perfluorocarbon-segmented side groups indicated that the surface characteristics of the material depend on the organizational state of the fluorocarbon segments. Drastic surface reorganization and lowering of the surface tensions was observed for annealed samples, when only a few percent of the fluorocarbon-containing comonomer units was incorporated into the polymer structure. The migration of high-energy units to the interface, which ensured strong adhesion interaction, was demonstrated by Falsafi et al. [32]. The authors studied the adhesion of cross-linked 2-EHA-*co*-acrylic acid elastomers prepared as model materials for pressure-sensitive adhesives (m-PSA) by the contact mechanics approach based on Johnson–Kendall–Roberts (JKR) technique [33]. The values of the advancing water contact angle showed that there was no change in the surface energy of the m-PSA material with acrylic acid content. The surface energies derived from the contact angle measurements were more consistent with the surface activity of alkyl chains of 2-EHA when the PSA was in contact with air. The system apparently tried to 'hide' higher energy carboxyl groups within the bulk materials. The XPS data suggested carbon enrichment in the vicinity of the surface, supporting this hypothesis. However, a surface free energy penalty for carboxyl groups did not exist in the polymer–polymer interface at the contact area. In the contact region, the carboxyl groups found each other across the interface and formed hydrogen bonds, which promoted the interfacial adhesion (Fig. 1).

An excellent series of reviews regarding current advances in the field of PSA materials has been recently published. In addition to an introduction of PSA materials [8] as various means for controlling surface response under external mechanical pressure and tensile stress, the authors considered: copolymers of reactive adhesives with controlled chemistry and composition [34], hot-melt adhesives from styrenic block copolymers and low-molar mass additives [35],

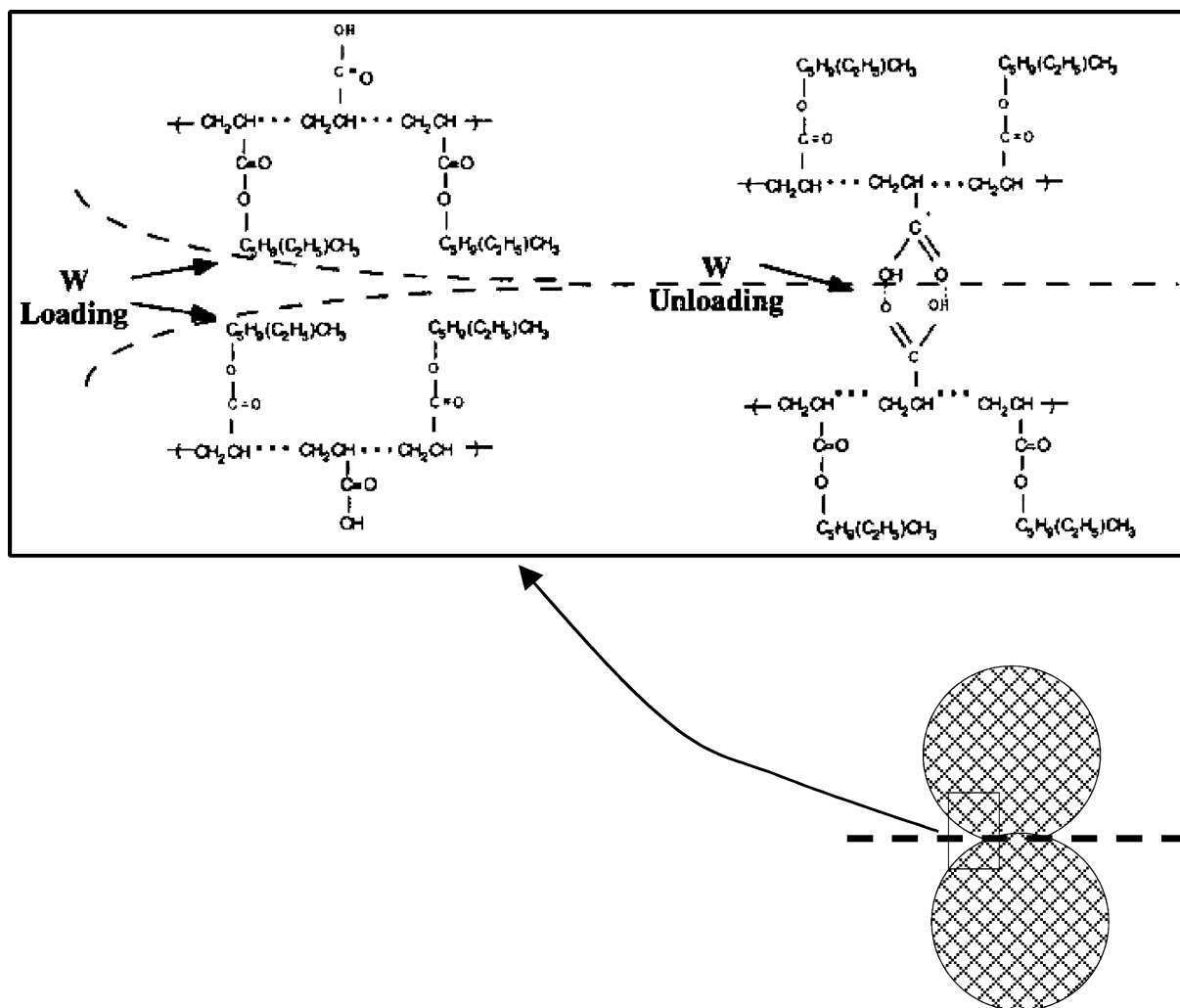


Fig. 1. Illustration of surface and interfacial rearrangements in the cross-linked PSA. Reprinted with permission from Ref. [32] (Langmuir 2000;16:1816, Copyright (2000) American Chemical Society).

and highly loaded polymer–metal nanoparticle adhesives [36].

2.3. Segmented polymers

Progress in synthesis and characterization of segmented (multiblock) polyurethanes has been, to some extent, driven by the idea to create the surface responsive materials [37]. A material exhibiting low-surface energies in both air and water (along with good flexibility, chemical stability, and mechanical properties) and possessing the potential for

minimizing adhesion and facilitating the release of soils and foulants (e.g. proteins) from its surface in both air and water has been sought. Thus, the polymeric materials should have switchable surface properties, which would spontaneously adjust with its environment in order to achieve the low-interfacial tension values.

In fact, segmented polyurethanes (SPUs) with alternating hydrophobic and hydrophilic segments demonstrated such a behavior [38–44]. For instance, the relationship between the surface properties and the structure of SPUs with various polyol soft segments

were investigated by Takahara et al. [43]. The polyols used in this study were poly(ethylene oxide) (PEO), poly(tetramethylene oxide) (PTMO), and poly(dimethylsiloxane) (PDMS). The hard segment of these SPUs was composed of 4,4'-diphenylmethane diisocyanate and 1,4-butanediol. XPS revealed that in the air-equilibrated state, lower surface free energy components were enriched at the air–solid interface, whereas in the water-equilibrated state, higher surface free energy components were enriched at the water–solid interface. The change in environment from air to water induced the surface reorganization in order to minimize the interfacial free energy. On the other hand, IR + visible sum-frequency vibrational spectroscopy has been used by Zhang et al. [44] to monitor structural changes of another polyurethane with PDMS segments grafted on as end groups (Fig. 2). The obtained data showed that the polymer surface underwent a significant restructuring when transferred from air to water. With the polymer exposed to air, the surface spectrum showed that the hydrophobic PDMS segments covered most of the surface. However, when immersed in water, the PDMS component retreated from the surface and the initially 'buried', more hydrophilic part of the polymer chain appears at the surface. The consistency was observed between the spectroscopic data and the contact angle measurement in characterizing the variable hydrophobicity of the polymer surface (Fig. 2).

Recently, a novel type of the SPU having both fluorocarbon and polyethylene glycol (PEG) segments was synthesized [37]. The polymers contained well-defined assemblies of perfluoropolyether (PFPE or hexafluoropropene oxide oligomer), PDMS, and PEG segments. These polymers exhibited a range of oleophobic, hydrophobic, and hydrophilic properties in the response to the polarity of the contacting medium. In fact, the contact angle decreased dramatically from 120 to 34° when it came into contact with water. The authors argued that the oleophobic and hydrophobic properties of the SPUs were due to the segregation of PFPE segments at the polymer–air interface. Wettability studies revealed that the same surface became hydrophilic, presumably due to the segregation of the PEG segments at the polymer–water interface.

This hydrophobic-to-hydrophilic transformation of the surface prevailed not only when the polymer was

in contact with liquid water but with water vapor as well. The overall kinetic of the surface reconstruction process could be tuned by suitably varying the quantity of different segments presented in the polymer (Table 1, Fig. 3). Interestingly, when droplets of hexadecane and water were placed on the same polyurethane surface, the contact angle of water gradually decreased from 115 to 54° after 20 min of exposure. On the other hand, the contact angle of hexadecane decreased only slightly (67–60°) (Fig. 4). Thus, in the case of non-polar hexadecane, the polymer surface exposed its low-energy, CF₃, groups, but its high-energy PEG groups were released after the contact with high-polar solvent, water.

2.4. Block and graft copolymers

Block copolymers, which refers to polymers that is composed of two or more chemically distinct blocks joined together end-to-end, are also found to demonstrate surface responsive/adaptive properties under certain conditions [8]. The typically observed immiscibility of the blocks results in the microphase separation of the dissimilar blocks into a variety of ordered, nanoscopic structures ranging from spherical to lamellar as the fraction and molar mass of the blocks are changed. The domain orientation and the resulting surface/interface composition of the films made of a block copolymer are strongly influenced by the boundary conditions at the polymer interface [45–52]. This interfacial behavior is controlled by a preferential segregation of the blocks to a substrate and a free surface owing to the difference in the surface energies of the components. This property of the copolymers has been used to design novel materials that reconstruct their surface in response to a change in the environment.

Block copolymers, which are both hydrophilic and hydrophobic (at the same time), have been synthesized [53–55]. At equilibrium, the lower surface energy hydrophobic block migrates to the air interface and the hydrophilic block is hidden beneath the surface. Upon exposure to water, a surface reconstruction occurs, opening channels to the underlying hydrophilic block to be exposed, as shown schematically in Fig. 5. The longer the exposure to water, the greater is the reconstruction, until only the hydrophilic block is in contact with

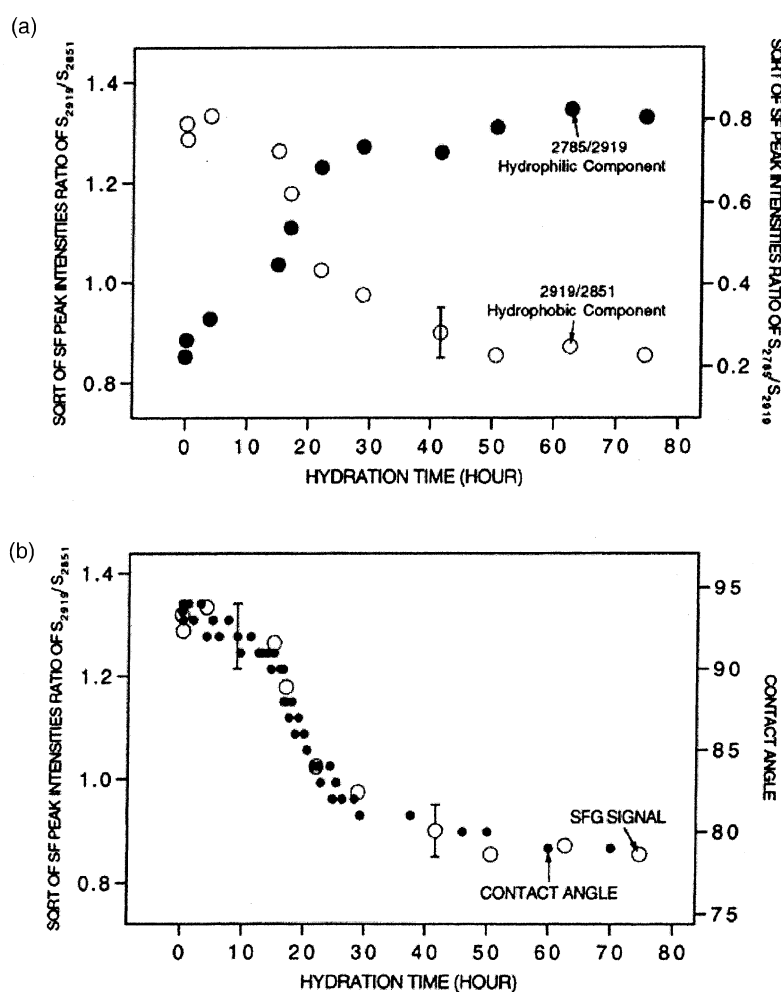
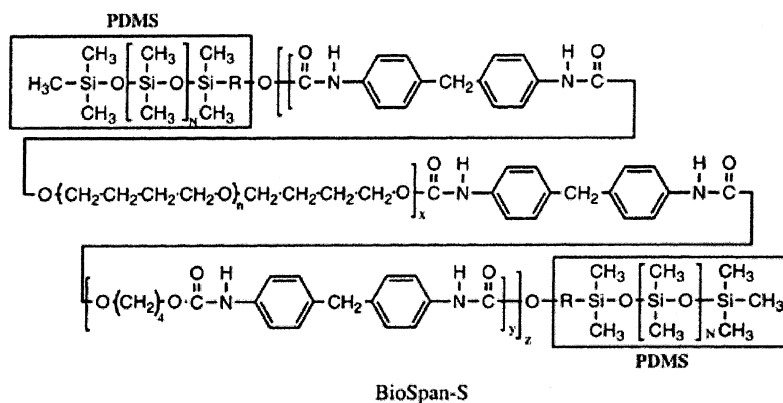


Fig. 2. (a) Square root of peak intensities ratios as functions of hydration time, with 2919/2851 cm^{-1} in open circles which represents the hydrophobic component of the polymer and 2785/2919 cm^{-1} in black dots which is related to the hydrophilic segment of the polymer chain. (b) A compilation of square root of the peak intensity ratio of 2919/2851 cm^{-1} in open circles and contact angle in black dots as functions of hydration time. Reprinted with permission from Ref. [44] (J Phys Chem B 1997;101:9060, Copyright (1997) American Chemical Society).

Table 1

Characterization of SPU (Reprinted with permission from Ref. [37] (J Coll and Interface Sci 2002;249:235, Copyright (2002) Elsevier)

Code	HO-PEG-PDMS-PEG-OH (1) (g) M Wt = 4000	MDI (2) (g)	PFPE (g) (% by weight) M Wt = 1359 g	FB (6) (g)	Mole ratio of (1)/(2)/(6)
SPU-001	— ^a	2	—	1	1:8:6
SPU-002	4	2	—	1	1:8:6
SPU-003	4	2	0.0176 (0.44%)	1	1:8:6
SPU-004	4	2	0.0344 (0.86%)	1	1:8:6
SPU-005	4	2	0.1 (2.5%)	1	1:8:6
SPU-006	4	2	0.4 (10%)	1	1:8:6

^a In the case of SPU-001, 4 g of 3-hydroxypropyl-terminated PDMS was used instead of HO-PEG-PDMS-PEG-OH.

water. Russell pointed out in his seminal article [8] that the prospective applications such as surface drug delivery mechanism could be enabled by such a morphological rearrangement quite effectively. Designing a specific functionality into the higher surface energy block allows it to be easily brought to the surface by a change in the environment.

In another recent example, Ratner and co-workers [53,56] investigated surface rearrangements of poly(HEMA-*block*-polystyrene) by XPS using a freeze-drying technique. The authors observed the rearrangement of the hydrated surface structure back to a dehydrated one under vacuum conditions. The reconstruction of the copolymer boundary could be

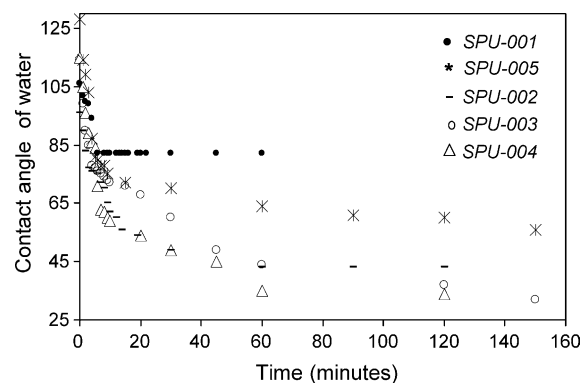


Fig. 3. Variation in contact angle of water (θ_w) as a function of on various SPU samples (SPU-001, 002, 003, 004, and 005) containing varied composition of PDMS, PFPE and PEG segments. See Table 1 for the designation of the various symbols. Reprinted with permission from Ref. [37] (J Coll and Interface Sci 2002;249:235, Copyright (2002) Elsevier).

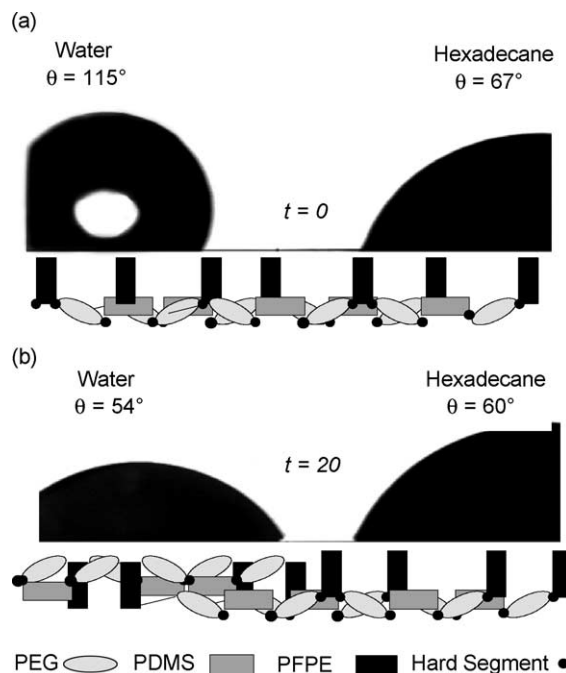


Fig. 4. Drops of water (left) and hexadecane (right) separated by a distance of 2 mm on a SPU-004 surface at $t = 0$ (a) and after 20 min. Reprinted with permission from Ref. [37] (J Coll and Interface Sci 2002;249:235, Copyright (2002) Elsevier).

conclusively identified as a movement of the PHEMA blocks to the surface of the hydrated polymer and the movement of the PS-blocks back to the surface upon drying. Another hydrophilic–hydrophobic diblock copolymer, poly(HEMA-*block*-polyisoprene), was synthesized and studied by Nakahama and co-workers [54]. The surface structures of the block copolymer film under dry and wet conditions were analyzed by transmission electron microscopy (TEM), contact angle, and angle-dependent XPS measurements. It was observed that the top surface of the films cast from DMF/THF and THF/methanol solvents were covered with a polyisoprene microdomain. When the as-cast film was exposed to water, the polyisoprene layer at the top surface disappeared and was replaced with HEMA blocks. It was directly confirmed by TEM that such surface rearrangement occurred at the microdomain scale controlled by the chemical composition of the block copolymer (Fig. 6). Contact angle measurement indicated that the surface rearrangement occurred repeatedly (Fig. 7).

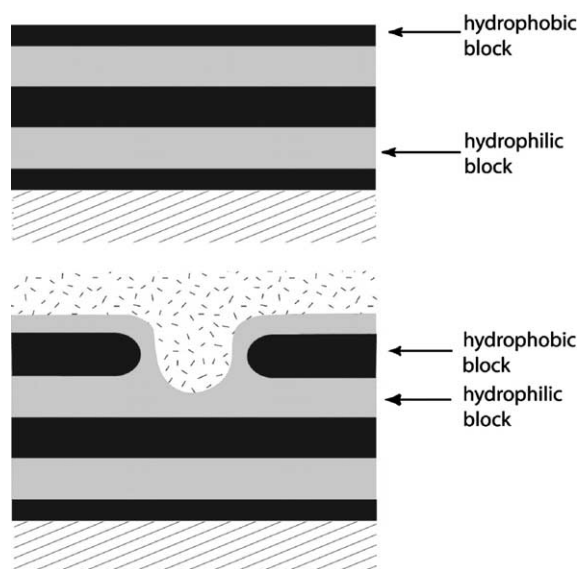


Fig. 5. Schematic of a symmetric diblock copolymer composed of a hydrophobic and hydrophilic block, with a lamellar microdomain morphology. In contact with air, the lower-surface-energy hydrophobic block is located at the surface. Changing the environment to water induces a surface reconstruction in which the hydrophilic block is located at the surface. Reprinted with permission from Ref. [8] (Science 2002;297:964, Copyright (2002) AAAS).

In an earlier publication from the same research group, the surface reconstruction of block copolymers containing polystyrene, poly(4-octylstyrene), or polyisoprene as a hydrophobic segment, and poly(2,3-dihydroxypropyl methacrylate), poly(DIMA), as a hydrophilic segment was studied [55]. XPS measurement of the as-cast film surfaces of the three block copolymers indicated the enrichment of the hydrophobic segments in the outermost surfaces. Furthermore, the XPS and contact angle measurements revealed that the poly(DIMA) segment was enriched in the surface of poly(styrene-*b*-DIMA) soaked in water and that reconstruction of the surface occurred again by annealing the sample in air. Nakahama and co-workers also reported on adaptive properties of poly(HEMA-*block*-styrene-*block*-HEMA) triblock copolymer surface [57]. The responsive behavior of the triblock samples, synthesized by the anionic living polymerization, was quite close to that observed for the diblock copolymers.

Graft copolymers as well as block copolymers, comprised of covalently connected immiscible polymer segments, generally show a well-developed

microphase separation structure in bulk. Their boundaries tend to be covered by one component that can insure lower interfacial tension at the phase border [58]. Therefore, the graft copolymer surfaces are also known to undergo a notable reorganization by responding to the change of the contacting medium within a short time scale. Tezuka et al. reported on the surface formation and environmentally induced surface rearrangement occurring on poly(vinyl alcohol) (PVA) [58–61] and polyurethane-based [61–64] graft copolymers containing uniform size polysiloxane, polyether, polyamine, and PS graft segments. In particular, the PVA–PS graft copolymer exhibited noteworthy behavior. During the film preparation by casting, the PS component was favored to accumulate on the topmost surface due to its lower surface energy, which was confirmed by XPS as well as contact angle measurements. Remarkable was that, by immersion into water, the contact angle of an air bubble at the surface was gradually changed from the value, which is characteristic for the PS homopolymer to that closer for the PVA homopolymer within a few hours.

An environmentally induced surface rearrangement occurring on the PVA–PS surface has been studied by means of atomic force microscopy (AFM) technique [58]. In a dry state, it was observed that the graft copolymer film surface was covered by a thin flexible layer of PS components on a PVA sub-layer. The topmost PS layer became unstable when the film was immersed in water. The surface dewetting process took place to generate a ‘hole-with-rim’ pattern for the graft copolymers with 12–23 mol% PS content (Fig. 8). The number of the hole-with-rim structures increased along with the immersion time, while their sizes were not appreciably varied. The dewetting process for the graft copolymers with 26–41 mol% PS content, alternatively, produced a ‘wormlike’ pattern, which corresponded to the microphase separation morphology observed in the dry state (Fig. 9). The graft copolymer film recovered from water and dried at 120 °C (above glass transition temperature, T_g , of both polymer components) reproduced the original smooth surface morphology, while the film dried at the ambient temperature maintained a notably rough surface morphology. Contact angle analysis also showed a distinct difference between the two graft copolymer surfaces prepared by the different treatments [60].

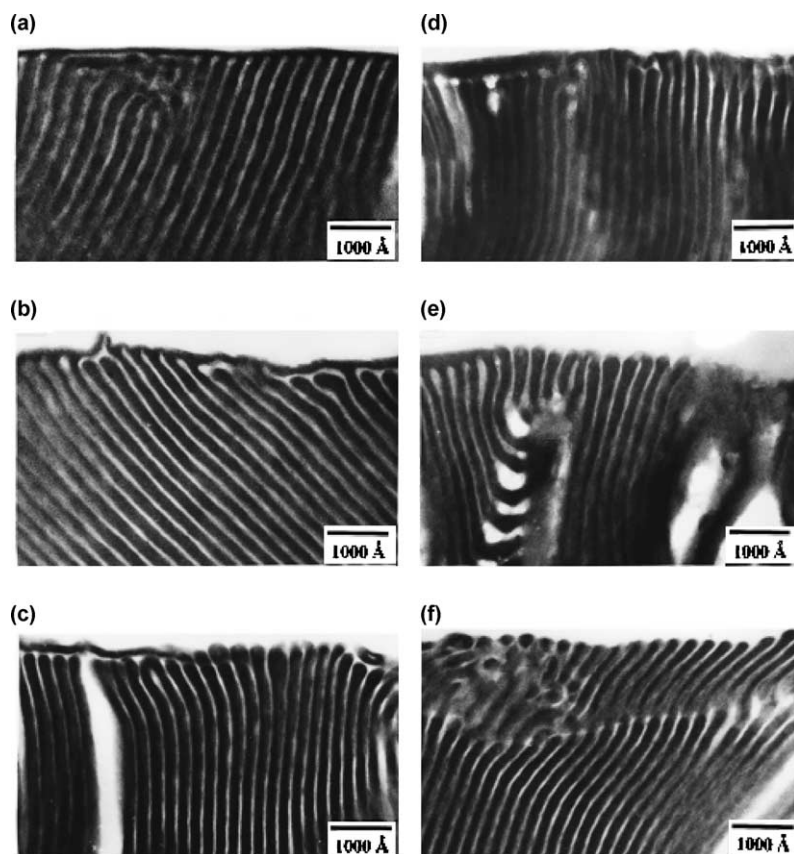


Fig. 6. Transmission electron micrographs (cross-sectional view) of the ultrathin sections of the poly(HEMA-*block*-polyisoprene) cast film from THF/methanol (5/1, v/v): (a) as-cast and (b) soaking in water for 5, (c) 10, (d) 30, (e) 60, and (f) 300 s. Reprinted with permission from Ref. [54] (Langmuir 1999;15:1754, Copyright (1999) American Chemical Society).

Thus, the surface morphology, once rearranged by the immersion of the polymer into water, is thought to be preserved at least to a certain extent. This behavior is unique for the PVA–PS graft copolymer surface. In fact, this is not applicable for the relevant graft copolymer having polysiloxane graft segments, where the contact angle was completely reversible during transformation from the dry state to water and back.

2.5. Liquid crystalline polymers

In order to obtain a material with switchable tackiness and wettability, De Crevoisier et al. [65], proposed to use a fluorinated liquid crystalline polymer that undergoes a first-order phase transition from a highly structured state towards a disorganized state. The polymer used in the study was a side-chain

liquid crystalline copolymer, obtained by radical copolymerization of 50 mol% of an acrylate monomer bearing a long perfluoroalkyl side chain ($C_2H_4-C_8F_{17}$), and 50% of a methacrylate monomer bearing a long alkyl chain ($C_{17}H_{35}$). At room temperature, this copolymer was highly organized into a partially crystallized lamellar phase. In those lamellae, both the hydrogenated and the fluorinated side chains could co-crystallize. A wide transition between a mesomorphic and an isotropic phase centered at 35 °C (Fig. 10) was observed for the polymer and resulted in dramatic changes of the polymer surface properties.

The variation of tack properties of this copolymer was studied using a technique that enabled one to measure the true area of contact between the adhesive and the probe in addition to the adhesive energy. In the smectic phase, the energy needed to separate

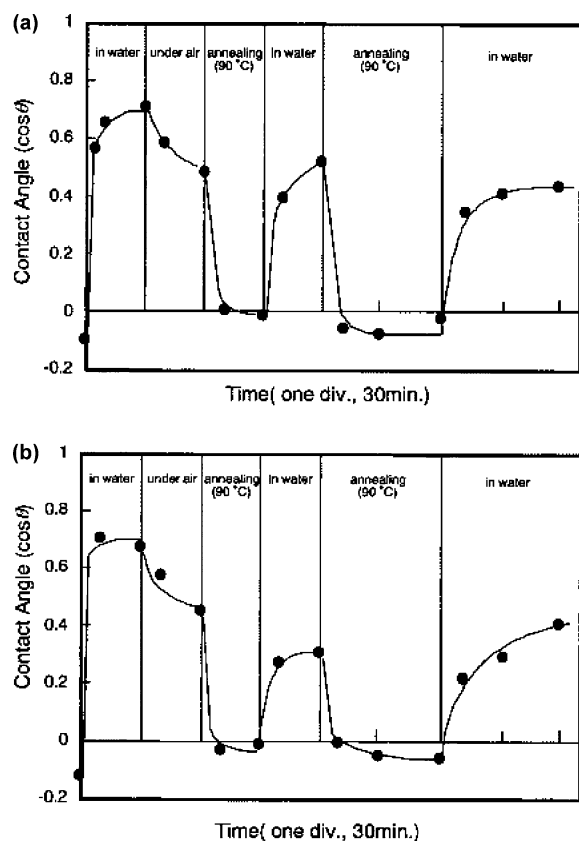


Fig. 7. Static contact angle ($\cos \theta$) of a water droplet on poly(HEMA-*block*-polyisoprene) (a) cast film from DMF/THF (9/1, v/v) and (b) from THF/methanol (5/1, v/v) as a function of treating period under dry and wet conditions. Reprinted with permission from Ref. [54] (Langmuir 1999;15:1754, Copyright (1999) American Chemical Society).

the adhesive from the probe was zero within the experimental accuracy, whereas in the isotropic phase, the energy decreased from 50 J/m^2 at 37°C to 14 J/m^2 at 50°C (Fig. 11). These values are typical for polymers well above its glass transition. A remarkable feature of this transition between a non-adhesive and an adhesive regime is that it occurred very abruptly at the smectic-to-isotropic transition. The tack energy increases within a 2°C temperature range, compared with the usual $60\text{--}70^\circ\text{C}$ transformation range for the conventional PSA with conversion point centered around a glass transition. The experiments showed that during the transition, the true area of contact between the adhesive and the probe increased from less than 10% in the smectic phase to nearly 100% in the isotropic phase (Fig. 11). It was also found that there was a large variation in the surface wettability at the transition temperature. Hence, by using the liquid crystalline materials with abrupt order-disorder structural transitions, one can tune the adhesive and wetting properties of a substrate. According to the authors, this opens interesting possibilities for many applications in which precise surface control is important, such as in areas as diverse as biotechnology, industrial coatings, and cosmetics. Everyday examples of switchable adhesive applications might include antisoil grips for tennis rackets or golf clubs.

3. Modified polymer materials

Many well-known polymers have excellent bulk properties, low cost, and are well suited for some

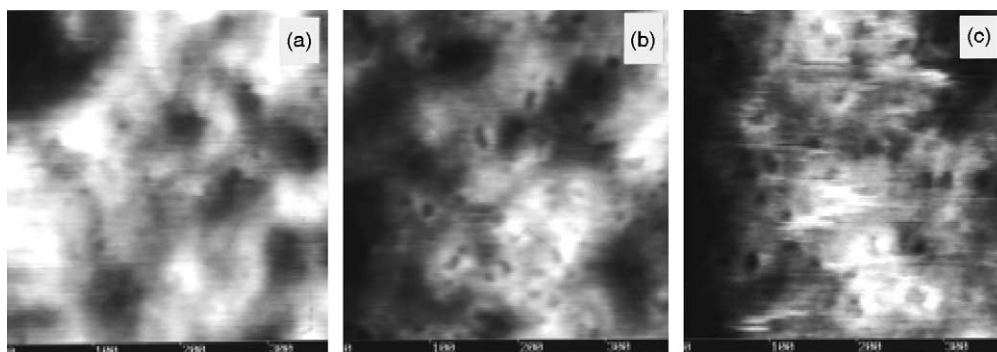


Fig. 8. AFM height images of the surface of PVA-PS graft copolymer of 12.9 mol% PS content in water for (a) 20, (b) 425, and (c) 1320 min. The scan size is $375 \text{ nm} \times 375 \text{ nm}$. The contrast covers 7.5 nm for (a), 7.3 nm for (b), and 8.1 nm for (c). Reprinted with permission from Ref. [58] (Langmuir 1999;15:3197, Copyright (1999) American Chemical Society).

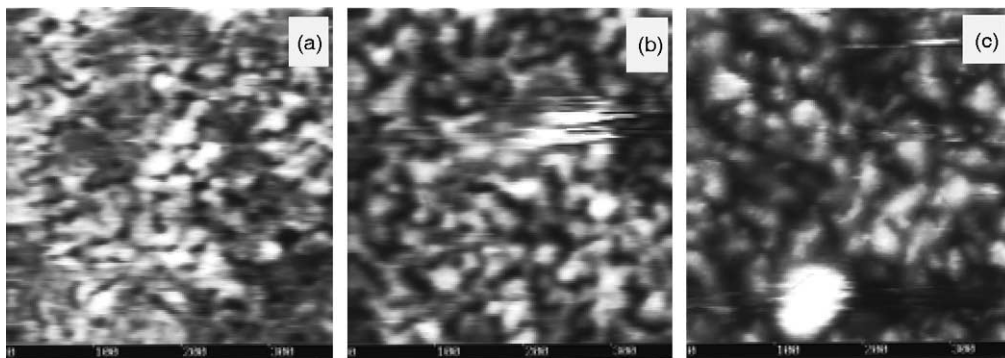


Fig. 9. AFM height images of the surface of PVA–PS graft copolymer of 26.5 mol% PS content in water for (a) 4, (b) 35, and (c) 1150 min. The scan size is 375 nm \times 375 nm. The contrast covers 8.4 nm for (a), 10.5 nm for (b), and 10.8 nm for (c). The bright spots with scanning traces observed in (b) and (c) correspond to a droplet on the surface. Reprinted with permission from Ref. [58] (Langmuir 1999;15:3197, Copyright (1999) American Chemical Society).

particular applications. For these reasons, various surface modification techniques that could transform these well-understood materials into sophisticated elements of the complex adaptive/responsive systems are under development in various laboratories. Modification strategies, which are supposed not to affect the bulk properties significantly but change their surface behavior, involve either blending of a virgin material with a small amount of (macro)molecular additive and/or the surface modification by chemical or physical treatment to alter the surface properties.

3.1. Modification of polymer surface behavior by blending

One of the key features of many surface modification approaches is the phenomenon of the preferential segregation of one (or more) constituent(s) of a multicomponent polymer material to its boundary [66]. Molecular fragments, functional groups, or polymer chains might preferentially segregate from the bulk to the surface/interface in order to decrease the interfacial energy and minimize the overall free energy of the system. The segregation is controlled by a balance between the free energy gain associated with the surface tension reduction accompanying the surface adsorption and the free energy cost of demixing surface-active species from the bulk. The surface segregation may have some distinct advantages over the other methods of surface modification.

In fact, because the segregation is a thermodynamically driven process, the surface composition can be controlled and the resulting surface structure is in equilibrium, thus, assuring the system stability [67]. Moreover, the segregation of the constituents is an in situ method, thus, limiting the need for additional processing. It also allows the possibility of a ‘self-healing’ surface, whereby the removal of the segregating component would trigger further segregation from the bulk to replenish the surface. Adaptive/responsive polymer surface can be created if several (macro)molecular additives (that may be covalently connected) coming to the surface of a polymeric material in a response to an environment variation or stimuli application.

Another strategy may rely on the presence of a single additive component that can migrate to the surface under certain conditions when necessary, but be hidden beneath the boundary, but in close

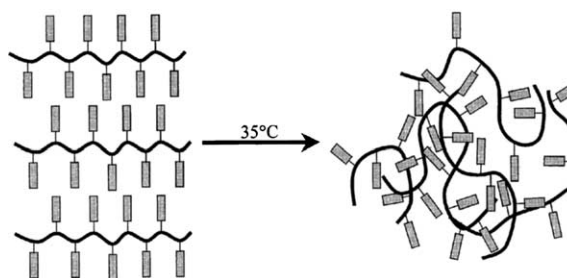


Fig. 10. Schematic representation of the transition between the smectic and the isotropic phase. Reprinted with permission from Ref. [65] (Science 1999;285:1246, Copyright (1999) AAAS).

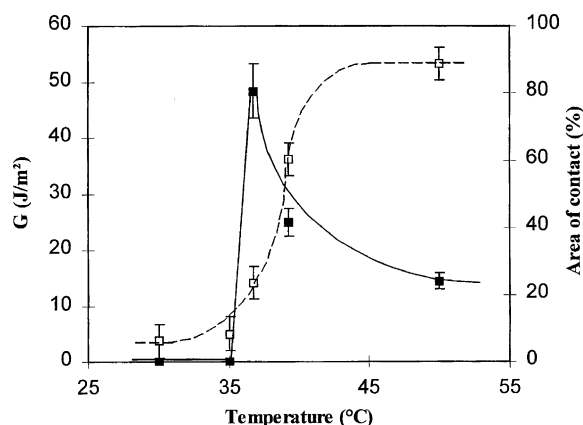


Fig. 11. Tack (■) and percentage of the probe wet by the film (□) for the fluorinated copolymer as a function of temperature. The lines serve as a guide to the eye. The smectic-to-isotropic transition is located at 35 °C. Reprinted with permission from Ref. [65] (Science 1999;285:1246, Copyright (1999) AAAS).

proximity to it. This component can diffuse to the topmost surface layer under certain conditions if the environment is changed or some external stimulus is applied to the system. The practical importance of the surface segregation in polymer mixtures and blends has provided strong motivation for the understanding of the fundamental factors that control it [68–71].

Miscible polymer blends have proven to be important systems demonstrating specific surface segregation, and their surface properties have been studied in some detail [69]. It was first evidenced by surface tension measurements, wherein the addition of small amounts of the lower surface energy constituent was found to bring about an incommensurably large decrease in the surface tension [72]. Later, XPS was employed to provide direct and quantitative evaluation of the surface composition and the surface composition gradient for the miscible polymer blends [73,74]. Jones et al. [75,76] utilized forward-recoil spectrometry and X-ray reflectivity technique to reveal that the surface of a blend of deuterated and protonated polystyrenes that were enriched with the deuterated compound relative to the bulk. The excess of poly(vinyl methyl ether) (PVME) on the surface of miscible PVME/PS blends was determined by static secondary ion mass spectroscopy (SIMS) [77]. This excess increased even more with increasing PVME content in the blend and with increasing PS molecular weight. A number of surface

segregation theories have been developed for the miscible polymer blends and successfully applied [78–80].

The effect of the interplay between bulk and surface free energy terms on surface segregation in miscible blends has been recently probed by comparing angle-dependent X-ray photoelectron spectroscopy (ADXPS) measurements for PS/PVME blends with those for analogous dPS/PVME blends [69]. The magnitudes of the bulk interaction parameters for these two systems differ markedly while the surface interactions are essentially identical. Experimentally determined concentration depth profiles are almost identical for these two systems indicating that their surface properties are affected a little by bulk interactions and are dominated by the surface energy effects.

The data were compared to the predictions of the square gradient theory developed by Schmidt and Binder [79] in order to gain a quantitative understanding of the factors that control the surface segregation in the miscible blends. While there was general qualitative agreement between the theory and experiment, the predicted surface composition fell significantly below the experimental value. Moreover, the predicted composition depth profile decayed more gradually than what was observed experimentally, especially in the case of low-PVME content. Careful analysis of the experimental behavior suggested that the configurational effect associated with the flattening of the adsorbed chains on the surface and differences in mer–mer interaction parameters in the bulk and near surface regions were possible origins for the discrepancies between the theory and experiment.

It is accepted that both energetic and entropic factors affect the segregation processes in polymer blends [67]. It was observed that the degree of surface segregation increases as molecular weight of a blend component decreases [71,80–82]. For instance, surface of PS/dPS blends was PS enriched, when PS molecular weight was much lower than that of its deuterated counterpart (typically located at the boundary) [81]. Walton et al. [67] reported on entropically driven segregation of a higher-energy component to the surface of a polymer blend due to the architectural modification of the macromolecular additive. In this work, thin film miscible blends of

PMMA and a branched random copolymer of methyl methacrylate and methoxy poly(ethylene glycol) monomethacrylate, P(MMA-*r*-MnG), were investigated by neutron reflectivity. The branched copolymer, which has a higher surface tension than PMMA, was, nevertheless, found to segregate to and completely covered both the free surface and a silicon substrate after annealing of the films. This was in a contrast to linear polyethylene oxide, which was depleted at both film interfaces when blended with PMMA and annealed.

The reflectivity results were confirmed by contact angle studies, which indicated that the surfaces of P(MMA-*r*-MnG)/PMMA blends behaved like that of pure P(MMA-*r*-MnG), resulting in a hydrophilic surface that was stable against dissolution in water-based environments and possessed protein-resistant properties. This proposed method allows, in general, for the possibility of creating a highly controlled surface coverage of a higher-energy polymer additive via architectural modification.

Considering similar aspects, Hester et al. [83] reported on the preparation of the protein-resistant surface of a poly(vinylidene fluoride) (PVDF) membrane via the surface segregation. Blends of an amphiphilic comb polymer having a poly(methyl methacrylate) (PMMA) backbone and PEO side chains in PVDF have been examined as a means to create foul-resistant, self-healing surfaces on polymer membranes. XPS analysis of phase inversion membranes prepared from these blends indicated a substantial surface segregation of the amphiphilic component, which occurred both during the coagulation step of the phase inversion process and in subsequent annealing of the membranes in water. With annealing, a near-surface coverage of nearly 45 vol% comb polymer was produced on a membrane with a bulk comb concentration of only 3 vol%. XPS analysis of membranes treated with concentrated acid showed that hydrophilic surface layers removed by acid exposure could be regenerated by further surface segregation during a subsequent heat treatment in water.

As was mentioned previously, an end-functionalized polymer possessing the same chemical nature as a bulk polymer and added at small fractions to this polymeric material, can sufficiently change its surface and interfacial properties. For instance, ADXPS was

used to measure end group concentration depth profiles for blends of surface-active ω -fluorosilane PS with non-functional PS [66]. The fluorine signal indicated the surface segregation of fluorosilane end groups with much lower surface tension. The end group segregation was enhanced by an increase in the concentration of ω -fluorosilane PS, an increase in the non-functional polystyrene molecular weight, or a decrease in the molecular weight of the ω -fluorosilane PS. A SCF lattice theory was developed to model the surface structure and the surface properties of blends containing end-functional polymers. Two end-functional PS architectures were considered in this work: α -functional PS for which the lattice reference volume was set equal to that of the entire fluorosilane end group and α , β -functional PS where the fluorosilane end group was assumed to occupy two adjacent lattice sites at the chain end. The lattice model considered both architectures and provided an excellent representation of experimental ADXPS data over a wide range of blend compositions and constituent molecular weights.

Indeed, the ability of the end groups to segregate to the phase boundary may be conveniently employed to formulate polymer materials with responsive/adaptive surfaces, where the polymers with different end-functional groups are added to the bulk polymer. In that case, the surface properties of the material might vary in a response to environmental variation when different end groups are migrating to the boundary. However, if a low-surface energy additive has a strong thermodynamic reason to move to the surface as soon as the material is fabricated, the component with higher surface energy often tends to remain in the bulk and not become concentrated in vicinity of the surface.

Ohgaki et al. [84] described a strategy to force a compound with high-surface energy to migrate onto the surface by the aid of a low-surface energy substance. To this end, B(AB)_{*n*} multiblock copolymers, of which the A block and the B block are hydrophobic and hydrophilic, respectively, were blended into cross-linkable polyisocyanate and acrylic coating compositions. The main constituent of A block was PDMS and that of B block was PEO. While the block copolymer slightly increased the hydrophobicity of the surface, it quickly became hydrophilic upon a contact with water. Elementary analysis with XPS

demonstrated that both the silicon atoms and ether groups were concentrated on the very top of the surface in the films. In spite of their propensity to remain in the bulk due to their high-surface energy, hydrophilic PEO moieties in the block copolymers migrated onto the near-surface region accompanying the movement of the hydrophobic polydimethylsiloxane, because their mobility would be restricted by the bonding of both sides. Generally, the surface polarity of materials that contain block copolymers can easily be altered over a wide range according to the substance that is in contact with them. The advantage of the block copolymers as a surface modifier was further developed as an effective adhesion promoter by the introduction of a larger amount of the hydroxyl group into the hydrophilic block.

In a different approach, PE–PEG co-oligomers were used to functionalize the surface of polyethylene films by a process named by the authors as ‘entrapment functionalization’ [85]. One of the goals in this work was to prepare surface-functionalized PE films containing polymer grafts that exhibit inverse temperature-dependent solubility typical for poly(alkene oxide) in water. In the reported procedure, the synthesized co-oligomers were modified by addition of pyrene butyric acid chloride that added a pyrene fluorophore to the hydrophilic end of the co-oligomer. Once prepared, the pyrene-tagged PE–PEG diblock co-oligomers were used in the entrapment functionalization. In a typical procedure, a 1 wt% functionalized film was prepared by mixing a 100-fold excess of virgin linear high-density PE with the block co-oligomer. Complete mixing was ensured by completely dissolving both the host virgin polyethylene along with the co-oligomer in *o*-dichlorobenzene at reflux.

Cooling of the solution precipitated the entrapped powder. Films were then produced by solvent casting from *o*-dichlorobenzene solutions. The pyrene groups of the diblock copolymer were located at the surface of the product film in part because of the PE–PEG incompatibility. When the film was immersed in water, the PEG groups at these surfaces showed solvation behavior that resembled the known inverse temperature-dependent solubility properties of PEG in water. The study of responsiveness of these films showed that the interface micropolarity was higher at low temperature and lower at high temperature.

Repeated heating and cooling of the same sample demonstrated that these interface changes were substantially reversible. The interface solvation was also measured in ethanol and toluene solutions. The results indicated that interface solvation was independent of temperature in toluene and directly dependent on temperature in ethanol.

Koberstein et al. [86,87] introduced another concept for polymer surface modification to create polymeric materials with smart surfaces. The particular approach centered on the attainment of two specific objectives: (1) the development of surface-active additives that promote adhesion and (2) the development of molecular design criteria that impart selective adhesion promotion toward particular target substrates. This method employed surface-active ω -functional block copolymers that were composed of three components: a low-surface energy block that causes the copolymer to segregate to the surface, an anchor block that tethers the copolymer into a matrix, and a functional group located at the terminus of the surface-active block (Fig. 12). The functional end group was selected to interact selectively with a complementary receptor on the target substrate. Fig. 13 illustrates schematically how the surface-active ω -functional block copolymers can be employed as selective adhesion promoters. The first step in the overall approach is the adsorption of the diblock copolymers at the matrix surface (Fig. 13a), a process driven by the surface tension reduction that occurs when the low-surface energy copolymer sequences segregate to the air–polymer interface.

As a result, the diblock copolymer forms a layered structure at the surface, consisting of a top layer of

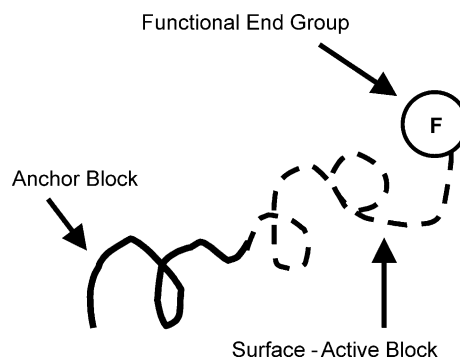


Fig. 12. Schematic structure of a surface-active ω -functional diblock copolymer. Figure redrawn after Ref. [86].

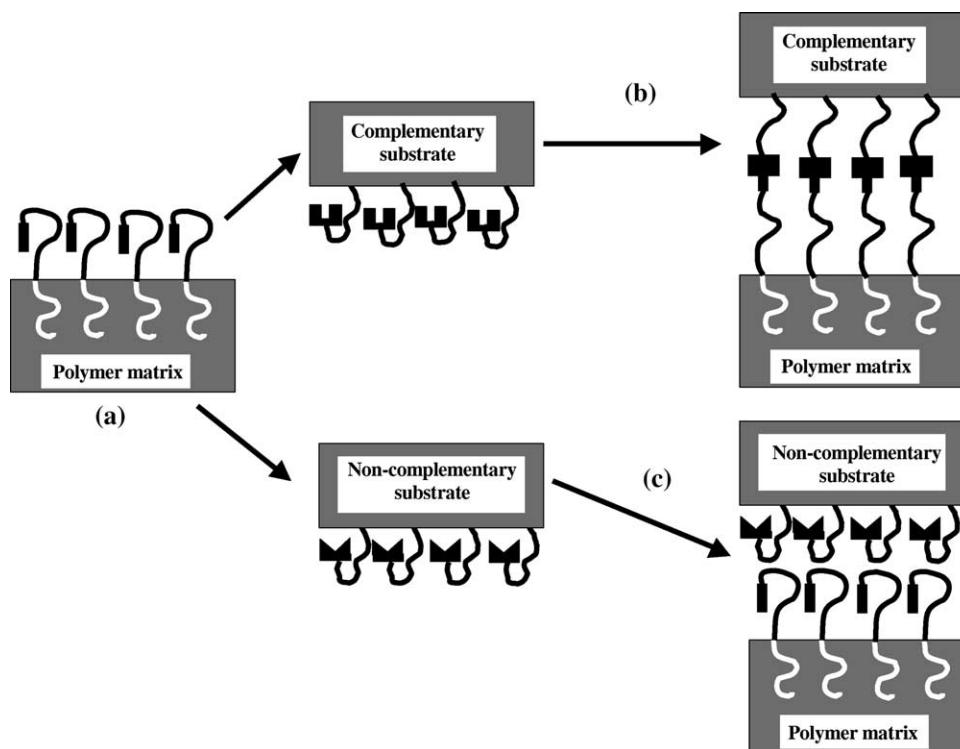


Fig. 13. Schematic diagram illustrating the concept of surface-active ω -functional block copolymers as selective adhesion promoters. (a) The surface is non-adhesive after preparation. (b) A target substrate containing complementary receptors binds specifically to the polymeric matrix modified with surface-active ω -functional block copolymer. (c) A target substrate with non-complementary receptors does not bind to the modified polymeric matrix. Figure redrawn after Ref. [87].

the surface-active sequence followed by a layer of the anchor block entangled with the host matrix. The functional ends are carried to the surface along with the surface-active sequences, and if their surface energy exceeds that of the chain backbone, they reside just beneath the surface. When the modified surface is contacted with a substrate, the functional groups are exposed to a stimulus associated with the new thermodynamic environment imposed by the proximity of the substrate. Whether or not the functional groups respond towards this stimulus determines whether adhesion or release is promoted. If the functional end groups find complementary receptors on the substrate specific interactions are formed (Fig. 13b). This enhances the adhesive strength between the host matrix and the substrate. If appropriate receptors are not found (Fig. 13c), the functional groups do not interact with the substrate. In this case, the low-energy surface layer on the matrix acts as a release coating that effectively separates the host

matrix from the substrate and thereby minimizes any potential adhesive interactions that might occur between the two surfaces in physical contact.

The model systems chosen to prove this concept were ω -functional poly(styrene-*b*-dimethylsiloxane) diblock copolymers PS-*b*-PDMS-X added to a PS matrix, where X represents the end group. The adhesion enhancement of the surface-modified PS matrices toward PMMA and PDMS substrates illustrates how selective adhesion behavior can be controlled by an appropriate choice of the functional end groups. In the next publication, Koberstein and co-workers [88] demonstrated that PS-*b*-PDMS-X diblock copolymers could also be used to deliver a precise amount of carboxylic acid groups to a polymeric surface.

Thanawala and Chaudhury [89] reported on bulk modification of PDMS using a perfluorinated moiety to obtain the elastomeric surface possessing adaptive/responsive characteristics. The surface properties of

PDMS have been modified by reacting an allyl amide functional perfluorinated ether (PFE) to the siloxane network by a hydrosilation reaction. PFE was added to the PDMS mixture prior to curing it. Examination of the surface with contact angle and XPS revealed that the PFE migrates to the surface of the polymer, thus, reducing its surface energy without affecting its bulk material properties. The resultant surface, however, exhibits higher contact angle hysteresis than that seen with the PFE-free elastomer. These results indicated that the higher energy amide functionalities of the PFE were available for interfacial interaction, even though they were buried below the PFE layer. This study once again demonstrates that a high-energy group can be pulled to the free surface of a polymer by exploiting the driving forces provided by the lower energy groups segregating to the surface.

3.2. Modification of polymer surface behavior by chemical/physical treatment

Surface modification of polymeric materials with chemical or physical treatments has been accomplished by a variety of procedures [90–92]. Flame, corona, and plasma treatments are generally applicable methods that serve to introduce various oxygen, nitrogen, and other functionalities. Plasma polymerization process has also been used to tailor the polymer surface. As a result, thin modifying surface films, which are usually highly cross-linked, can be obtained on a polymeric surface. Solution oxidation using reactive oxidants has successfully produced oxygenated and sulfonated surfaces. Ion-beam treatment, photon and γ -radiation have also been utilized to modify polymer surfaces. Once functionalized, the next step is often attachment of some functional molecules and/or polymer grafting is required to produce a surface with necessary properties. Some of the above mentioned modification methods are confirmed to be capable of converting an inert polymer substrate into a material with the adaptive/responsive surface behavior.

To this end, Whitesides and co-workers [93,94] studied reconstruction of the interface of oxidatively functionalized polyethylene and derivatives on heating. Oxidation of low-density polyethylene (PE) film with chromic acid resulted in the material (PE-COOH) bearing hydrophilic carboxylic acid

and ketone groups in a thin oxidatively functionalized surface. This interface was indefinitely stable at room temperature. The functionalized hydrophilic interfaces of oxidized PE film became hydrophobic and similar in the wettability to the non-functionalized PE film upon heating under vacuum. This indicated the surface reconstruction after the annealing. The progression of the contact angle with water from the initial value of 55° to the final value of 103° followed kinetics, which suggested that the polar functional groups disappeared from the interface by diffusion. The migration of functional groups away from the interface was dominated by the minimization of the interfacial free energy and by dilution of the interfacial functional group in the polymer interior. The rate of the surface reconstruction decreased with increasing size of the functional groups deposited on the surface. When the annealed film was contacted with reactive aqueous solutions, the functional groups that had migrated into the bulk polymer were still available for the chemical reactions even when the wetting properties of the surface had become similar to those of unmodified PE film. Samples that had previously reconstructed by the heating could, to a limited extent, be made to become hydrophilic again by heating in water.

The next paper examined the surface wetting by water of the functionalized PE [95]. It was determined that the wettability of the PE-CO₂H surface depends on pH: for $\text{pH} \leq 4$, the carboxylic acid groups are protonated and the surface relatively hydrophobic (advancing contact angle is $\sim 55^\circ$); for $\text{pH} \geq 10$ the carboxylic acid groups are present as the more hydrophilic carboxylate ions, and the contact angle drops to 20° . Wilson and Whitesides [96] reported that anthranilate amide of the PE-CO₂H surface showed an exceptionally large change with pH in its wettability by water. Indeed, the advancing contact angle of the PE-anthranilate decreased from 110° at pH 1 to 33° at pH 12 (Fig. 14). Comparison of these values with those for corresponding amides of *m*- and *p*-aminobenzoic acid and aniline suggested that both conformational mobility of the polar functional group at the solid–water interface and the surface roughness contributed to the large change in wettability with pH (Fig. 14).

Generally, enthalpic forces (e.g. hydrogen bonding, Lewis acid–base interactions, and van der Waals

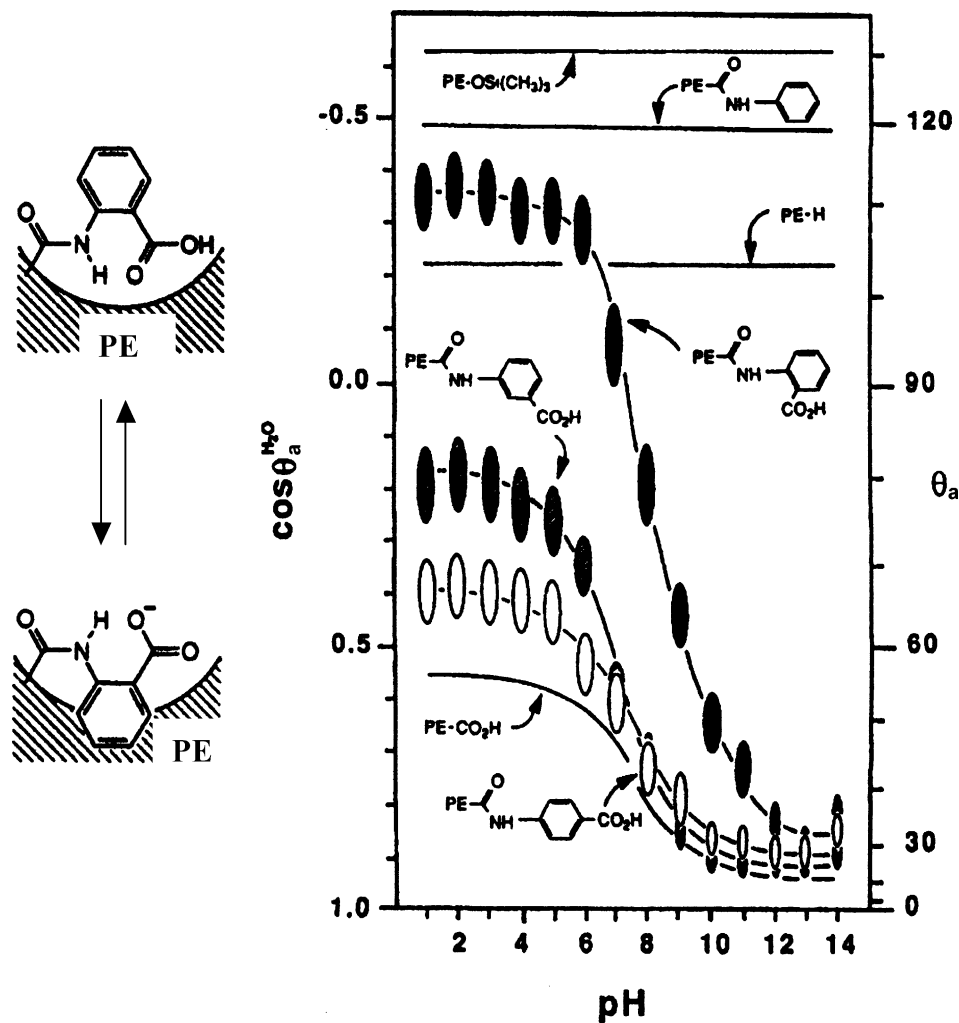


Fig. 14. Right figure: advancing contact angle of water on PE-CO₂H and anilide derivatives as a function of the pH of the liquid. Data for PE-H and PE-CONH₂ are included for reference. Left figure: proposed change in conformation for PE anthranilate used in rationalizing the extraordinary change in wettability observed between low and high pH (upper and lower conformations, respectively). Reprinted with permission from Ref. [94] (Langmuir 1990;6:87, Copyright (1990) American Chemical Society).

forces) between a polymer and any contacting phase determine the relative concentrations of polar and non-polar groups in the outermost portion of the polymer material with a modified/functionalized surface. Nevertheless, when Bergbeiter and Kabza studied annealing and the surface reorganization of sulfonated PE (in order to produce surface-modified films of varying hydrophilicity) some unanticipated surface response was found [97]. The sulfonation of PE surfaces resulted in relatively hydrophilic films

whose hydrophilicity, however, was increased upon thermal annealing. This behavior was in a contrast to that seen for the PE-CO₂H and its derivatives. The extent to which such surfaces did not reorganize to a less hydrophilic surface was affected by the presence of alkylammonium salts. Films with long chain alkylammonium salts at their surface reorganized thermally to less hydrophilic surfaces while films with short chain alkylammonium salts had contact angles which decreased upon heating.

According to the authors, the reason for this unanticipated behavior might be due to a change in the uniformity distribution of sulfonic acid groups during the annealing.

In a series of papers, Ferguson and co-workers reported on a responsive polymer material with a chemically modified surface for which entropy plays a central role in determining the composition of the polymer surface when it is in contact with water or a polar substrate [98–101]. The authors studied the surface/interfacial behavior of syndiotactic 1,2-polybutadiene (PBD) modified by the oxidation of the surface with aqueous $\text{KMnO}_4/\text{K}_2\text{CO}_3$. When heated against water, the surface of PBD-ox became more hydrophobic, a result apparently contrary to that expected based on the tendency of systems to minimize interfacial free energy. The advancing contact angle of water for this system, in fact, increased with increasing temperature of the water against which it was equilibrated. Initially, the hydrophilicity of the surface varied reversibly as a function of temperature, reflecting reversible changes in the relative concentrations of hydrophilic and hydrophobic groups at the interface (Fig. 15) [98,99]. Eventually, however, the surface remained hydrophilic against water, independently of temperature. The temperature dependence of this phenomenon suggested the importance of entropy in determining the state of minimum interfacial free energy in this system.

This entropic effect was due to rubber elasticity arising from crystallinity in the polymer, and its loss

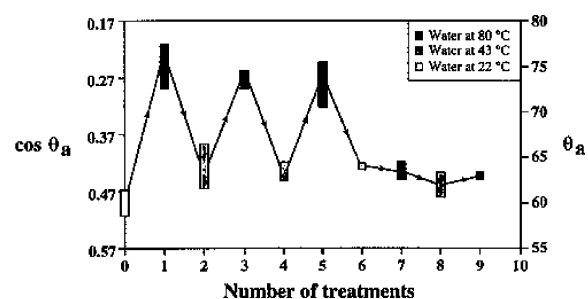


Fig. 15. The range in advancing contact angles of water (pH 1) on two separate samples of PBD-ox that were heated sequentially against water at 80 and 43 °C. After three such complete cycles, the wettability of these samples became independent of the temperature. Reprinted with permission from Ref. [98] (J Am Chem Soc 1996;118:9780, Copyright (1996) American Chemical Society).

was associated with a change in the amount and type of crystallinity [99]. The authors suggested that in lightly cross-linked elastomers, the rubber elasticity might compete with the tendency to minimize the interfacial free energy and perhaps dominate the interfacial behavior at high temperatures. As a result, the migration of functional groups attached to the mobile segments would require the extension of chains out of their relaxed, random-coil conformations. When the temperature is increased, however, the polymer chains recoil, pulling these polar groups away from the interface. This hypothesis is analogous to the thermodynamic changes that accompany small extensions of an elastomer: while the stretching of an elastomer can be enthalpically favorable, an entropic restoring force determines the equilibrium extension (Fig. 16).

Khongtong and Ferguson [101] have employed the observed surface behavior of the PBD-ox for designing smart adhesive systems in which the surface adhesion itself is responsive to changes in environmental conditions. Specifically, the strength of adhesion in laminated PBD-ox/Al samples that had been equilibrated at room temperature and at elevated temperature was examined. Fig. 17 shows representative force-displacement curves for peel tests for the different types of samples. In fact, the PBD-ox/Al interface displayed temperature-dependent adhesion. It was proposed that the temperature dependence in this system arises from the rubber elasticity of the polymer and mirrors the interfacial behavior of the same polymer against water. The interface produced a strong adhesive joint at room temperature due to enthalpically favorable chemical interactions between the added functional groups and the surface of the metal substrate. However, the migration of these functional groups into the contact with the aluminum (oxide) required the extension of the polymer chains out of their random coil conformations, thus reducing the entropy in that region of the polymer.

At high temperature, in turn, these functional groups were pulled away from the interface by the elastic restoring force induced by the entropic loss in the extended polymer chains. As a result, adhesion at the oxidized-1,4-PBD interface decreased dramatically when temperatures increased. The change in the adhesion at the PBD-ox/Al interface was reversible; the interfacial adhesion slowly recovered and reached

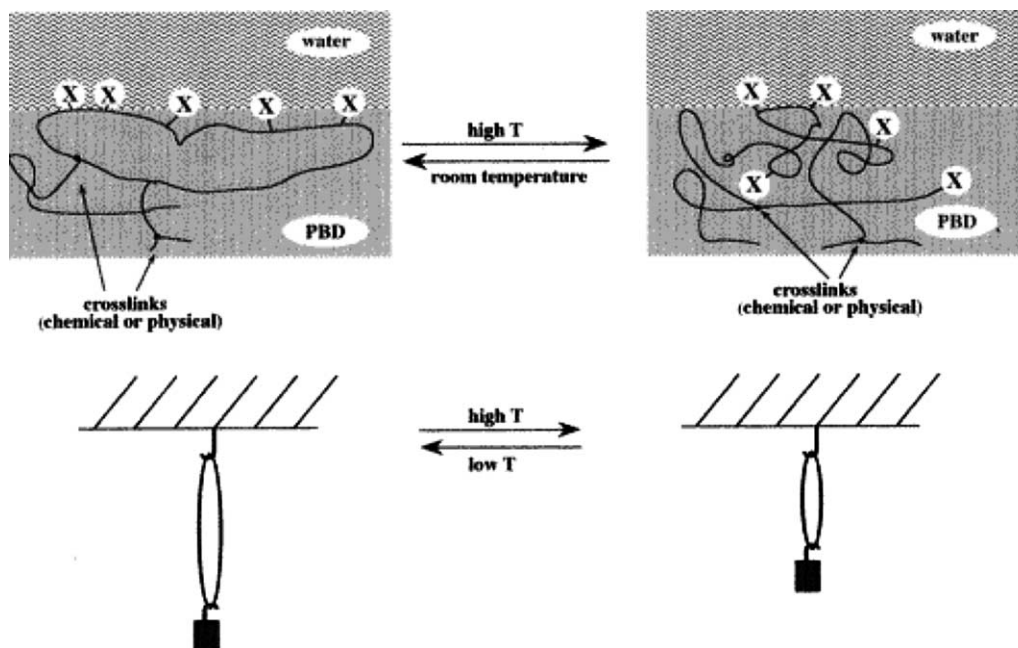


Fig. 16. Stylized illustration of the proposed model for explaining the entropically controlled reconstruction of PBD-ox against water (top). A lack of mobility near branch points requires entropically unfavorable chain extension to bring hydrophilic (X) groups into enthalpically favorable contact with the water. The resulting temperature-dependent behavior is analogous to that expected for a rubber band under constant stress (bottom). Reprinted with permission from Ref. [99] (*Macromolecules* 2000;33:8802, Copyright (2000) American Chemical Society).

its initial steady-state level within about 40 h (Fig. 18). This reversibility extended through several cycles of heating to 80 °C and cooling to room temperature.

Another example of a very different polymer material demonstrating the responsive surface behavior could be a cross-linked polymer in its rubbery state with chemically modified surface. The material can be easily stretched or contracted, causing significant increase or decrease in the surface area. Thus, the surface concentration of the functional groups introduced on the polymer surface can be varied by the extension or retraction of the elastomer. Genzer and Efimenko have used this change in surface area for the generation of hydrophobic polymer surfaces that can change the hydrophobicity level when the rubbery material is stretched or relaxed [102]. At the first step, they oxidized the surface of the stretched PDMS film by ultraviolet/ozone (UVO) treatment to introduce –OH functionalities (Fig. 19). Next, perfluoroalkanes possessing low-surface energy were deposited on the surface from vapor, and a hydrophobic self-assembled monolayer was formed

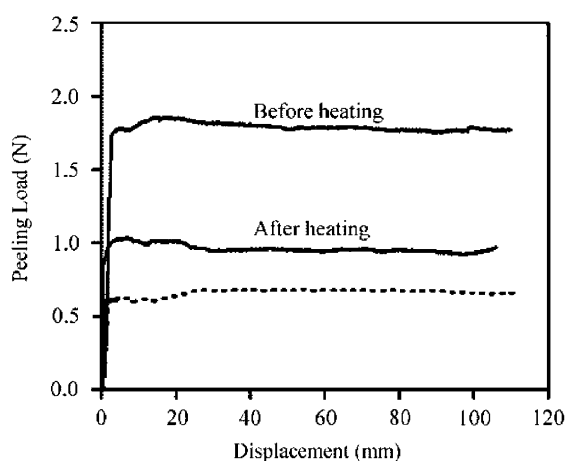


Fig. 17. Adhesion at the oxidized-1,4-PBD/aluminum interface before and after heating at 80 °C for 15 min. The heated specimen was quickly cooled to room temperature under a stream of nitrogen before measuring the adhesion. The dashed line shows the adhesion at the unoxidized-1,4-PBD/aluminum interface, for comparison. Reprinted with permission from Ref. [101] (*J Am Chem Soc* 2002;124:7254, Copyright (2002) American Chemical Society).

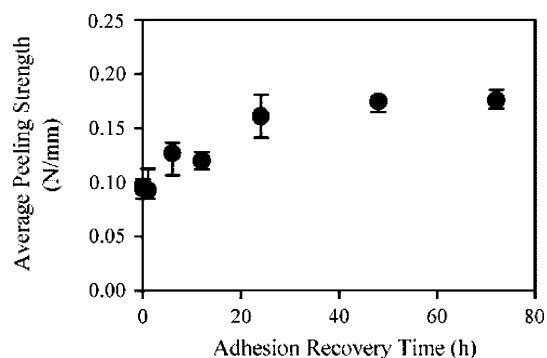


Fig. 18. The kinetics of recovery of adhesion at an oxidized-1,4-PBD/aluminum interface after samples heated at 80 °C for 15 min were subsequently equilibrated at room temperature. Reprinted with permission from Ref. [101] (J Am Chem Soc 2002;124:7254, Copyright (2002) American Chemical Society).

on the rubbery substrate. When the modified PDMS samples were relaxed, its contact angle with water significantly increased. The values of the contact angle were strongly dependent on the degree of stretching of the PDMS substrate before the UVO treatment (Fig. 20). Genzer and Efimenko proposed that any external force or stimulus (e.g. heat or solvent exposure), that causes the elastomer to deform will change the wetting characteristics of the surface and can be used to tailor its wetting properties in a predictable manner.

Lampitt et al. reported another mechanism of switching of liquid repellent surfaces through generation of polyelectrolyte-surfactant complexes on a substrate surface [103]. They employed plasma polymerization of maleic anhydride as direct and interfacially specific approach to the functionalization. The plasma polymer layer was deposited by pulsing the electrical discharge on the submicrosecond time scale in order to achieve high-structural retention of the anhydride groups. Next, a complex between the plasma polymer and cationic fluorinated surfactant was obtained. The fluorocontaining surfactant-plasma polymer layer was found to repel oil but allow the spreading of water. Thus, the cationic fluorosurfactants complexed to maleic anhydride polymer layers readily underwent the surface reconstruction in a response to their local liquid environment. It was shown that this ability to switch between hydrophobicity and hydrophilicity could be repeated at least 20 cycles.

Actually, in the aforesaid work by Lampitt et al., glass slides were used as model substrates for the plasma polymer deposition to obtain the material with responsive/adaptive surface. However, the proposed method can be readily applied to a polymer boundary, since the deposition of a functional layer on a polymer surface by the plasma polymerization has been successfully used for the treatment of polymeric materials [90]. In fact, once a stimuli-responsive

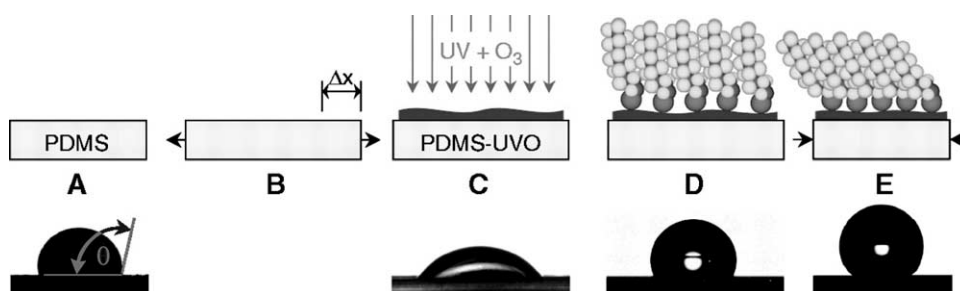


Fig. 19. Top panels are schematics illustrating the technological steps leading to the production of the hydrophobic surfaces. (A) A pristine PDMS network film is prepared by casting a mixture of PDMS and a cross-linker into a thin (≈ 0.5 mm) film and curing it at 55 °C for about 1 h. (B) After soxhlet extraction in chloroform for 24 h, which removes any non-cross-linked PDMS oligomers, the film is cut into small strips ($\approx 1 \times 5$ cm²) and mechanically stretched by a certain length, Δx . Subsequent exposure to a UVO treatment) produces hydrophilic PDMS surfaces (PDMS-UVO) composed mainly of hydroxyl groups. (C) By increasing the length of the UVO treatment, the number of the surface hydrophilic groups increases, causing the water contact angle to decrease. (D) The FyHx molecules are deposited from vapor onto this stretched substrate and form an organized SAM. (E) Finally, the strain is released from the PDMS-UVO film, which returns to its original size, causing the grafted FyHx molecules to form a densely organized MAM. To remove weakly physisorbed FyHx molecules, we wash the samples thoroughly in warm (≈ 60 °C) distilled water for 1 min and dry them with nitrogen. The bottom panels show photographs of a water droplet spreading on each of the substrates. Reprinted with permission from Ref. [102] (Science 2000;290:2130, Copyright (2000) AAAS).

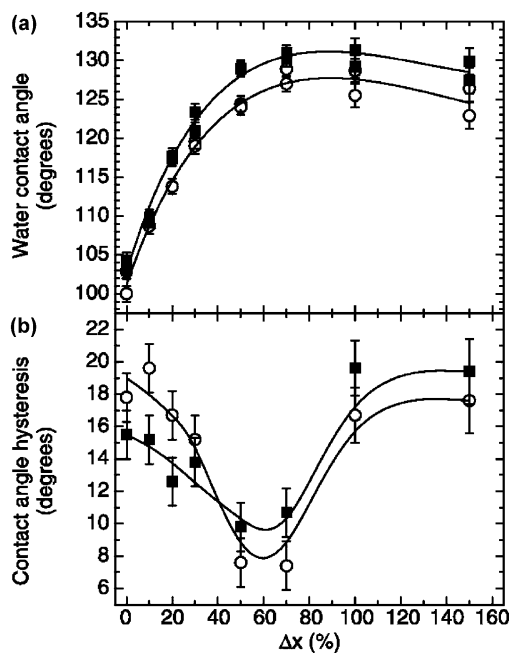


Fig. 20. (a) The dependence of the water contact angle, θ_w , on F6H2-MAM (circles) and F8H2-MAM (squares) samples on the degree of stretching of the PDMS substrate before the UVO treatment, Δx . (b) The corresponding contact angle hysteresis (defined as the difference between the advancing and receding water contact angles). The lines are meant to guide the eye (32). Symbols as in (a). Reprinted with permission from Ref. [102] (Science 2000;290:2130, Copyright (2000) AAAS).

(macro)molecular system is identified and its behavior understood, the modification approach can be translated to other polymer and any inorganic substrate of interest. Then, the problem to create materials with the smart surface can be viewed from another angle and more general questions can be formulated; what are the optimum structures, compositions, and properties of the stimuli-responsive layer grafted to a surface that can bring adaptive/responsive behavior to any non-polymer (e.g. metals, semiconductors) material? How this layer should be attached to the underlying surface to perform its function the best? How the substrate nature and morphology affect the polymer layer responsiveness? For that reason, significant efforts have been made to prepare, characterize and understand the functional surface layers. The next sections of the present review are devoted to progress in this area.

4. Grafted layers with adaptive/responsive behavior

Grafted organic and polymer layers are, in fact, capable of responding communally to very subtle changes in the surrounding environment such as pH [104], temperature [105], and solvent quality [106–108]. These reorganizations are responsible for physical properties important in applications of colloid stabilization [109], drug delivery and biomimetic materials [110,111], chemical gates [112], and tuning lubrication, friction, adhesion, and wettability for tailored surfaces [113–115]. Surface composition and, hence, related properties of grafted polymer layers such as surface energy, adhesion, friction, and wettability could be ‘tuned’ to the necessary physical state. This provides the fabrication of robust ‘smart surfaces’ with some new sophisticated properties such as self-cleaning and self-refreshing abilities, or ultrahydrophobic behavior [116,117]. The grafted polymer chains located at the interface can be attached to the surface in several configurations. The macromolecules may form multiple connections with the substrate or be connected to the surface at one or both ends. Tethered polymer chains that are grafted to a solid substrate by one chain end may be definitely distinguished from other anchored polymer layers, since they form polymer brushes if relatively high-grafting density is reached [118,119]. Brush-like layers are formed due to the excluded volume effect, that occurs when the substrate is completely covered with a relatively dense monolayer of grafted chains stretched normal to the surface (Fig. 21).

The responsive surface polymer layers can be designed by using a number of various approaches including several major designs represented in Fig. 21. The known and proven designs include reversible photoisomerization reaction of grafted photochromic segments, reversible swelling/collapse of water-soluble grafted polymers, and phase separation in binary grafted brushes or grafted diblock copolymers (Fig. 21). In this section, we primarily focus on the first two types of responsive layers with mixed brushes and diblock copolymers brushes being considered in Section 4.1.

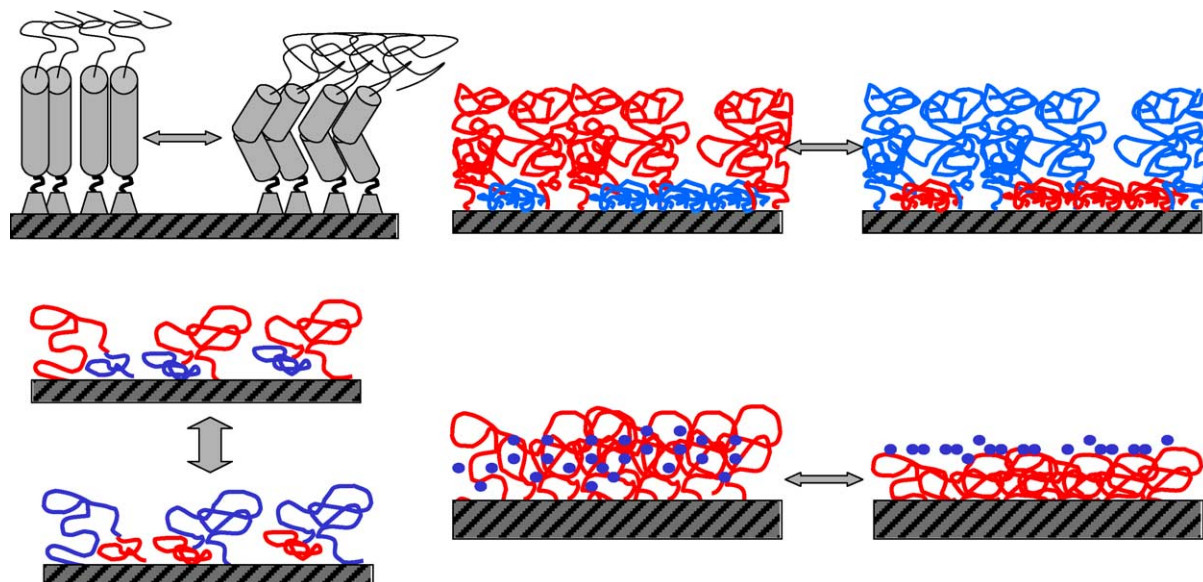


Fig. 21. Several representative designs of switchable grafted layers: light-sensitive molecules with photochromic groups (top left), mixed binary brush layers (top right), grafted diblock copolymers (bottom left), grafted polymer with LCST (bottom right).

4.1. Photoresponsive surface layers

Photoresponsive polymeric materials based upon photoactive groups capable of changing their configuration due to the interaction with incoming UV light are very well known and studied in great detail [120]. The vast majority of such materials are designed to utilize the ability of azo-benzene chromophores to show effective and reversible photoisomerization under UV-illumination. Initial rod-like, *trans*-configuration of these molecules, which is stable under ambient light conditions is transformed to folded, kinked *cis*-configuration due to the photoisomerization of central $-N=N-$ group after the adsorption of UV-photons with a wavelength of around 360 nm (Fig. 22). This transformation results in dramatic changes in the adsorption properties of the molecules with virtually complete disappearance of the initial strong band at 365 nm and appearance of a weak band at 450 nm (Fig. 22). This change of the UV spectrum is a signature of the photoisomerization reaction and is used for monitoring corresponding transformations. *Cis*-configuration is stable in complete darkness or upon the vitrification of the photochromic material. However, it can be converted back to the *trans*-configuration by additional UV

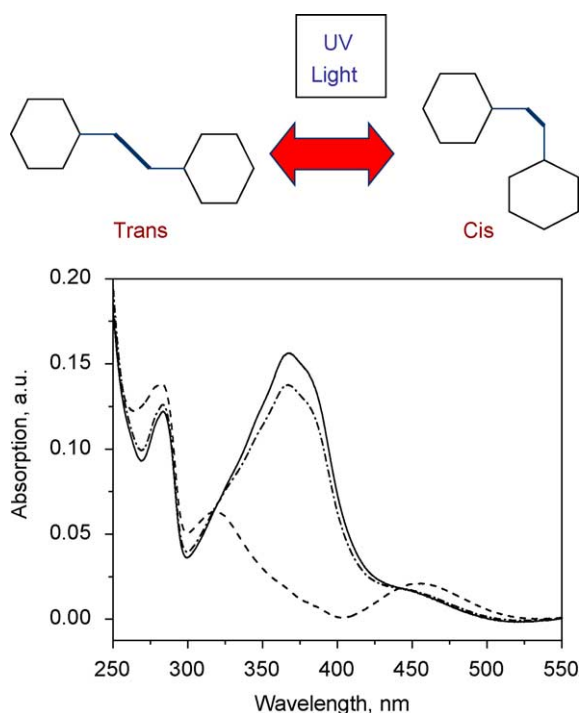


Fig. 22. UV spectra of azobenzene solution in *trans*-state (solid) and in *cis*-state after illumination (dash) and after 5 min after relaxation to the initial state (dash-dot).

illumination with wavelength of 450 nm. Photochromic, azobenzene-containing polymers of amorphous, gel, fiber, and liquid-crystalline types have been synthesized to date. Their photochromic properties and the photoisomerization phenomena of these materials were observed and utilized for various applications including optical storage, optical filtering, and grating [121–123].

It has been suggested that this phenomenon can be used for controlling surface wettability, film permeability, surface reactivity, and phase separation in polymer blends. However, the fabrication of the photoresponsive surface films based on azo-containing molecules and polymers have been realized relatively recently. One of the first attempts included the fabrication of Langmuir–Blodgett monolayers from amphiphilic molecules/polymers and self-assembled monolayers from alkylsilane molecules [124–126]. These surface layers, called ‘command layers’, demonstrated the ability of reversible photoisomerization within certain limits, which affected dichroism and other optical properties of quartz slides used as substrates.

Another interesting phenomenon is the so-called photomechanical response, which is observed within Langmuir monolayers formed from photochromic amphiphilic molecules directly at the air–water interface [127]. It consists of reversible changes of the surface pressure of azo-containing monolayers under illumination with different wavelengths that indicated a direct change of intramonolayer packing density caused by changing the shape of the molecules. Direct photomechanical phenomenon was also observed for the surface layers of chemically grafted polypeptides with incorporated azo-benzene groups [128]. The authors used a single molecule force-spectroscopy to demonstrate that the contour length of the grafted macromolecules can be reversibly shortened or lengthened by the photoisomerization reaction. This proves the ability of a single polymer molecule to conserve photomechanical energy, which is critical for designing future molecular level nanomachines.

Effective photoisomerization was also demonstrated for ultrathin *multilayered* polymer surface films fabricated by electrostatic layer-by-layer self-assembly [129]. As was observed, the kinetics of the photoisomerization in these films was hindered by

their organized multilayered structure. However, this ordering did not prevent completely reversible switching behavior controlled by UV illumination. The photoisomerization reaction of azo-containing fragment incorporated in polyelectrolyte backbones organized within these films resulted in detectable reversible changes of film thickness along with the usually observed changes of optical adsorption.

Unfortunately, a vast majority of results published to date do not go beyond proving the same fact of switching of the photochromic groups and rarely addresses the corresponding changes in the surface properties associated with this photo-induced switching. Only a few recent studies reported significant variation of the surface wettability caused by the photoisomerization reaction with a reversible increase of the contact angle after UV illumination. For instance, a spectacular phenomenon of light-driven motion of a liquid droplet on a photoresponsive, azobenzene-containing surface layer has been recently observed by Ichimura et al. [130]. The authors demonstrated that the liquid droplet placed on a surface of an azo-containing SAM can be moved along a certain direction by applying gradient UV-illumination to the surface (Fig. 23). The authors suggested that the gradient illumination caused a gradient of the photochromic transformation resulting in the corresponding gradient of the surface wettability. Thus, the horizontal driving force arised along a certain direction due to the unbalanced surface

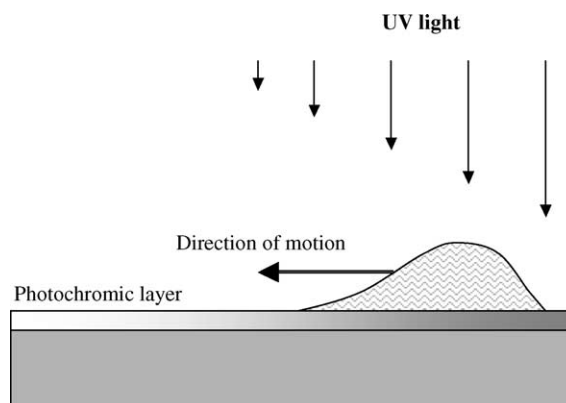


Fig. 23. Asymmetric shape of the liquid droplet moving on a gradient surface created by gradient UV-illumination of azobenzene surface layer.

tension caused by different contact angles on two sides of the droplet (Fig. 23). This example demonstrates a potential, far-reaching application of this photo-driven surface switching in chemical processing and microfluidic systems.

4.2. Thermally responsive surface layers

The well-studied example of thermally driven switching of surface properties is related to a type of polymers exhibiting an easily accessible lower critical solution temperature (LCST) while mixed with water [131]. This phase behavior is frequently caused by the presence of a high concentration of hydrogen-bonding capable chemical groups in the polymer backbone, and is common for polymer systems. Below the LCST, the polymer is completely miscible with water, adopt a highly swollen coiled chain conformation, and can be considered as water-soluble and, hence, hydrophilic (Fig. 24). At elevated temperature above the LCST, the polymer–water homogeneous mixture undergoes phase separation resulting in the formation of compact, globular polymer phase separated from water-enriched phase. Under these conditions, the polymer can be considered as incompatible with water

and, hence, hydrophobic. Thus, a minute variation of temperature in the vicinity of the LCST point should result in reversible and dramatic changes of polymer properties from hydrophilic to hydrophobic and back.

The most studied polymer of this type is poly-*n*-isopropylacrylamide (PNIPAAm) for the reason that in solution, it demonstrates LCST point close to 32 °C [132]. Although, the majority of experiments in polymer–water system are devoted to macroscopic hydrophilic–hydrophobic properties, several recent investigations addressed an important question of surface switchable behavior of the grafted layer from this polymer. The most important result was related to the preservation of the bulk phase behavior in molecular thick and chemically grafted polymer films. It has been concluded that in these densely grafted and partially cross-linked polymer films; the LCST was still close to the known bulk value [133].

Potential for use of these polymers as switchable substrates for temperature-controlled cell harvesting has recently been demonstrated [134]. Controlling bacterial biofouling is desirable for almost every human enterprise in which solid surfaces are introduced into non-sterile environments [135]. Surface coating by thermally reversible polymers is a new approach for the recovery of cells from tissue culture substrata without the need for enzymes, e.g. trypsin, to digest the matrix responsible for attachment. Cells were recovered from tissue culture substrata simply by lowering the temperature below a critical threshold. It has been observed that the vast majority of cultured microorganisms and naturally occurring marine microorganisms that attach to grafted PNIPAAm surfaces were removed when the hydration state of the polymer was changed by means of a temperature shock [135]. Dramatic change in the physical state resulted in switching the surface wettability that was favorable for attachment (hydrophobic) to a wettability that was less favorable (hydrophilic). Neither solvated nor desolvated PNIPAAm layers exhibited intrinsic fouling release properties, indicating that the phase transition was the important factor in removal of organisms.

Another paper by these authors describes a convenient method for in situ polymerization of PNIPAAm on the surfaces of azo-initiator-derivatized SAMs of ω -terminated alkanethiolates on gold [136]. The resulting tethered PNIPAAm surface layers

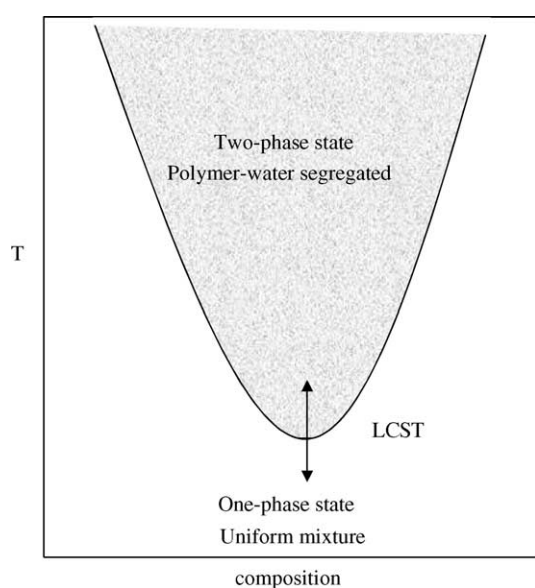


Fig. 24. Sketch of phase diagram for polymer–water system with LCST and illustration of transition across the phase line.

were characterized using ellipsometry, XPS, and contact angle goniometry and tested for their ability to attach and release bacteria. The synthetic method was considered to be very useful for the fabrication of ultrathin films that are compatible with common reflection (e.g. surface plasmon resonance) and transmission-based optical characterization techniques.

Confirmation of the formation of highly swollen polymer layers grafted to a solid substrate below LCST and its collapse to a dense compact state above this temperature was obtained from recent AFM studies [137]. It has been concluded that, indeed, not only does the effective thickness of the grafted PNIPAAm layer change during this temperature-controlled phase transformation, but their micromechanical response to the compression load also underwent dramatic changes. In fact, direct measurements of the elastic modulus of the grafted PNIPAAm layer with different cross-linking density in water solution revealed dramatic changes of surface properties at temperatures close to the bulk LCST value (Fig. 25) [138]. The elastic modulus changed by two orders of magnitude from a low value around 10–100 kPa in the highly swollen state below LCST to several MPa in the collapsed state above the LCST. These changes were completed within a narrow temperature interval of 3–6 °C.

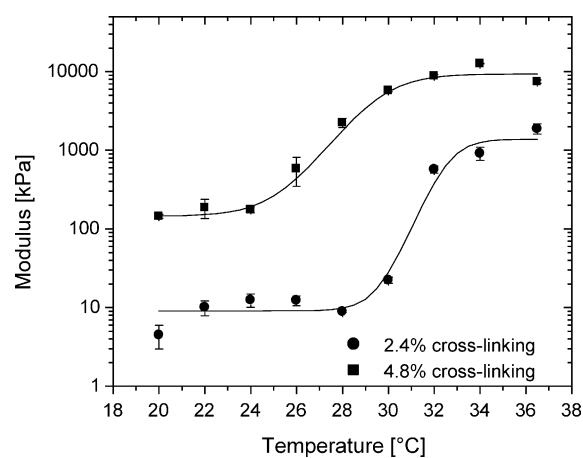


Fig. 25. The temperature variation of the elastic modulus of the grafted PNIPAAm layer in water undergoing the phase transformation from swollen to collapsed state. The plot is a courtesy of M. Harmon, D. Kuckling, and C. Frank.

The authors demonstrated that the range of variations and the limiting values in two different states can be controlled by the degree of cross-linking of the polymer layer.

Dramatic reversible changes of the surface morphology and adhesion were also demonstrated for the micropatterned grafted PNIPAAm layer, which formed elevated stripes alternating with an alkylthiol SAM on a gold substrate (Fig. 26) [139]. The authors observed that the height of the brush layer increased 3-fold when the aqueous solution temperature was reduced below LCST for this polymer. These reversible changes of the surface morphology were repeatedly observed during temperature cycling confirming that grafting of polymer chains to a solid substrate does not dramatically affect their phase behavior in aqueous solution. The apparent increase of the surface stiffness of the grafted layer accompanied its collapse.

The most convincing confirmation of switching of grafted PNIPAAm layers came from micromapping the adhesive surface properties using AFM force–distance probing (Fig. 26). Above LCST, the adhesive forces between the AFM tip and the collapsed, hydrophobic polymer layer were virtually identically to that for surrounding methyl-terminated SAM, which resulted in uniform, uni-modal surface histogram distribution (Fig. 26). However, crossing the phase line by cooling the grafted surface layer below LCST resulted in dramatic transformation of the surface properties. The adhesion of patterned surface areas coated with a swollen hydrophilic polymer layer increased dramatically and became very different from that measured for the surrounding, unchanged SAM areas. This reorganization caused major changes to its overall surface adhesive properties converting initial uniform surface to the patterned surface. A non-uniform character of this surface after phase transformation can be seen from a bimodal surface histogram of the adhesive forces below LCST (Fig. 26).

4.3. Responsive surface layers from dendritic polymers

Special attention has been paid to the fabrication of the responsive surface layers from photochromic dendrimers. These polymers possess unique

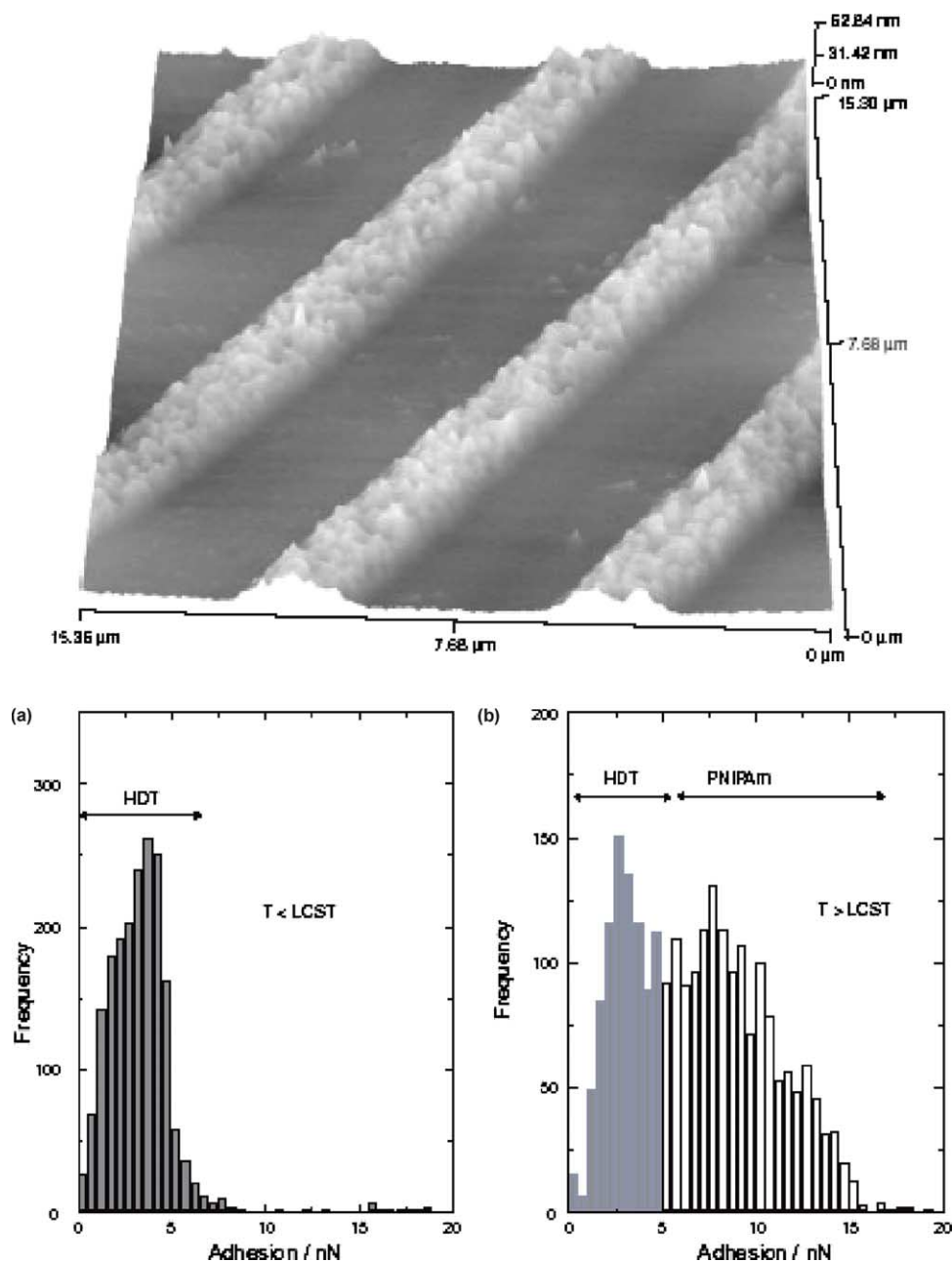


Fig. 26. AFM image of PNIPA/SAM patterned surface in water at 26 °C (top) and histogram of surface distribution of adhesive forces for this patterned surface below LCST (left) and above LCST (right). Reprinted with permission from Ref. [139] (Adv Mater 2002;14:1130, Copyright (2002) Wiley InterScience).

properties due to their tree-like architecture, high concentration of terminal groups on periphery, virtual monodispersity. Thus, they show peculiar surface behavior controlled by balance between polar heads

and crowded hydrophobic shell [140,141]. The first amphiphilic photochromic dendrimers capable of forming stable monolayers at the air–water interfaces and solid surfaces have been very recently

synthesized [142]. It has been demonstrated that polypropylene imine dendrimers of the fifth generation modified with a combination of hydrophobic alkyl tails and azo-benzene containing groups possess strong amphiphilic character and form stable, ordered Langmuir monolayers with the photochromic behavior at the air–water interface [143]. Despite a random shell structure of these molecules, the tree-like architecture prevents microphase separation of the azobenzene chromophores within those monolayers, thus facilitating reversible *trans*–*cis* photoisomerization of these large molecules.

In another series of papers, the results were reported on several different sets of amphiphilic monodendrons of different generations with a photochromic central group and different types of outer alkyl shells and polar groups have been synthesized and studied (Fig. 27) [144–146]. These monodendron monolayers were studied at both air–water interface and solid substrates. Amphiphilic monodendrons of four different generations,

AD12-N, containing a benzyl-15-crown-5 polar focal point, photochromic spacer, and different number of alkyl tails as peripheral groups ($N = 1–16$) have been investigated for their ability to form uniform organized monolayers. The surface pressure–area behavior, the photomechanical behavior, and the morphology of the monomolecular films confirmed that all compounds studied were capable of forming stable Langmuir and Langmuir–Blodgett monolayers with virtually flat packing of molecules. Higher generation dendrimers formed very uniform, featureless monolayers on the solid surface without the usual domain microstructure observed for crystallizable, alkyl-containing amphiphilic compounds (Fig. 28).

Fast reversible photochromic response was observed for all monolayers with a conversion level of 50% and higher at the initial stage of the photochromic conversion [147]. Two different kinetic regimes of photoisomerization were observed for a full time scale of observation. Initially, as was

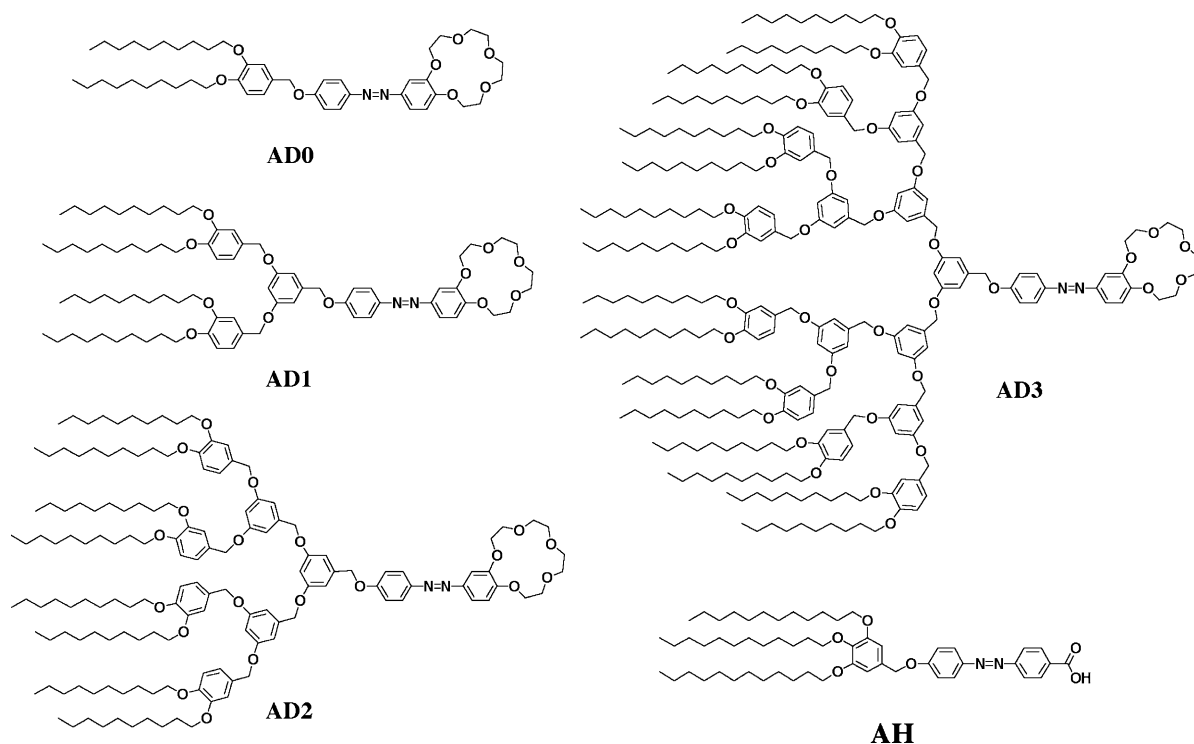


Fig. 27. Chemical structures of several representative photochromic monodendron molecules.

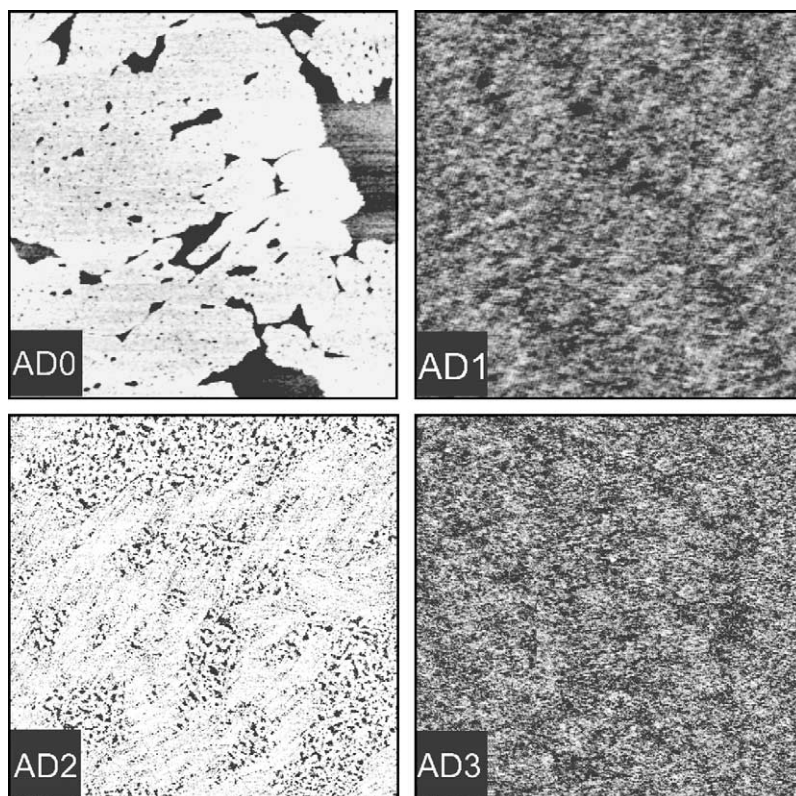


Fig. 28. AFM images ($1 \times 1 \mu\text{m}^2$) of Langmuir–Blodgett monolayers from photochromic monodendrons with chemical structures represented in Fig. 27.

mentioned above, a fast regime obeying first-order kinetics was observed within the first several minutes until conversion reached a slower stage. Following this stage, a slow photoisomerization regime was found obeying zero order kinetics. The resulting spectra of the monolayers after full conversion were close to the spectra of the corresponding dendrimers in solution after UV illumination, which confirmed the completeness of the corresponding transformation in the surface monolayers.

In fact, UV spectrum recorded after 5 min of illumination was still far from the corresponding spectrum of the monodendron in solution and significant presence of the main band at 365 nm was recorded (Fig. 29). Such ‘incomplete’ photoisomerization is common for many photochromic polymer films containing azo-benzene fragments. The changes of the spectrum were completely reversible at this stage and the monolayer reached its initial state after 20 h of storage in

darkness. The multiple reversible switching of the solid monolayer is shown in Fig. 29 as monitored by the intensity of the characteristic band at 365 nm. Illumination for longer periods (up to 72 h) resulted in a dramatic decrease of the 365 nm band intensity, ultimately resulting in complete disappearance of the band indicating full transformation. All monolayers from amphiphilic dendrimers of different generations studied demonstrated similar behavior with only minor differences.

A possible scenario has been suggested for the inhibition of the photoisomerization process and appearance of the two-step transformation of the photochromic dendritic monolayers. As known, *trans*–*cis* isomerization is accompanied by a change in geometry of the azobenzene group. Such a transition may be in conflict with the monolayer microstructure and the presence of the solid substrate if the molecule is oriented in a certain manner. On the other hand, no significant changes of

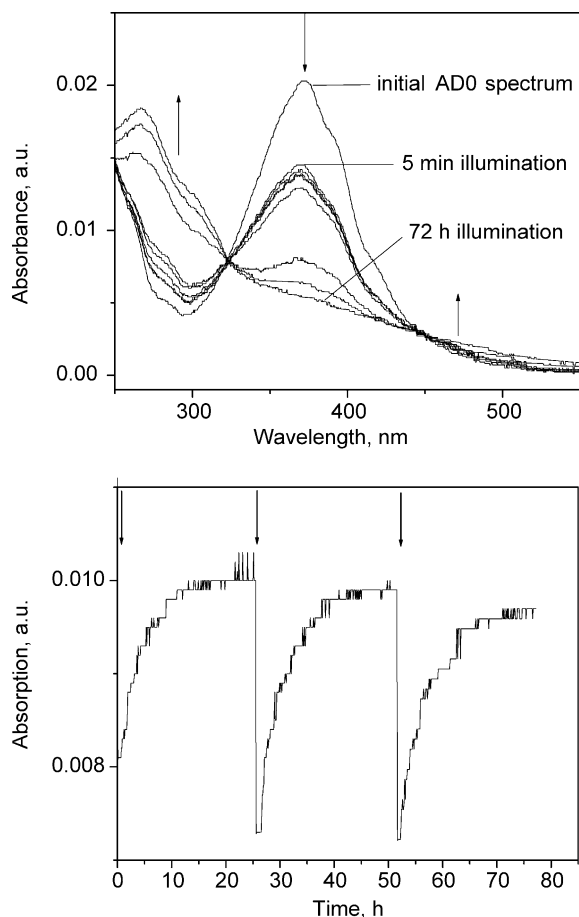


Fig. 29. UV spectra of photochromic molecule at different stages of photochromic isomerization (top) and the kinetic of variation of intensity of the adsorption band at 360 nm during switch on/off cycling (bottom).

the monolayer thickness were observed during photoisomerization reaction. This suggested that the two-stage photoisomerization kinetics was governed by intramonolayer mechanisms related to lateral mobility/reorganization of the dendrons. The fast kinetic regime was attributed to the occupation of free volume available in the initial monolayer by a fraction of molecules in folded configuration that requires much larger cross-sectional area. After this initial fast stage, the process turned to a very slow diffusion-limited reorganization of the intralayer structure.

In addition, it was found that only intermediate generation monodendron monolayers showed

significant changes in surface area at air–water interface under UV-illumination that can be unambiguously detected [148]. Corresponding temporal variations of the surface area under UV-illumination clearly showed photomechanical phenomenon caused by the photoisomerization transformation (Fig. 30). Photochromic transformations for the dendron monolayers of intermediate generations were completely reversible and were repeated many times. The photomechanical response of the surface area (or surface tension) of Langmuir monolayers was used as a measure of conversion of *trans*–*cis* photoisomerization. It has been concluded that only the optimal balance between cross-sectional areas of dendritic shells and polar groups in monodendron molecules could cause significant photomechanical response due to the fact that ‘more crowded’ dendritic shells provided loose packing for a central fragment with azo-benzene groups.

The photoinduced structural reorganization of the monodendron monolayer on the solid substrate was revealed with AFM imaging [149]. The authors observed that photoinitiated *trans*–*cis* isomerization of the photochromic dendrimer molecular film resulted in microstructural reorganization, which manifests itself in breaking regular strip-like intralayer organization (Fig. 31). *Trans*–*cis* isomerization occurred as *in-plane intralayer reorganization*

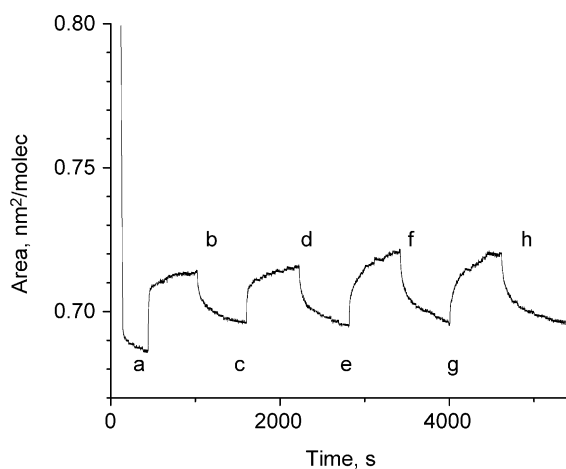


Fig. 30. Reversible photoinduced deformation of the Langmuir monolayer from AD1 monodendron as a response to multiple switching the illumination UV-lamp on (points a, c, e, g) and off (points b, d, f, h) at $\pi = 34$ mN/m.

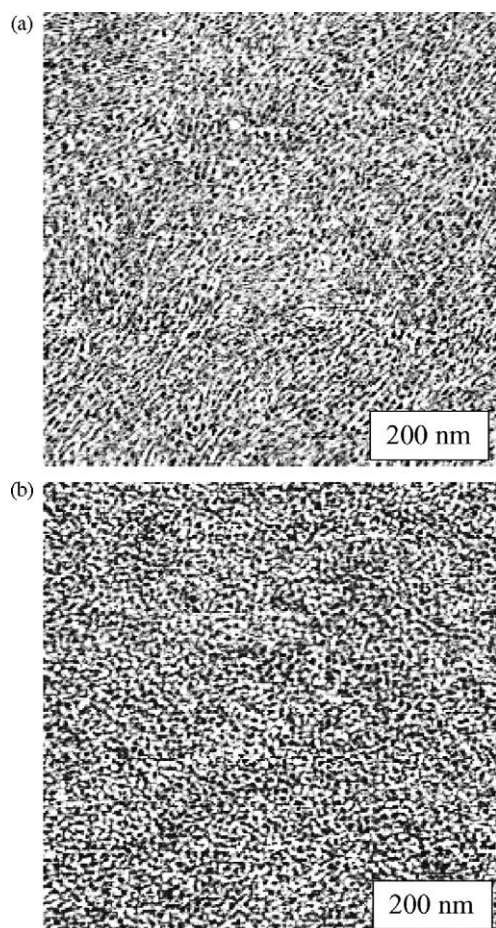


Fig. 31. The AFM phase images of the initial (a) and UV-illuminated (b) monolayer from photochromic monodendron, Z-scale is 10° .

without an affect on the monolayer thickness. Taking into account that a constant thickness during photoisomerization was observed for many azo-containing films, it was speculated that this type of intralayer reorganization is common for photochromic molecular films with azo-benzene fragments tethered to the solid surface.

On the other hand, it was observed that this photochromic microstructural reorganization changed the surface properties such as wettability of the monolayer similar to bulk azo-containing polymers. After UV illumination, the monolayer became more hydrophobic as indicated by the increase in contact angle from 56 to 79° . The contact angle value, observed for the UV-treated monolayer, was close to

the one measured for azobenzene monolayers with terminal alkyl chains. Obviously, the intramolecular structural reorganization leads to additional surface exposition of the hydrophobic tails of the dendrimer molecule shells. In addition, it has been observed that the friction coefficient, which reflects the dissipation of energy during shear stresses, decreased two times after photochromic reorganization. The friction coefficient of the initial monolayers was in the range from 0.05 to 0.1 and this value decreased to 0.03–0.05 after *trans*–*cis* isomerization.

A different type of branched molecules, hyper-branched polyesters (HBP) with different terminal groups (P-OH, P-COOH, P-OAc) were prepared as thin films and tested for their ability to swell in different vapors as a means to detect traces of solvent [150]. The surface properties of these films were studied using zeta potential and contact angle measurements. The variation in surface properties between different HBP layers was suggested to be promising for sensoric applications. The vapor of the homologous series of alcohols (from methanol to pentanol) was exposed to the thin HBP films. Changes in thickness were monitored with highly sensitive reflectometry interference spectroscopy and used to demonstrate that the detection and discrimination of different molecules using P-OH as a sensitive layer is possible.

4.4. Responsive surface layers from polyelectrolytes

The physical properties of polyelectrolyte molecules attached to a surface are fundamentally different from that of uncharged polymers [151–153]. In contrast to those of neutral polymer films, the structure and properties of the polyelectrolyte layers are almost exclusively dominated by electrostatic interactions. Mutual repulsion between the charged polymer segments and electrostatic forces between the polyelectrolyte molecules and the surface to which the chains are attached (especially if the latter one also carries a charge) influence the strength of interaction with the substrate and the physical properties of the surface layers strongly.

Polyelectrolytes are known for their ability to undergo abrupt changes in conformation, optical properties, and volume, in response to external stimuli such as pH, temperature, ionic concentration, solvent

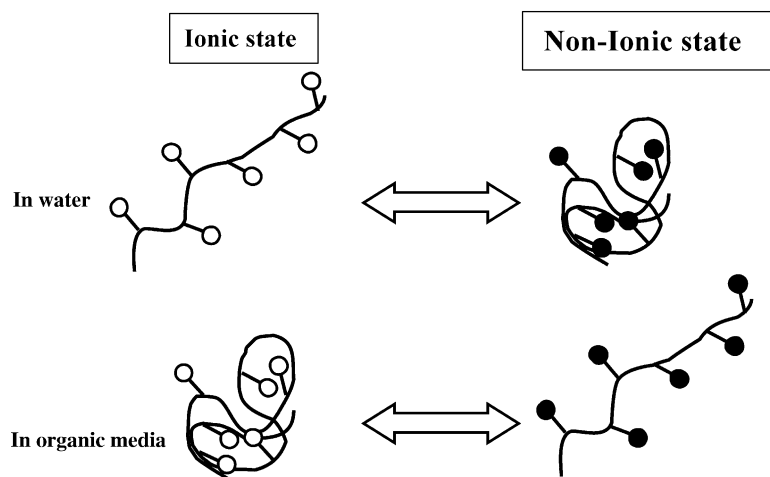


Fig. 32. Two different types of polyelectrolyte behavior. Figure redrawn after Ref. [154].

components, electric fields, and chemical reactants [154]. The responsiveness of the polyelectrolyte layers is attributed to the high concentration of the ionic groups in the polymer backbone, which are reversibly deionized in response to the stimuli (Fig. 32). The ionic state significantly affects the polymer conformation, which results in drastic changes in the physical properties. Therefore, design of responsive/adaptive surfaces frequently employs polyelectrolytes tethered to a substrate that continually expand and contract under external stimuli. Several recent comprehensive reviews devoted to the fabrication and the surface behavior of thin polyelectrolyte layers as well as their application in signal responsive systems are published [152, 154–156]. Thus, in this section, we will limit

the discussion on the polyelectrolyte responsive layers to several recent examples and refer an interested reader to the reviews for further information.

Ito and co-workers [157] reported pH-controlled gating of a porous glass filter by the surface grafting of polyelectrolyte layers. Poly(acrylic acid) (PAA is a strong polyelectrolyte) was grafted onto a porous glass filter in order to construct a pH-dependent system for the control of liquid permeation. The porous glass filter was treated with octadecyldimethyl(*N,N*-diethylamino)silane and subjected to the glow-discharge treatment to facilitate graft polymerization of the acrylic acid (Fig. 33). The surface wettability of the glass filter decreased following silane-coupling treatment and increased following PAA grafting. Thus, it was suggested that water

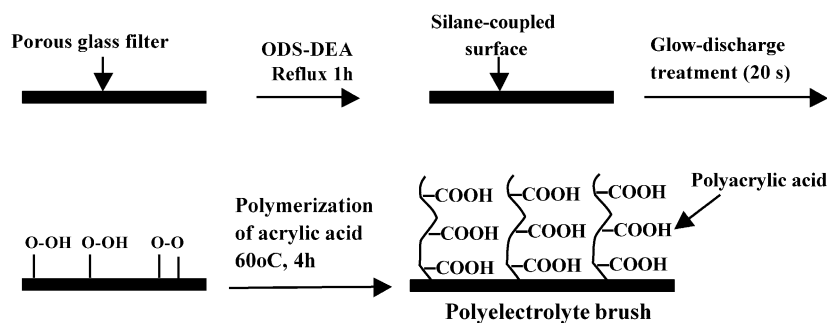


Fig. 33. Preparative scheme of surface-grafted glass filter. Figure redrawn after Ref. [157].

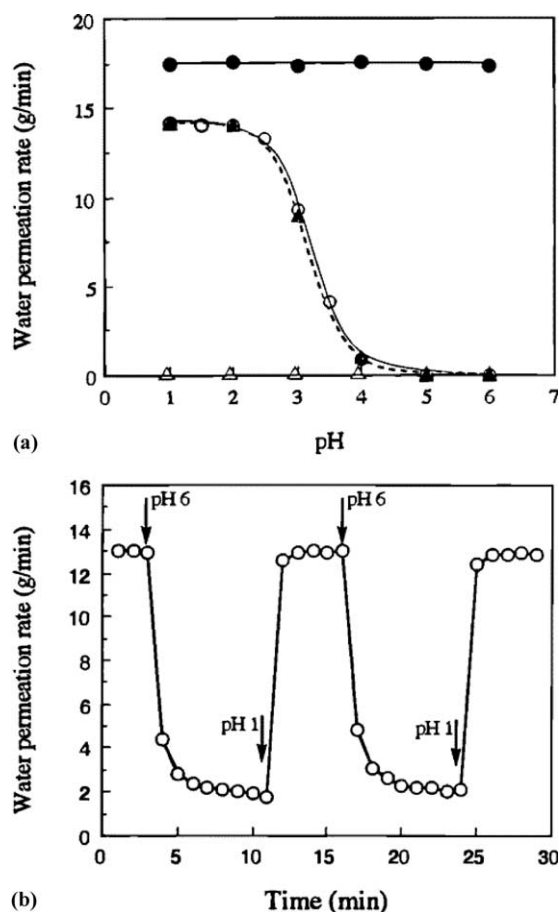


Fig. 34. (a) pH-dependent water permeation through PAA-grafted glass filter; pH 1 \rightarrow pH 6 (\circ), and pH 6 \rightarrow pH 1 (\blacktriangle), silane-coupled glass filter (\triangle) and glow-discharged glass filter (\bullet). (b) Time course of water permeation through PAA-grafted glass filter at different pHs. Reprinted with permission from Ref. [157] (Chem Mater 1997;9:2755, Copyright (1997) American Chemical Society).

permeation of the PAA-modified glass filter was pH dependent (Fig. 34).

In fact, it was observed that the permeation rate was higher under low-pH conditions and lower under high-pH conditions. The permeation rate of a water/acetone mixture through the grafted glass filter was also pH dependent. Authors proposed that under low-pH conditions, protonated PAA chains shrink, thereby opening the pores of the filter, and that under high-pH conditions dissociated PAA chains are extended to cover the pores (Fig. 35). Another publication from the same group was dedicated to pH control of

the fluid transport through a porous membrane self-assembled with a PAA loop brush [158]. Side chains of PAA backbones were conjugated with cysteamines for self-assembly on a gold-coated membrane. It was found that the amount of assembled polyelectrolytes significantly depended upon the concentration of the polyelectrolytes, the content of cysteamine in the polyelectrolyte, solution pH, and the ionic strength. Transport through porous membranes, which was gold-coated and subsequently self-assembled with the polyelectrolyte, showed that the water permeability through the membrane was reversibly regulated by pH and ionic strength.

In another approach, Bergbeiter et al. [159] synthesized PAA-grafted polypropylene (PP) using block co-oligomers of PP and acrylate esters. Co-dissolution of such co-oligomers with excess of isotactic PP and film casting produced functionalized films via an entrapment process. In the next step, acidolysis of the *tert*-butyl esters at the surface of these films resulted in the formation of the PAA layer attached to the PP surface. A substantial portion of the acid groups of the PAA grafted layer formed this way were accessible to base. The resulting carboxylate groups could then be reprotonated by treatment with acid. When the PAA graft was labeled with a fluorescent dansyl probe, the probe was found to be responsive to pH changes of solvent. In the presence of acid and solvents such as *tert*-butyl alcohol or THF, these dansyl groups could be reproducibly protonated and deprotonated with HCl and Et₃N, respectively. It was observed that the fluorescence intensity detected altered from zero to a much higher value that was roughly 60–80% of the intensity of the functionalized film's fluorescence in pure *tert*-butyl alcohol.

5. Block-copolymer brushes

Di- or tri-block-copolymers grafted to a solid substrate constitute a separate class of block-copolymer brushes. In general, thin films of block copolymers (BC) are the focus of intensive investigations due to their ability to self-assemble into well ordered, nanoscale periodic structures [160,161]. BC demonstrates a variety of bulk and surface morphologies (spherical, cylindrical, gyroidal, and lamellar) depending on the ratio of block lengths

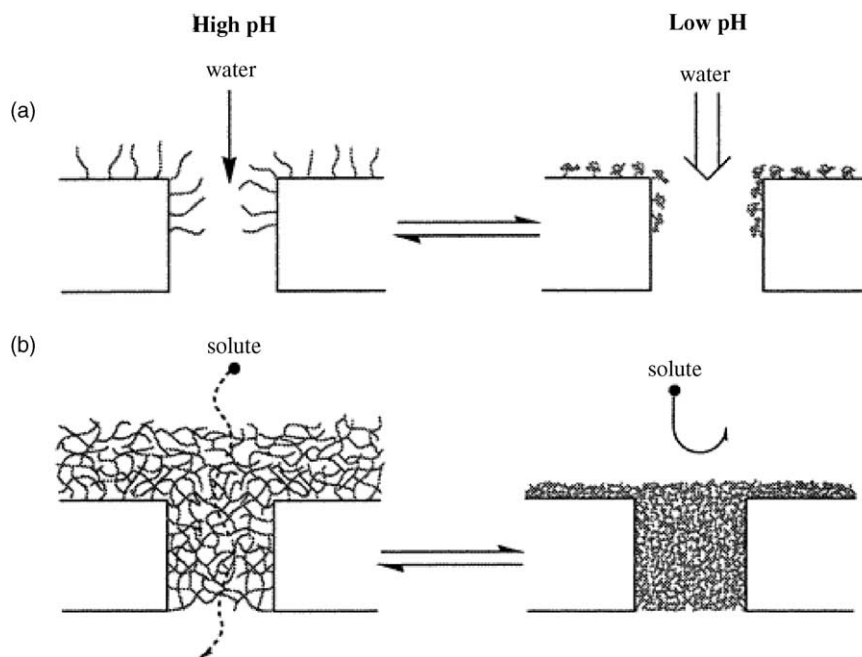


Fig. 35. Schematic drawing of permeation mechanism through PAA-grafted porous glass filter (a) and PAA-based hydrogel (b) Under high-pH conditions, deprotonation of PAA reduces pore size to decrease water permeation in (a) and leads swelling to enhance solute permeation in (b). Under low-pH conditions, protonation of PAA increases pore size to increase water permeation in (a) and leads deswelling to reduce solute permeation in (b). Reprinted with permission from Ref. [157] (Chem Mater 1997;9:2755, Copyright (1997) American Chemical Society).

and the segment–segment interaction parameter. The periodicity of these structures is determined by molecular weight and chemical composition in the BC and typically is in the range from 10 to 100 nm. This class of ordered materials is promising for sophisticated applications in many fields of nanoscience and nanotechnology such as surface patterning, lithography, and templating for the fabrication of information storage devices of terabits per cm^2 capacity, magnetic and optical materials, and nanowires and nanomembranes [162,163].

The grafted block-copolymer surface layer strongly differs from physically adsorbed thin films of mobile block-copolymer chains due to confinements introduced by tethering to a solid surface. However, even for the case of the immobilized polymer chains, a very rich phase behavior can be observed upon exposure to different media and external stimuli, which can be much more complicated than in the case of physisorbed films. The basis for the responsive behavior of BC brushes is in the phase segregation mechanism, specifically if

the solvent affinities to the different blocks are significantly different. The polymer–solvent interactions will govern the formation of the segregated phases within the grafted layer.

5.1. Self-assembly of block-copolymer brushes

In corresponding theoretical analysis, Zhulina et al. used both SCF calculations and scaling arguments to predict the structures formed by BC brushes upon exposure to different solvents [164,165]. With the SCF model, they demonstrated the formation of novel types of pinned micelles such as ‘onions’ and ‘garlics’, in which the less soluble blocks formed the inner core and the more soluble fragments formed an outer coating. Through scaling approach, they determined how the size and shape of these structures varied with the solvent quality and the properties of the diblocks. In a series of publications, they considered a variety of flexible AB diblock copolymers grafted onto a flat surface. The blocks contain N_A and N_B symmetrical units of size a (see Fig. 36).

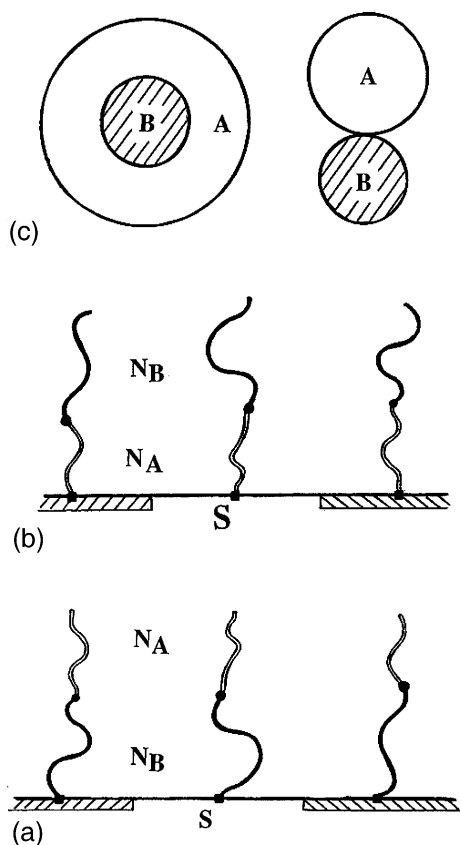


Fig. 36. Schematic diagram of (a) chains tethered by the less soluble B block, (b) the diblock chains grafted onto the surface by the more soluble A block, and (c) 'onion' and 'dumbbell' conformations for a single chain. The parameter s marks the area per chain. Reprinted with permission from Ref. [164] (Macromolecules 1996;29:6338, Copyright (1996) American Chemical Society).

For this system, they investigated two cases. *In the first case*, the layer was immersed in a solution that is a poor solvent for both components.

If each chain is tethered at the end of the less soluble B component (see Fig. 36a), the block copolymers associate themselves into 'onion' structures, where the less soluble B's form the inner core and the more soluble A's form the outer layer. In this conformation, the encircling A's shield the B's from the unfavorable solvent and the surface tensions within the system are minimized. Comparing the losses in the free energy at the boundaries for both the onion and the dumbbell conformations (see Fig. 36c) the authors found that forming an onion structure is

more favorable than splitting into a dumbbell. An increase in polymer incompatibility will lead to an increase in the surface tension between the A and B blocks and will eventually drive the onion to separate into a dumbbell.

On the other hand, if N_A increases further, the losses at the boundaries of the A layer become sufficiently large that the two adjacent shells are driven to merge and, thereby, minimizing their contact with the solvent. This merging into a common shell causes the structural rearrangement of the B cores. The two cores, which are shielded by the same A layer, rearrange themselves to move closer to each other. Since the multiple cores are simultaneously shielded by a common A shell, the micelle resembles a 'garlic-like' structure. As N_A increases, the density of A-block near the surface increases while that of B-block decreases. As a result of these changes, the B-block is somewhat more extended in the Z direction.

When the diblock chains are tethered by the ends of the more soluble A blocks (see Fig. 36b), and N_A is small, each A block contributes to forming the legs of the micelles, whose cores are composed of the more solvent-incompatible B. As N_A is increased, the legs become less stretched and the A's again form an outer shell around the inner core to minimize the contact between the B's and the solvent. With further increases in N_A , the density of A around the poorer component gradually increases and, thus, becomes more effective in shielding the B's. Since the A's are closer to the surface, increasing N_A causes the B core to be pushed away from the grafting surface in the vertical direction. In addition, less and less of the B's contribute to the legs of the micelle, and once N_A is sufficiently long, the legs are composed entirely of A. Whether the chains are grafted by the A or B blocks, increasing the grafting density significantly beyond the overlap threshold ultimately causes one or both components to form a continuous surface layer. For long blocks and high-grafting densities, the surface layer eventually forms a laterally homogeneous brush.

In the second case, the authors studied the system where the solvent acted as a theta or good solvent for one block but was a poor solvent for the other. Under these conditions, it was anticipated that the self-assembly of the layer would be affected by

the swelling of the solvophilic component. If the chains are grafted by the ends of the soluble A blocks, and when the length of the soluble A block is small, the layer is laterally homogeneous. Here, the chains are too short to stretch and associate into multichain aggregates.

However, when N_A increased significantly, the chains self-assembled and the B blocks formed pronounced micelles. The A blocks stretched in the lateral direction and formed a coating or shell around the B cores. The A coating shielded the B's from the unfavorable solvent and, thereby, lowering the interfacial tensions in the system. When the length of the soluble blocks is increased further, the A's form a polymer brush. The density of A's, however, was not monotonic in the normal direction. On the contrary, it was higher around the B cores since the A's shield this solvophobic region. If the increase in N_A is continued, the height of the A layer increased monotonically, as expected for planar brushes, and the micelles formed by the B blocks move farther away from the grafting surface.

When the solvophobic component B is grafted onto the planar surface the solvent-incompatible B blocks form a dense micellar core and the soluble A blocks form a shield around the B micelles. Again, this A coating reduces the extent of B-solvent contact. Thus, the structure resembles a 'flower' whose core is formed by the B blocks and the 'petals' are formed by the A blocks. As the length of the A block is increased, the solvent-shielding layer remains unchanged and the rest of the A blocks form a stretched layer, or brush. With further increase in N_A , the brush extends to larger distances in the Z direction. At relatively uniform grafting, the diblocks formed an ordered array or a pattern on the surface. The size and spacing of the micelles, and thus the dimensions of the pattern, could be controlled by varying the chain length, solvent quality, or the grafting density.

Thus, this theoretical study clearly demonstrated the mechanism of the surface reconstruction in BC brushes controlled by the incompatibility between polymers and selective interaction with solvent enhances the top of the layer with one of blocks. Recently, Zhao and Brittain for the first time have presented the experimental evidence of the theoretical prediction [166]. They have synthesized

a tethered block copolymer of polystyrene-*block*-PMMA (PS-*b*-PMMA) films by a sequential carbocationic polymerization of styrene followed by radical polymerization of MMA, and have reported large changes in surface composition that were induced by solvent treatment. The tethered diblock copolymer underwent reversible changes in water contact angles as the film was treated with different solvents. Initially, the film exhibited a contact angle characteristic of PMMA (75°). However, the following treatment with methylcyclohexane (a better solvent for PS than for PMMA), resulted in the contact angle value increasing to a characteristic value for PS (98°). Finally, a subsequent treatment of the same sample with CH₂Cl₂ (a good solvent for PMMA and PS components) reverses this change.

A series of investigations of Zhao et al. on BC brushes of different structures [167–169] proved the mechanism of the phase segregation predicted by the theoretical investigations of Zhulina et al. [164,165]. For example, in the case of the tethered PS-*b*-PMMA and PS-*b*-PMA, CH₂Cl₂ is a good solvent for PS, PMMA, and PMA. When the sample is immersed in this solvent, the polymer chains are forced to stretch away from the interface to avoid contact with neighboring polymer chains. Removing the PS-*b*-PMMA brushes from CH₂Cl₂ condenses the polymer brushes and localizes PMMA blocks at the air interface. The T_g 's of PS and PMMA in the bulk state are both around 100 °C, and there is little difference in the surface free energies of PS and PMMA. Therefore, the PMMA blocks remain at the air interface, which is supported by contact angle measurements and XPS results. Fig. 37 illustrates this process.

If the sample was immersed in cyclohexane, PMMA chains migrated from the solvent interface and formed aggregates with neighboring PMMA blocks to avoid contact with solvent. Although PS blocks have a low mobility because of the covalent bond to the silicon wafer surface and to the PMMA block, they are miscible with cyclohexane and migrated to the solvent interface to form a shield around the PMMA aggregates. The phase segregation mechanism and the formation of corresponding surface morphologies in these brushes was proven with AFM experiments (Fig. 38).

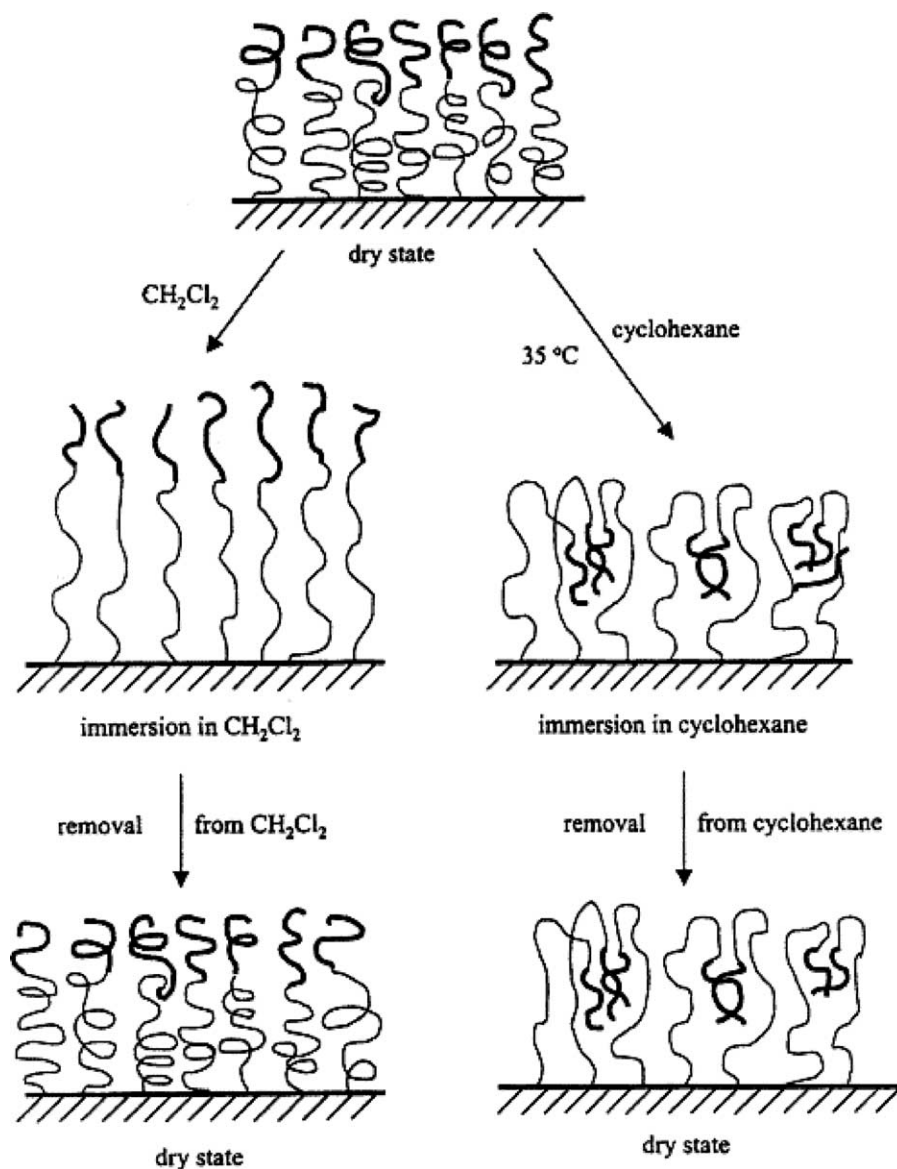


Fig. 37. Responses of tethered PS-*b*-PMMA brushes to different solvent treatments. Reprinted with permission from Ref. [167] (Macromolecules 2000;33:8813, Copyright (2000) American Chemical Society).

5.2. Synthesis of block-copolymer brushes

As mentioned above, Zhao and Brittain synthesized block-copolymer brushes by sequential carbocationic polymerization and ATRP [166]. They started with surface immobilization of functional trichlorosilane-1, which is an initiator for carbocationic polymerization (Fig. 39). The silane layer was deposited on the silicate

substrate. Treatment of the modified substrate-2 with styrene under carbocationic polymerization conditions led to the formation of tethered PS layer. This PS film was immersed in a solution of MMA and polymerized using typical ATRP conditions resulting in the block-copolymer brush.

In another recent development, Matyjaszewski et al. developed a two-step ATRP routine for

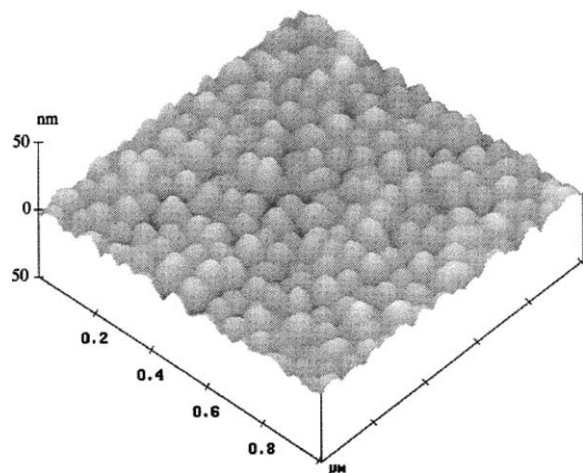


Fig. 38. AFM image of a PS-*b*-PMA brush after treatment with CH_2Cl_2 at room temperature. Reprinted with permission from Ref. [169] (Macromolecules 2000;33:8821, Copyright (2000) American Chemical Society).

the fabrication of BC brushes [170]. ATRP was successfully used for the fabrication of triblock copolymer brushes on planar surfaces [171] and BC brushes polymerized directly on the surface of nanoparticles [172].

Recently, the reversible addition fragmentation chain transfer techniques were applied for synthesis of BC brush PS-*b*-PDMA (*N,N*-dimethylacrylamide), PDMA-*b*-PMMA on silicon wafers, and poly(3-[2-(*N*-methylacrylamido)-ethyl]dimethyl ammonio]propane sulfonate-*b*-PDMA on gold surface [173,174]. These brushes displayed reversible surface properties upon treatment with block-selective solvents. Finally, several research groups suggested and developed living anionic polymerization for the synthesis of BC brushes [175,176].

All the above-mentioned synthetic methods are based on the approaches, which are very similar to that developed for synthesis of similar block-copolymers in solution polymerization. The main challenge of the synthesis of chemically grafted layer on solid substrates concern an appropriate choice to immobilize the initiator on the surface and, then, performing the process under conditions that does not allow any reactions, which can dramatically decrease the quality of the brushes.

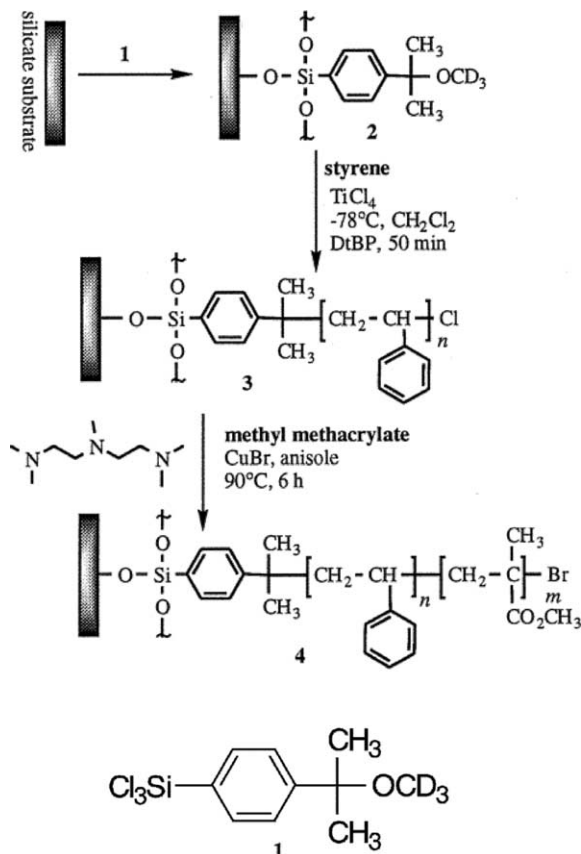


Fig. 39. The synthetic scheme for tethered PS-*b*-PMMA block copolymers. Reprinted with permission from Ref. [166] (J Am Chem Soc 1999;121:3557, Copyright (1999) American Chemical Society).

5.3. Y-shaped copolymer brushes

A specific case of BC brushes is represented by Y-shaped brushes when Y-shaped AB copolymers are grafted onto a flat surface. One 'arm' of the Y-shaped brush is an A homopolymer, and the other arm is an incompatible B chain, and the short 'stem' tethers the entire copolymer to the surface. This type of BC brush builds the bridge between end-tethered BC brushes and mixed binary polymer brushes (see below).

Zhulina and Balazs [177] have investigated the behavior of the Y-shaped brush in the melt, and in the presence of a solvent, with a sophisticated theoretical treatment. Specifically, they determined how solvent quality, grafting density, and chain length affects

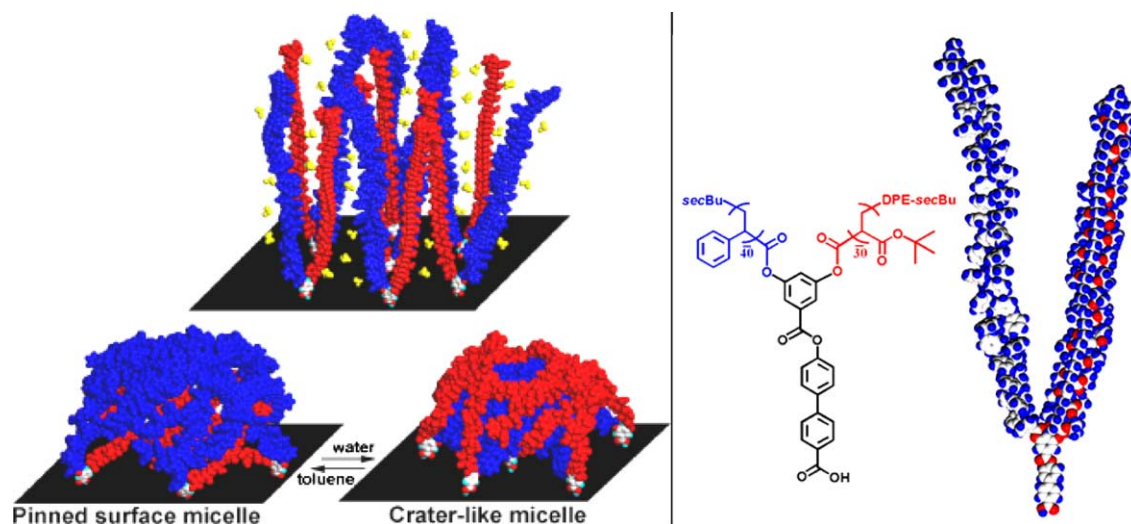


Fig. 40. Stimuli-responsive amphiphilic Y-shaped brush with dissimilar PS and PAA arms attached to a single grafting point (see right image for chemical formula and molecular model): switching of surface nanostructures upon treatment with selective solvents (left). Reprinted with permission from Ref. [178] (Langmuir 2003;19:7832, Copyright (2003) American Chemical Society).

the structure of the grafted layer and calculated a phase diagram that delineated the regions where the different structures appeared. Using scaling arguments, the authors have found that the brushes under poor solvent conditions segregated laterally forming an array of pinned micelles. Morphology of the micelles strongly depends on AB interaction, grafting density, and solvent quality. The phase diagram was calculated under poor non-selective solvent condition demonstrating the rich phase behavior of the system. They suggested that for realistic values of the incompatibility parameter, one expects two main regimes of microsegregation at sparse grafting: internally segregated, ‘polarized’ micelles or single-component, split micelles. By varying the solvent quality, one can initiate the reorganization of the system from one regime into another and, thus, affecting partial mixing or demixing of the A and B components in the system.

Recently, Julthongpipit et al. for the first time synthesized and studied Y-shaped mixed brushes with two highly incompatible PS and PAA arms [178]. It was observed that these arms are capable of local reversible rearrangements leading to a reversible surface structural reorganization in different solvents. AFM investigation found that the nanoscale surface structures of segregated

pinned micelles of grafted Y-shaped molecules, and the reversible structural reorganization was verified by molecular modeling of surface clustering (Fig. 40). The spatial constraints induced by a chemical junction of two dissimilar (hydrophobic and hydrophilic) polymer arms in such Y-shaped molecules and low-molecular weight of the arms lead to the formation of a novel type of segregated *crater-shaped* pinned micellar structures in chemically grafted brush layers at the scale of several nanometers (Fig. 41).

6. Mixed brushes

Two or more different polymers *randomly grafted* to the same substrate form a mixed polymer brush layer. Macrophase separation in the mixed brush with the formation of large separated phases is suppressed due to the chemical grafting. Under constrained conditions, to avoid non-favorable interactions the tethered polymers segregate microscopically forming nanoscopic domains scaled with the molecular dimensions (end-to-end distance R_e) of the grafted chains. The mechanism of the microphase separation and behavior of the mixed brushes are very similar to

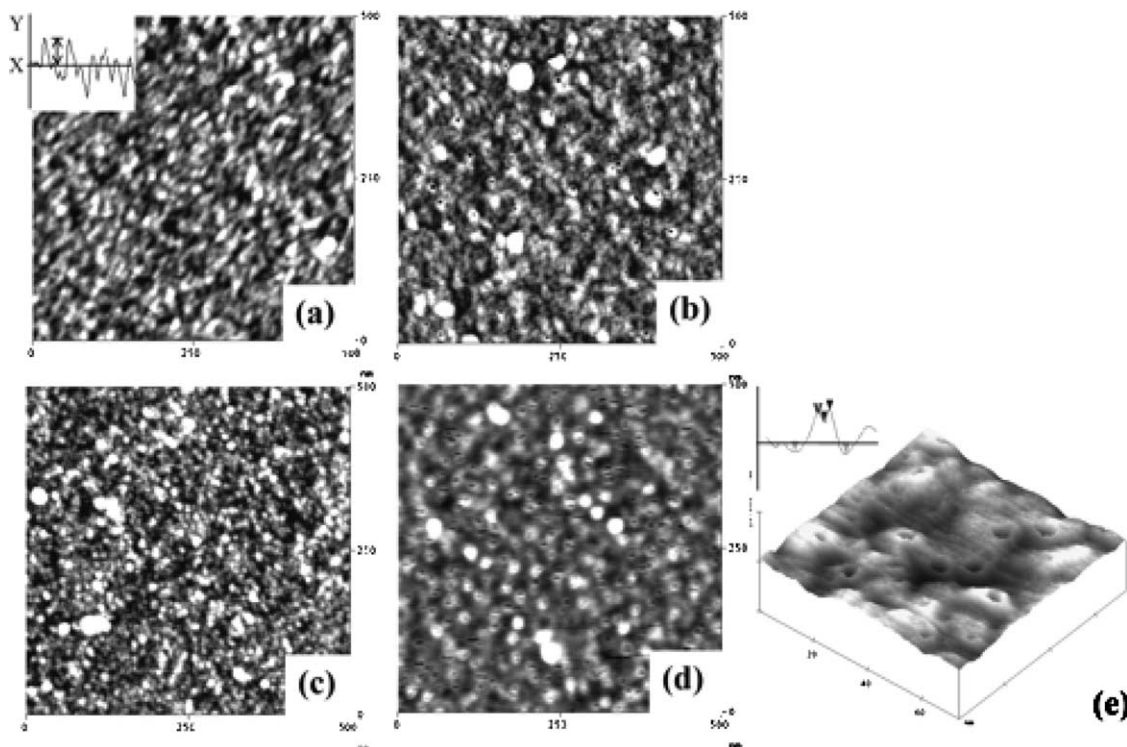


Fig. 41. AFM topographical images ($500 \times 500 \text{ nm}^2$) of the Y-shaped PS-PAA brushes treated with toluene (a, c) and water (b, d). Images a and b show the surface of the short-stem brush, whereas images c and d show the surface of long-stem brush. The vertical scale is 5 nm. (e) High-resolution three-dimensional topographical image ($70 \times 70 \times 10 \text{ nm}^3$) showing the craterlike surface structures in the long-stem brush treated with water. Representative cross-sections ($30 \times 3 \text{ nm}^2$) are shown. Reprinted with permission from Ref. [178] (Langmuir 2003;19:7832, Copyright (2003) American Chemical Society).

block-copolymer brushes. The main differences are caused by the polymer layer architecture.

First, by increasing the grafting density, the block-copolymer that is grafted onto a substrate would tend to localize on the bottom, therefore will tend to segregate into layers, a term known as lateral segregation. However, at moderate grafting densities, both brushes demonstrate the interplay between layered and lateral phases resulting in a rich phase behavior. Second, in block-copolymer brushes, both polymers always have the same grafting density and they are homogeneously grafted. However, in mixed brushes, the deviation from random grafting will cause strong fluctuations in the distance between grafting points and, consequently, it may increase the average size of lateral phases. On the other hand, the grafting densities of both polymers can be tuned independently in mixed brushes.

6.1. Mechanism of phase segregation in mixed brushes

The first theoretical analysis of the phase segregation in mixed binary brushes based on SCF theory was performed by Marko and Witten [179], then Zhulina and Balazs [177,180,181], and Müller [182]. Chemical difference of the unlike polymer molecules gives rise to a mixing free energy in the mixed brush implying that the system tends to phase separate. The separation is opposed by the loss of entropy and stretching energy of the grafted chains. The phase diagrams of the mixed brushes were calculated considering this principal for varying incompatibility (Flory–Huggins parameter), difference of the solvent quality, total grafting density, difference of chain length, and the relative grafting density of the dissimilar chains.

There are two limiting types of morphologies into which chains arrange themselves to avoid unfavorable interactions between different species (Fig. 42). The two tethered chains segregate perpendicular to the substrate forming the layered morphology of the polymer film (Fig. 42a). One component is enriched on the substrate, while other occupies the top of the brush. In this regime, the mixed brush retains laterally homogeneous. For the second limiting case, the two species self-assemble laterally into two-dimensional surface structures with a well-defined lateral length scale, which is of the order of the molecule extension (Fig. 42b). The lateral segregation in mixed brushes was predicted for the first time by Marco and Witten [179]. They have shown that mixed brushes undergo

the second-order phase transition from the disordered mixture to the ripple laterally segregated structure as the incompatibility between the two species increases. A further increase of the component incompatibility results in the transition to the layered phases. In this case, ripple morphology is formed, which is similar to the lamellar-like morphology in a free block-copolymer melt. In this case, self-assembled structures are periodic in two dimensions and have a brush-like structures perpendicular to the grafting surface.

Several numerical studies by Soga et al. [183] and Lai [184] demonstrated that the mixed brushes undergo true microphase separation under various solvent conditions. Soga et al. [183] found that the brush response to increasing immiscibility proceeds in two stages: an overall expansion stage and a microphase separation stage. In the expansion stage, where the immiscibility coefficient is relatively small, the brush relaxes by expanding outward in a laterally uniform fashion. At larger incompatibility, it is energetically more advantageous for the two polymer species to undergo microphase separation. Under these conditions, clear microphase separation in the lateral direction was indeed observed. They have also found clear evidence of the Z dependence in the microphase separation, by showing that the demixing of the two types of monomers is non-uniform along the Z direction. The phase behavior of the binary brush in a poor solvent reveals different conformations of tethered chains depending on the detailed path for microphase separation. In particular, either pure domains of the two different polymer types or mixed polymer domains were observed. For the case of symmetric binary mixtures, Lai [184] demonstrated that the chains of the same type clustered together laterally forming the ‘ripple state’ while the layered state was never observed. For asymmetric mixtures, layer structures, with the minority chains staying further away from the grafting plane, were observed.

Recently, SCF theory for the mixed brushes has been extended by Müller [182]. Using the calculation technique of Matsen and Schick [185], he has analyzed the phase stability of different lateral morphologies. The author found the phase transitions between the disordered phase to the different lateral morphologies, such as ripple, checkerboard, and hexagonal dimple phases. Thus, in addition to the ripple phase, the calculation showed dimple phases

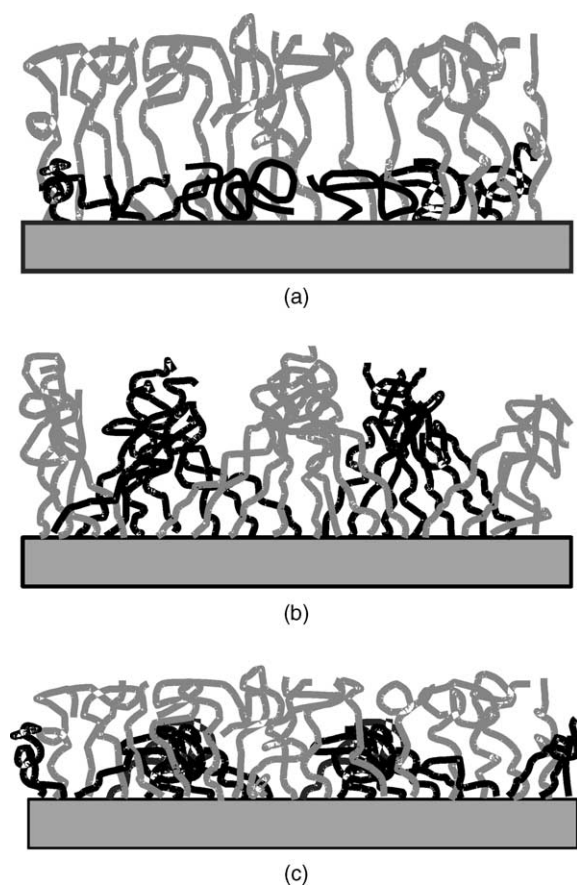


Fig. 42. Schematic illustration of possible morphologies of mixed brush irreversibly grafted to solid substrates (cross-section of the layer): layered disordered morphology in a solvent selective for gray chains (a), ripple morphology in a non-selective solvent (b), dimple morphology in a solvent poor for the black chains (c).

(Fig. 42c) in which one of the components segregates into clusters which arrange into a hexagonal or square (symmetrical dimple S) lattice (Fig. 43). The size of the lateral repeat units was about $1.9R_e$ for the ripple and symmetrical dimple phases and $2.2R_e$ for the hexagonal dimple phase.

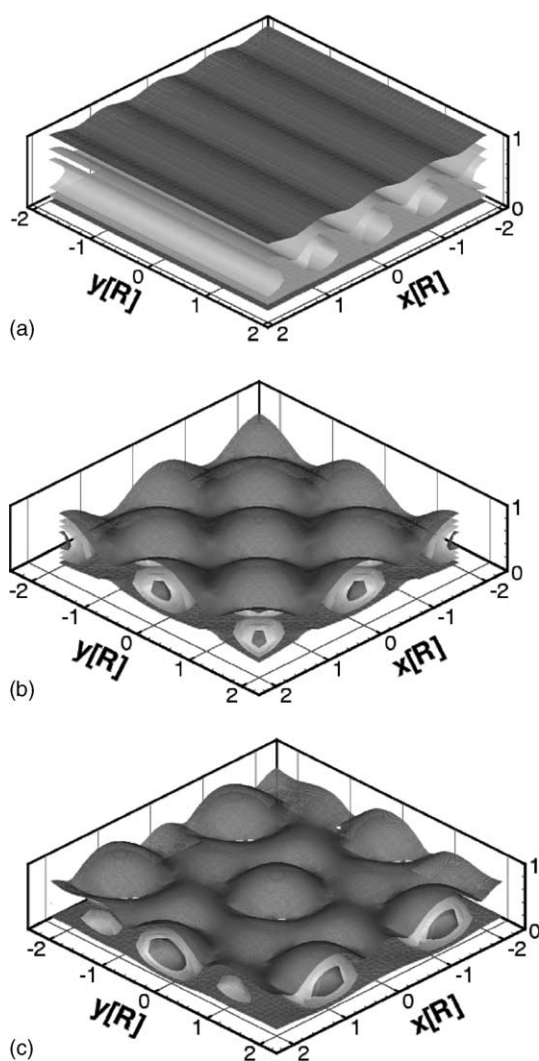


Fig. 43. Contours of the total density for the symmetrical mixed A/B brush. In the ripple phase (a) the species self-assemble into cylinders, every second cylinder is rich in the A-component. In the symmetrical dimple S phase (b) A and B clusters alternate on a quadratic lattice. In the dimple A phase (c) the A component clusters form a hexagonal lattice, while the B component is collapsed and fills the space between A-rich clusters. Reprinted with permission from Ref. [182] (Phys Rev 2002;E65:030802(R), Copyright (2002) American Physical Society).

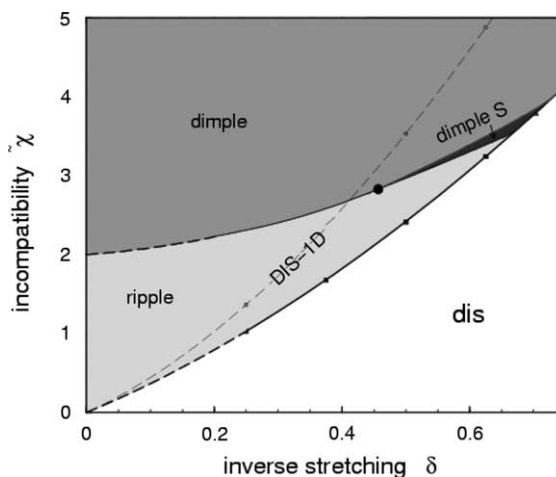


Fig. 44. Phase diagram for a symmetric mixed polymer brush. Under conditions of a moderate incompatibility ($\chi < 2$) the brush undergoes a transition between a disordered (dis) and a ripple phase. At higher incompatibility the disordered, the ripple and two dimple phases are stable. The transition between the disordered and the layered (1D) phases is indicated by a dashed line. Reprinted with permission from Ref. [182] (Phys Rev 2002;E65:030802(R), Copyright (2002) American Physical Society).

The phase diagram for a non-selective solvent calculated in this paper is presented in Fig. 44. As shown, increasing of incompatibility between polymers (χ) initiated a second-order phase transition from the disordered phase to the ripple phase. For strong stretching of the brush and strong incompatibility ($\chi > 2$), a transition from the ripple phase to a hexagonal dimple phase was observed. In the less stretching regime, the mixed brush transformed from ripple into symmetrical dimple S phase. At even larger incompatibility, the second transition into hexagonal dimple phase took place. The phase diagram for a moderate stretching as a function of the composition Φ is presented in Fig. 45. As was calculated, at high incompatibility or extreme composition asymmetry, the majority component formed a hexagonal array of clusters. Simultaneously, there was a pronounced perpendicular segregation: the majority component was enriched at the grafting surface, while the minority component was expelled from the surface. At lower incompatibilities or symmetrical composition, the minority component formed the hexagonal lattice of clusters. It was observed that the majority component acted like a very bad solvent for the minor component.

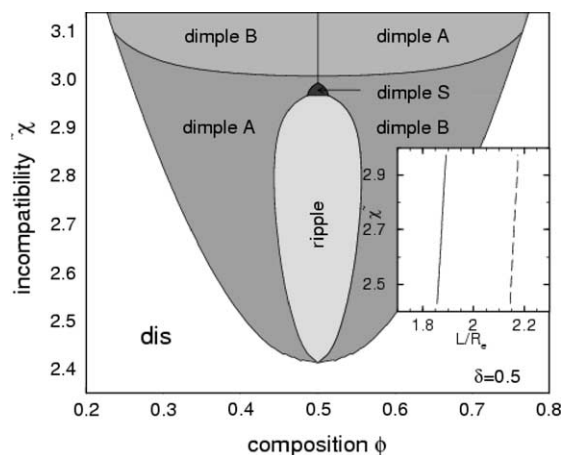


Fig. 45. Phase diagram for mixed brush at moderate stretching as a function of the composition. The inset displays the variation of the lateral unit cell size L along the dimple–ripple phase boundary. The solid line corresponds to the ripple phase, the dashed line corresponds to the dimple phase. Reprinted with permission from Ref. [182] (Phys Rev 2002;E65:030802(R), Copyright (2002) American Physical Society).

The first experimental observation of the lateral segregation in a mixed brush was reported for a PS/P2VP binary brush [186]. In good agreement with theory, the ripple and dimple phases were found in AFM study of the brush structure. However, no long-range order was observed for the laterally separated microphases. This disagreement with theory was explained by large fluctuations between grafting points [187] due to the synthetic procedure. The explanation seems to be quite reasonable, because the same situation (no long-range order) in conditions of a poor solvent was observed for homobrushes [188]. Later, the lateral segregation into either ripple and dimple microstructures was reported for mixed binary brushes of different compositions prepared with different synthetic approaches [189].

6.2. Responsive/switching/adaptive behavior

Sidorenko et al. [190] for the first time reported on the responsive behavior of the mixed PS/P2VP brush. XPS and contact angle experiments have shown that the surface composition of the brush and the surface wetting behavior switched upon exposure to different selective solvents. Recently, it was proven for various mixed binary brushes that they are capable of

switching their structure in response to solvent quality, temperature, pH, and confining wall signals [186,189,191].

The origin for the responsive behavior is in the reversible microphase segregation of the components in the mixed brush [182,191]. The phase diagram for symmetrical mixed brush as a function of the solvent selectivity ζ is presented in Fig. 46. In a non-selective solvent, $\zeta = 0$, a transition from laterally homogeneous phase to a ripple phase was observed upon increasing the incompatibility of A and B species. As solvent quality for the A-component ($\zeta < 0$) decreased, the ripple phase transforms to a dimple structure, where the A component segregated into clusters. Similarly, a dimple structure with a collapsed B polymer was observed when solvent was poor for the B component ($\zeta > 0$). At higher incompatibility (or poorer solvent quality), only dimple structures were stable.

On the other hand, the laterally averaged composition profiles demonstrated that in non-selective solvent both polymers are present on the brush top (Fig. 46, inset) forming alternating stripes. However, in selective solvent conditions the top of the brush is enriched by the favorable component. Contour plots of the composition at small and large solvent

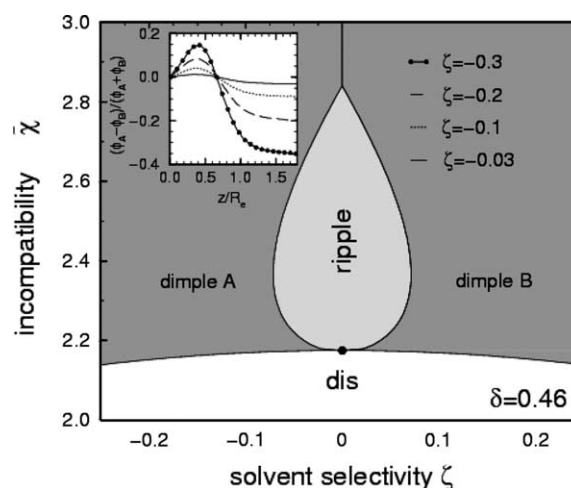


Fig. 46. Phase diagram of a mixed brush as calculated in SCF theory as a function of solvent selectivity. In addition to a laterally homogeneous phase (dis), the phase diagram comprises a ripple phase and dimples. The inset presents the laterally averaged composition profile at $\chi = 2.4$. Reprinted with permission from Ref. [191] (Phys Rev Lett 2002;88:035502, Copyright (2002) American Physical Society).

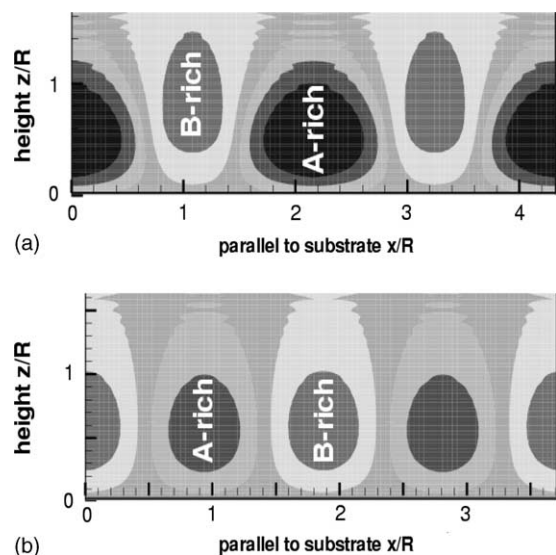


Fig. 47. Contour plot of the composition $(\Phi_A - \Phi_B)/(\Phi_A + \Phi_B)$ at $\chi = 2.4$. Each shading corresponds to a composition difference of 0.32: ripple phase $\zeta = -0.03$ (a), dimple A phase $\zeta = -0.3$ (b). Reprinted with permission from Ref. [191] (Phys Rev Lett 2002;88:035502, Copyright (2002) American Physical Society).

selectivity are presented in Fig. 47 indicating that as the solvent selectivity increases the B component segregates to the top of the brush, while the relative concentration of A is much higher at the substrate. Thus, the dimple morphology at larger ζ exhibits, in addition to the two-dimensional structure, a pronounced *vertical segregation*. That is the key property of the phase segregation responsible for the switching of mixed brushes.

Experimentally, this mechanism was proved by applying the combination of X-ray photoemission electron microscopy (XPEEM), contact angle, and AFM techniques for the binary mixed brush [191]. Component A was a random copolymer of styrene and 2,3,4,5,6-pentafluorostyrene (PSF), and component B was PMMA with grafting density of about 0.03 nm^{-2} for each component (4.5 nm average distance between grafted points) and molecular weight 500 and 800 kg/mol for polymers A and B, respectively. When the brush was exposed to the good non-selective solvent toluene, the contact angle of water in the mixed brush was 90° . This value was between the contact angles 110 and 78° on PSF and PMMA monobrushes, respectively. Thus, both components were simultaneously present on the top of the brush. The lateral

ripple phases were observed with AFM (Fig. 48a) and XPEEM (Fig. 49a). XPEEM probed the morphology with lateral resolution of 30 nm based on chemical contrast introduced by different X-ray adsorption of the fine structure spectra of C edges for PSF and PMMA. The XPEEM images taken at the energies corresponding to C edges for PSF (Fig. 49a) and PMMA (Fig. 49b) were inverse one to another and, thus, proved the lateral segregation of PSF and PMMA components.

After exposure to the selective solvent for PMMA (acetone), the morphology changed from ripple to the dimple structure and was observed with AFM imaging (Fig. 48b). The solvent was bad for PSF and this component formed small clusters embedded in the PMMA matrix. The contrast was reduced on the AFM phase image (Fig. 48b, right hand side) and XPEEM images (Fig. 49c and d), but the height contrast remained very pronounced. The contact angle of water on the top of the mixed brush was 81° , a value, which was close to the value 78° for pure PMMA. Thus, the lateral segregation is much reduced only at the top of the brush, and the component for which the solvent was good preferentially segregated to the top.

Lemieux et al. [192] have proven the mechanism of the structural reorganization by studying the nano-mechanical properties of the mixed binary brush prepared from two polymers with very different mechanical behavior, PSF and polymethylacrylate (PMA). This was demonstrated for the corresponding homobrushes [193]. The lateral and vertical reordering of the mixed brush was observed to be relatively quick (on the order of a few minutes), and reversibility between good and bad solvent states was observed for each component. Since PSF and PMA are mechanically dissimilar (glassy and rubbery, respectively) at room temperature, AFM phase imaging was used to verify the resulting laterally segregated structures. To determine the vertical segregation in addition to the lateral ordering, surface nanomechanical mapping was conducted to directly determine the surface distribution of the elastic modulus and adhesive forces (Fig. 50). Results show a clear bimodal response of the mechanically heterogeneous surface, with elastic modulus and adhesion contributions very different for the 'glassy state' and the 'rubbery state'. Furthermore, depth profiling of the elastic modulus was exploited to understand the vertical segregation in

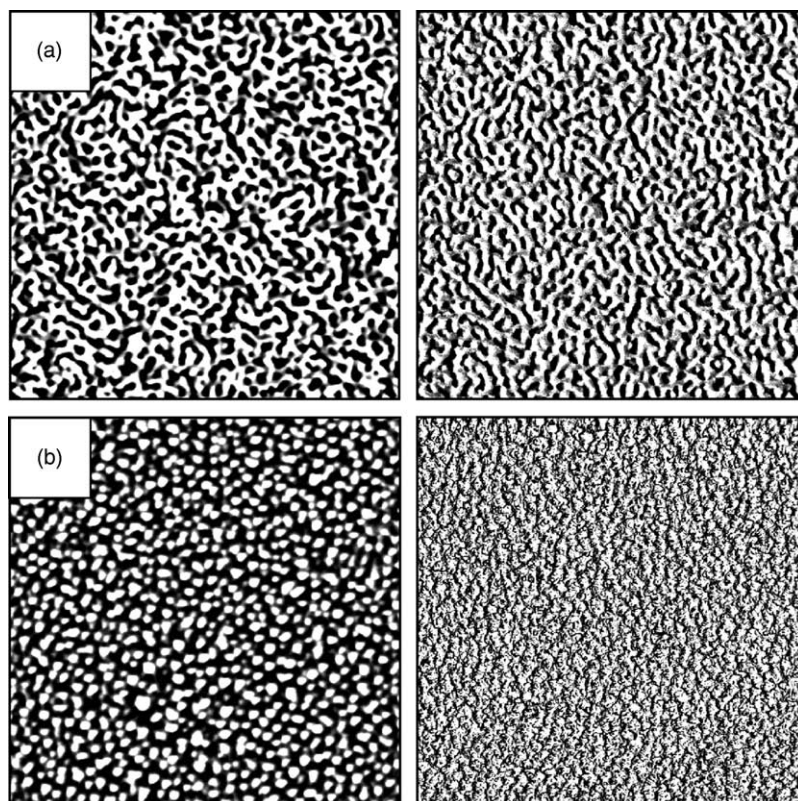


Fig. 48. AFM tapping mode images $5 \times 5 \mu\text{m}^2$ of the mixed brush after exposure to (a) the non-selective solvent (toluene) or (b) a good solvent for the B component (acetone). Topography-left, Phase-right. Reprinted with permission from Ref. [191] (Phys Rev Lett 2002;88:035502, Copyright (2002) American Physical Society).

the mixed brush and verify partial vertical segregation of dissimilar components. Results of this study quantified the elastic properties of PSF and PMA, demonstrated the dramatic mechanical contrast of the surface as a function of solvent conditions, and decisively revealed the lateral and layered modes of the phase segregation in a binary polymer brush.

Various external stimuli may be used to make a shift in the subtle interplay between lateral and vertical segregation. For example, temperature changes solvent quality and in this way it may change the structure of a mixed brush. The interplay between lateral and vertical segregation strongly depends on the solvent selectivity and, thus, the top layer composition and wetting behavior may be tuned by appropriate selection of solvent quality (Fig. 51). A special case constitutes polyelectrolyte mixed brushes. If one or more components in the mixed brush are polyelectrolytes, it makes the brush

sensitive to pH and salt signals. For instance, it was shown that PS/P2VP brush undergoes switching in acid aqueous solution ($\text{pH} < 3$) and demonstrates much more hydrophilic wetting behavior as compared with treatment in neutral water [186,189].

Unique and very special responsive behavior was found for the mixed brushes interacting with a confining wall [194]. This behavior constitutes an exciting combination of recognition and response. The phase diagram of the brush as a function of the component incompatibility and interaction with the confining wall (U_w) is presented in Fig. 52. The phase diagram contains a region of a laterally disordered phase in which the densities do not depend on the lateral coordinates. However, the preferred component segregates to the top of the brush. Increasing the selective interaction with the confining wall enhances the vertical segregation and leads to the enrichment of the preferred component on

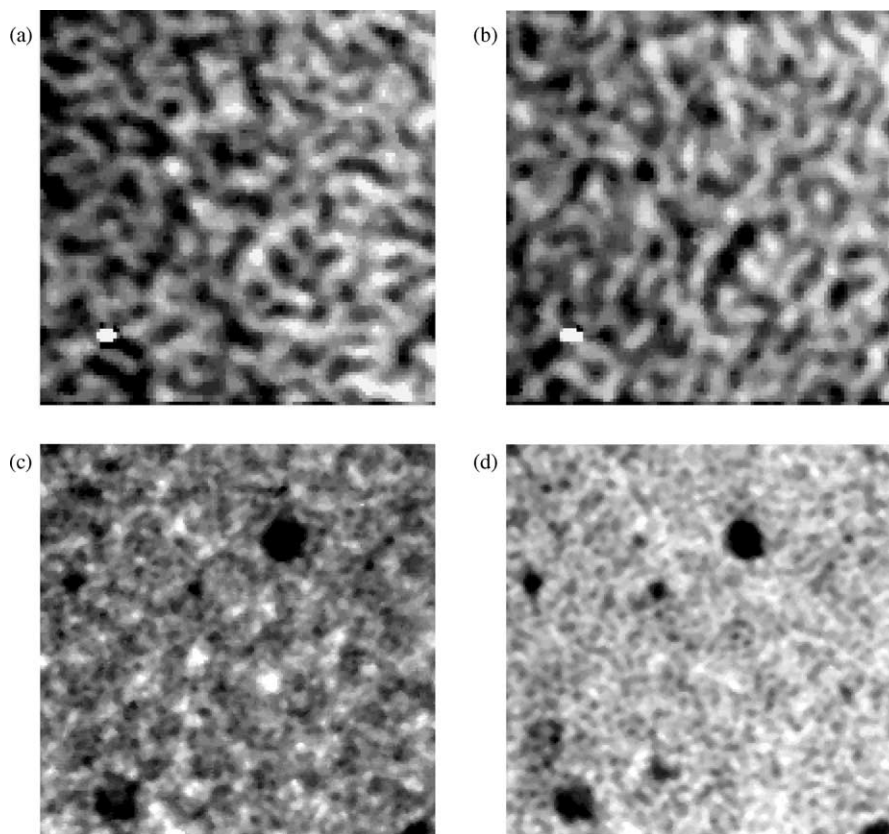


Fig. 49. XPEEM images $3 \times 3 \mu\text{m}^2$ after exposure to toluene showing contrast between C edges of both polymers at 286.1 (a) and 289.2 eV (b) for PSF and PMMA, respectively. (c) and (d) show the corresponding XPEEM images for the selective solvent (acetone). Reprinted with permission from Ref. [191] (Phys Rev Lett 2002;88:035502, Copyright (2002) American Physical Society).

the topmost layer. However, the coexistence of lateral and perpendicular segregation was found for the broad range of U_w and χ values. At a high-incompatibility level, an increase of the selective interaction causes the *first-order phase transition* from dimple B to dimple A structure. It is a remarkable example of the responsive behavior when even a small selective interaction effects the dramatic change of the brush morphology.

One of the most interesting properties of the mixed brushes concerns the mechanism of the interaction between two surfaces with grafted mixed brushes in selective solvent. This mechanism was analyzed theoretically by Singh et al. [180,181]. Using a two-dimensional self-consistent field theory, they investigated the interaction between two planar surfaces where each surface is grafted with the A and B homopolymer mixed brush. The chains are grafted at

low densities and the B polymers are chosen to be solvophobic. The theory analyzes the morphology of the layers and the energy of interaction as the layers are compressed at the varying solvent affinity of the A chains and the interaction between the A and B monomers. The energy of interaction versus distance profiles shows a wide region of attraction as the surfaces are brought together. This attractive interaction is due to the self-assembled structures that appear at low-grafting densities in poor solvents. The properties of the attraction can be tailored by change of the incompatibility parameter, solvent affinity and relative chain length. The analysis demonstrates a large diversity of possible interaction mechanisms between two mixed brushes in controlled environment. This behavior of mixed brush was not yet investigated experimentally. However, the theoretical predictions of Balazs et al. clearly demonstrate that

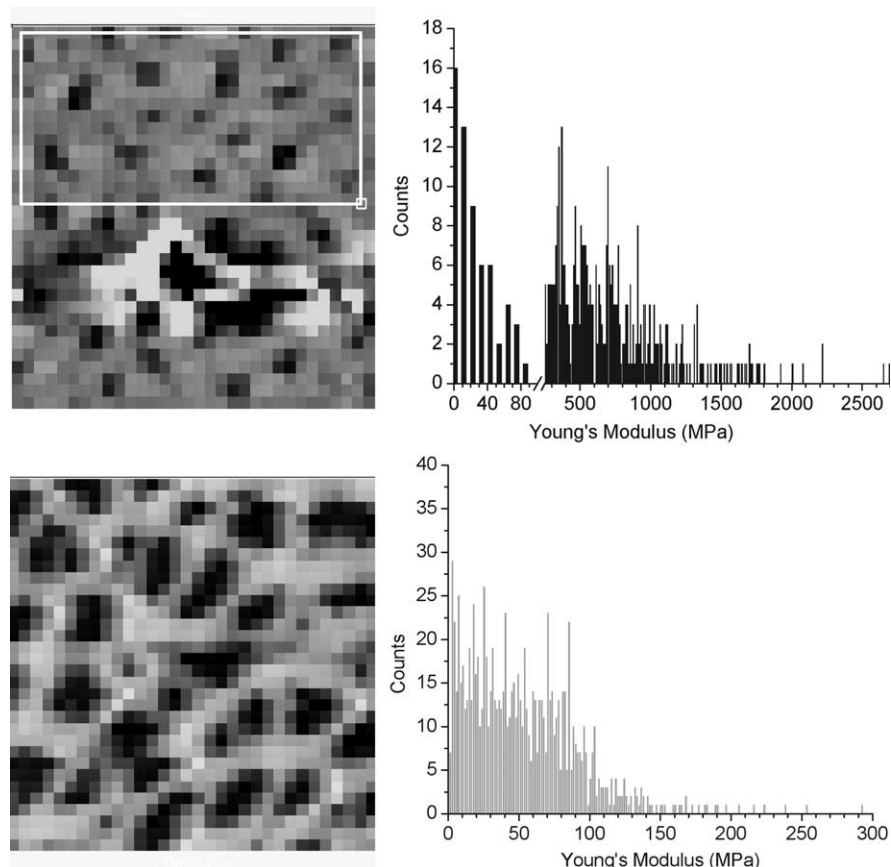


Fig. 50. Force volume topography distribution and corresponding elastic modulus histograms from the glassy (top row) and rubbery state (bottom row) using a soft tip. The histogram in the glassy state was derived from the region with the white frame to avoid incorrect data from the damaged surface region. The bimodal distribution is enhanced in the glassy state. Histograms are taken from 32×32 force volume scans at $1 \times 1 \mu\text{m}^2$.

the phase segregation in the mixed brush is a powerful tool to tune interaction for numerous very promising and important applications implying the regulation of interactions in colloidal and nanoparticle systems, protein and cell adsorption and adhesion [181].

6.3. Polyelectrolyte mixed brushes

The phase segregation mechanism is strongly modified by electrostatic interactions in the binary mixed brush constituting of two oppositely charged polyelectrolytes (Fig. 53). The first theoretical analysis of such a brush was performed by Shusharina and Linse [195,196]. Recently, the mixed brush from oppositely charged polyelectrolyte components,

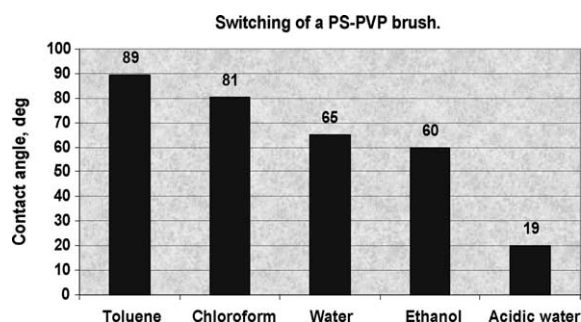


Fig. 51. Switching of the surface composition of the mixed PS/P2VP brush represented in terms of water contact angle measured upon exposure of the brush to different media.

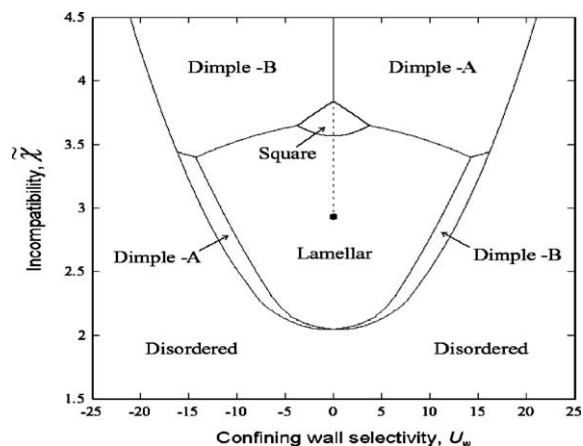


Fig. 52. Phase diagram of the binary mixed brush interacting with a confining wall. Reprinted with permission from Ref. [194] (Polym Preprints 2003;44(1):478, Copyright (2003) American Chemical Society).

P2VP and PAA, was synthesized and studied by Huobenov et al. [197]. The experiments demonstrated a very pronounced response of the mixed brush to pH signal when the wetting behavior, surface charge and the brush thickness were switched by change of pH. The isoelectric point of the mixed PAA/P2VP brush ($pK = 4.9$) was found to be in between the isoelectric points of the corresponding P2VP ($pK = 6.7$) and PAA ($pK = 3.2$) homopolymer brushes (Fig. 54). A shift of solvent pH away from the isoelectric point results in switching of the surface charge and the chemical composition of the topmost layer of the polymer film. The switching is effected by the preferential swelling of P2VP at $pH < 3.2$ and by the preferential swelling of PAA at $pH > 6.7$.

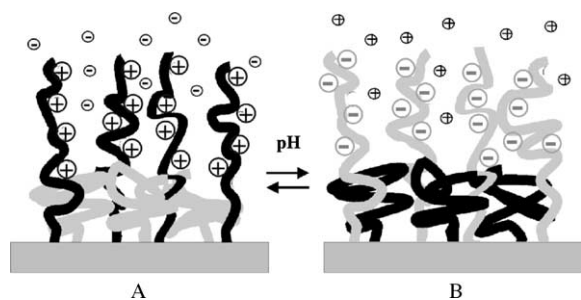


Fig. 53. Schematic representation of switching behavior of mixed PE brush upon change of pH: below isoelectric point (A), and above the isoelectric point (B). Reprinted with permission from Ref. [197] (Macromolecules 2003;36:5897, Copyright (2003) American Chemical Society).

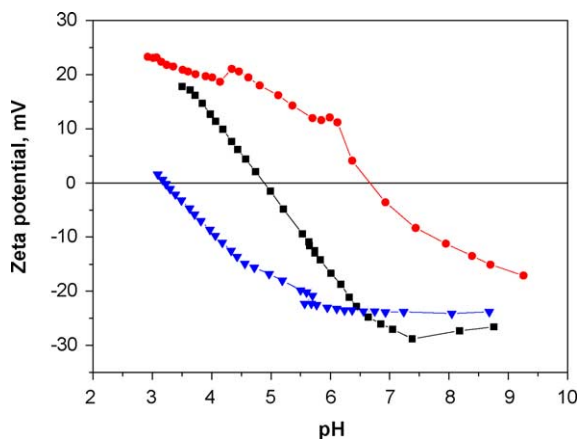


Fig. 54. Zeta-potential plotted as a function of pH for the PE brushes: homopolymer P2VP brush (circles), homopolymer PAA brush (triangles), mixed PAA/P2VP brush (squares) Reprinted with permission from Ref. [197] (Macromolecules 2003;36:5897, Copyright (2003) American Chemical Society).

In the vicinity of the isoelectric points, the uncharged and non-swollen surface polymer film is formed by the polyelectrolyte complexes. The pH-dependent swelling results in an U-shape variation of the brush thickness versus pH (Fig. 55). Changing the topmost layer composition only by a small pH adjustment strongly affects the wettability of the brush, showing a triple hydrophilic–hydrophobic–hydrophilic transition through an acidic–neutral–basic aqueous medium (Fig. 56).

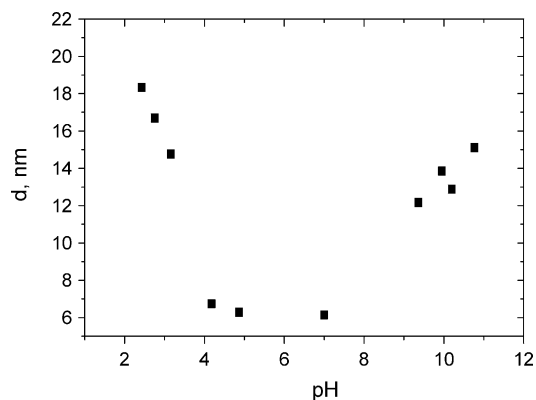


Fig. 55. Influence of pH on the thickness (d) of the swollen PAA–P2VP brush. The thickness in dry state was measured to be 6.4 nm. Reprinted with permission from Ref. [197] (Macromolecules 2003;36:5897, Copyright (2003) American Chemical Society).

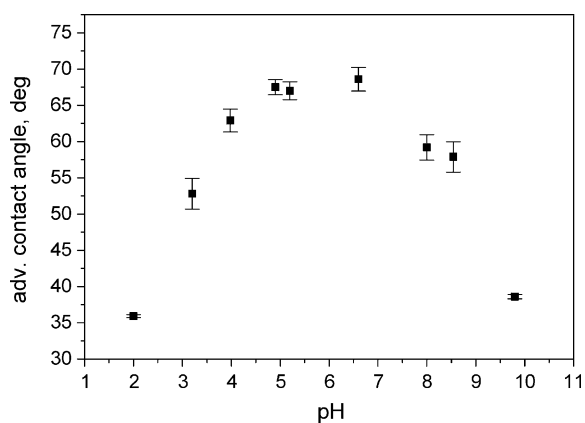


Fig. 56. Advancing contact angle as function of pH of aqueous bath for treatment of the PAA–P2VP mixed brush measured on dry brush (rapidly dried after exposure to the bath for 10 min). Reprinted with permission from Ref. [197] (Macromolecules 2003;36:5897, Copyright (2003) American Chemical Society).

6.4. Synthesis of mixed brushes

Two well established approaches are usually used to synthesize mixed brushes: the ‘grafting to’ and ‘grafting from’ methods. The grafting from method refers to the approach when the initiator is attached to the solid substrate and polymerization is done in situ on the solid surface.

For instance, Sidorenko et al. [190] applied the grafting from approach suggested by Tsubokawa et al. [198] to introduce the initiator on the solid substrate. First, ω -epoxysilane was used to introduce the epoxy functional groups on the surface of silicon wafers. Afterward, 4,4'-azobis(4-cyanopentanoic acid) (ACPA) was anchored using the catalytic reaction of the epoxy groups on the surface with carboxyl groups of the azoinitiator. Another approach [199] was based on the method of Boven et al. [200] where ω -aminosilane was grafted on the silicon wafer and then the chloride derivative of ACPA (Cl-ACPA) was bonded to the substrate. Both methods were found to have disadvantages. In the first case, the reaction of epoxy groups with ACPA was not very well controlled. Moreover, during chemisorption a large fraction of epoxy rings is lost by a catalytic effect of the surface and adsorbed water. In the second case, due to the high reactivity of amino groups, the chemisorption of ω -aminosilane was not a well-controlled process.

Recently, Usov et al. [201] suggested a solution to the problem when, in the first step, 3-glycidoxypropyl trimethoxysilane (GPS) was used to modify the surface of Si-wafers resulting in the chemisorbed layer with epoxide and hydroxyl groups. A high-density monolayer can be formed with epoxy groups that are available for further reaction as was discussed in detail [202,203]. In the second step, the epoxy-terminated silicon wafer was treated with ethylene diamine to transform epoxy groups into more reactive amino groups. Finally, Cl-ACPA was attached by the reaction with amino and hydroxyl groups on the surfaces in the presence of a catalytic amount of triethylamine to bind released HCl. The latter method demonstrated very good reproducibility. In another approach, Motornov et al. [204] modified polyamide substrates by oxygen and NH_3 low-pressure plasma to introduce hydroxyl and amine groups on the surface of the polymers. Then, Cl-ACPA azoinitiator was attached to the substrate with the same procedure as mentioned above.

A novel method to introduce epoxide and hydroxyl groups on the surface of different substrates by the deposition of a thin (1–2 nm) film of poly(glycidyl methacrylate) (PGMA) has been reported [205,206]. Upon heating, this film was cross-linked and formed a stable smooth polymer ‘carpet’ with high density of hydroxyl and epoxy group on the surface. This method is universal and can be applied for the modification of different substrates because the cross-linked PGMA forms the stable surface film due to the multi-point interactions between backbones and the surface even in the case of the participation of weak van der Waals attractive interactions between PGMA monomer units with the substrate.

Once the initiator was attached to the solid substrate, the two-step radical polymerization procedure was performed to graft two different polymers. The first polymerization step was done for the controlled periods of time to use only a fraction of the initiator. Afterwards, the obtained monobrush was thoroughly rinsed to remove the non-grafted polymer after first reaction. After this, the second grafting polymerization was performed using the residual initiator on the surface. With this procedure, the mixed binary polymer (and random copolymer) brushes were synthesized in the range of grafting

densities from 0.005 to 0.2 nm⁻² with molecular mass from 100,000 to 900,000 g/mol.

An alternative strategy for the synthesis of mixed polymer brushes consists of the combination of atom transfer radical polymerization (ATRP) and nitroxide-mediated radical polymerization (NMRP) [207,208]. These two controlled radical polymerization techniques depend upon different mechanisms and can be performed at very different temperatures. A nitroxide-terminated and ATRP-initiator terminated organotrichloro- or triethoxy silanes were used to graft the initiators to the solid substrate. Then, two-step polymerization procedure is applied to fabricate mixed brushes. ATRP of MMA was performed at 60–80 °C in the first step, and NMRP of styrene was carried out at 115–125 °C.

On the contrary, the “grafting to” method employs end-functionalized homopolymers or random copolymers, or functionalized block-copolymers with functional groups located near the point connecting different blocks. The polymers are grafted onto the substrate via chemical reaction of the polymer functional precursor groups and complimentary functional groups on the surface.

Grafting density of polymer brushes prepared with the grafting to method usually is relatively low because of the kinetic limitations resulting from the very low-diffusion rate of polymer chains penetrating through the already grafted brush layer. In the framework of this approach, the largest grafting density was obtained for the grafting from concentrated solutions or polymer melt when the concentration of the polymer segments with the functional groups have approached the maximum possible level [190]. Under these grafting conditions, two incompatible polymers segregate macroscopically when one of polymers preferentially occupies the substrate surface. One of the problems with this approach is that, upon heating, the film can dewet the substrate and the grating may result in a very inhomogeneous polymer film. Thus, the two-step grafting procedure avoiding the phase segregation during grafting was developed. For example, the mixed brush from carboxyl-terminated homopolymers PS and P2VP was prepared with the two-step procedure [189]. First, PS was grafted to the GPS modified silicon wafer. The PS film on the wafer surface was prepared by spin-coating. The grafting was performed upon heating

above the glass transition temperature for controlled periods of time to assure that the first grafting step was terminated at the grafting density less than the plateau value. Then, the non-grafted polymer was removed and the same procedure was repeated to graft carboxyl terminated P2VP. This routine was also successfully used to graft PS/PBA mixed brush and, after hydrolysis, PS/PAA binary brushes [209]. These mixed brushes showed clearly defined switchable behavior with dramatic rearrangements of surface morphology upon expose to different solvents. The authors observed that not only the surface wettability changed significantly, but also surface nanomechanical properties were altered by this reorganization (Fig. 57).

This procedure was the most successful if a less polar polymer (PS) was grafted first. It gives the additional

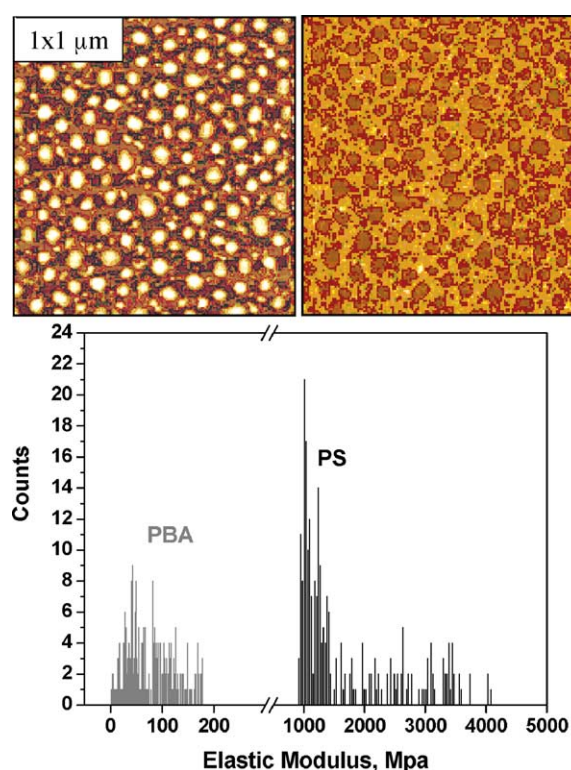


Fig. 57. AFM topographical images of PS/PBA mixed brush after treatment with toluene (left) and *n*-butanol (right) and corresponding surface histogram of surface elastic modulus for PS and PBA brushes (bottom). Reprinted with permission from Ref. [192] (Macromolecules 2003;36:7244, Copyright (2003) American Chemical Society).

driving force for the second polymer to penetrate the layer of the first grafted polymer. With the grafting to approach, the mixed brushes with the grafting densities ranging from 0.01 to 0.2 nm⁻² and molecular mass from 4 to 200 kg/mol were synthesized.

Recently, the synthesis of the PS/PBA mixed brush by the combination of the grafting to and grafting from methods was reported in Ref. [210]. The silicon wafer substrate was modified with the PGMA thin layer. Then, the sample was treated with a vapor of 2-bromoisobutyric acid, which can serve as an initiator for ATRP. In the first step, the carboxyl-terminated poly(*tert*-butylacrylate) was grafted to the silicon wafer via grafting to method involving the reaction of the end carboxyl groups with the epoxy groups of the PGMA modified substrate. In the second step, ATRP of styrene was carried out. The high-density brushes were synthesized with this approach. The advantage of this method refers to the possibility to substantially extend the range of polymers, which can be exploited for the fabrication of mixed brushes.

It is worth noting that mixed brushes prepared by different grafting methods show very similar surface behavior. The general tendency reveals that the higher grafting density results in the larger range of switching until the limiting state (e.g. complete switching between properties of polymers A and B) is approached. In other words, the increase of the grafting density within the practical experimental region of the grafting densities enhances the tendency of both vertical and lateral phase segregation of dissimilar components.

To approach the maximum switching range controlled by the phase transition mechanism, the mixed brush should be randomly grafted. However, the microphase segregation even before or during grafting tends to deviate from random grafting. Modifications of grafting procedures aim to overcome this inhomogeneous grafting affected by the microphase segregation.

Inhomogeneous grafting can be identified from experimental results by measuring the spatial distribution of segregated areas. Theory of mixed brushes predicts that the lateral size of segregated phases should be roughly twice larger than the end-to-end distance of polymer chains in θ -solvent (R_θ) [182]. The lateral size of domains observed in the experimental studies of the mixed brushes synthesized by

different methods is somewhat larger (often three times larger than R_θ). It is worth noting that monobrushes in poor solvent demonstrate the same result when the size of laterally segregated clusters is also larger than that predicted by theory. This effect is not fully understood. Recently, Müller et al. have demonstrated that even small fluctuations of averaged distance between grafting points in polymer brushes may result in a large increase of the lateral phases [187]. Such fluctuations can be introduced in the course of any grafting procedure. The fabrication of uniform, dense and homogeneously grafted mixed brushes is still a non-trivial challenge.

6.5. Methods to study responsive behavior

The main problem in studying the phase transition and responsive properties of the mixed brushes is effected by the high sensitivity of the polymer chain conformation to a change of environment. In addition to this, the simultaneous segregation on lateral and vertical directions makes the problem much more difficult. It implies that in situ study of the morphology of the brushes should be performed with methods sensitive to the brush profile with a lateral resolution at the molecular dimension scale. There are only a few methods known for investigations of thin polymer films, which can, in principal, fit the requirements: AFM with direct scanning under solvent (in a liquid cell) and neutron reflectivity from solid–liquid interfaces. Only two reports are published in the literature about the investigation of the mixed brush morphology performed with AFM in situ in a selective solvent and demonstrating reversible switching of surface morphology [211,212]. So far to our knowledge, there were no attempts at the present time to employ neutron reflectivity for the study of mixed brushes.

The task of studying mixed brushes is much easier if we make an assumption that the original brush morphology is frozen in the dry state due to the rapid evaporation of solvent. Indeed, during drying the brush undergoes collapse mainly in Z direction, so that the lateral morphology remains almost unchanged [186]. The latter statement can be applied for the case of non-selective poor solvent. If the solvent selectivity increases, a selective swelling may cause larger differences between the swollen and the dry layers.

The profile in the Z direction is strongly modified because of solvent evaporation, however, the relative distribution of the polymers A and B in the Z direction still reflects the layered or vertical segregation [169, 191]. Practically, it means that after the rapid evaporation of solvent one can measure the surface composition of the dry mixed brush with an appropriate lateral resolution and then reconstruct the morphology of the brush, which corresponds to that in solvent. That assumption is quite reasonable because the solvent evaporation time from of

the brush layer is much smaller than the characteristic time of polymer diffusing in a swollen state.

In fact, it is a commonly used practice to freeze the morphology of multicomponent polymer materials by rapid drying or cooling. There are also several experimental evidences supporting the assumption: (1) the morphology of the dry brush reversibly switches upon exposure to different solvents; (2) the morphologies after the treatment by a particular solvent are reproducible and can be repeated many times; (3) the AFM scanning under solvents proved

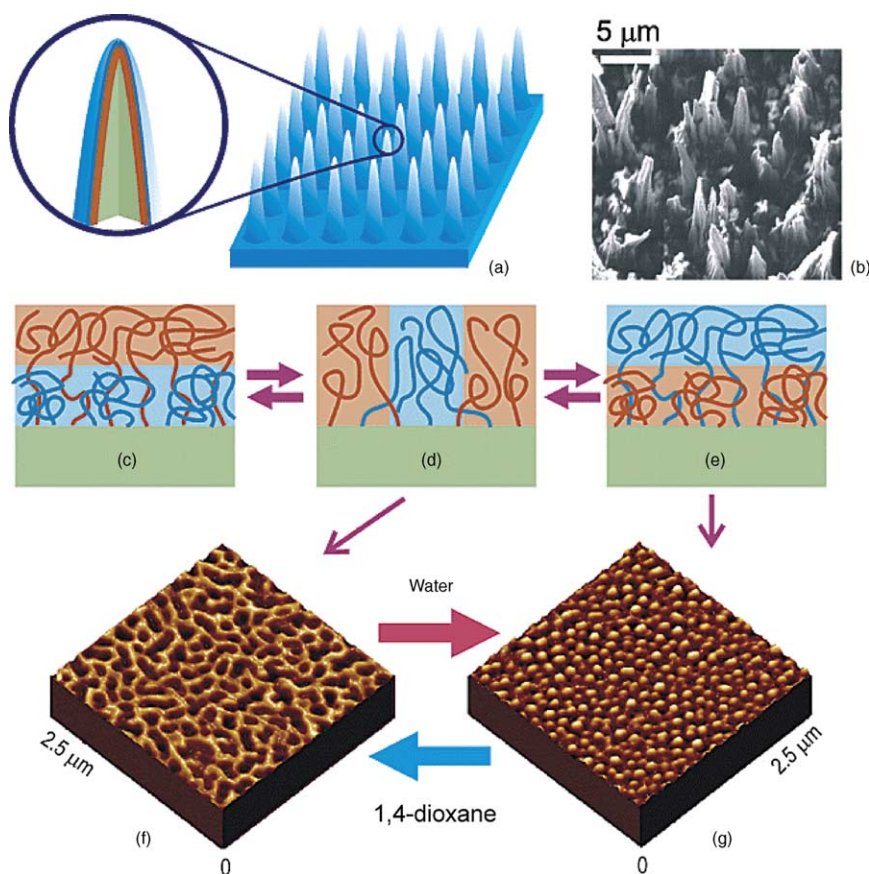


Fig. 58. Two-level structure of self-adaptive surfaces (SAS): schematic representation of needlelike surface morphology of the PTFE surface (first level) (a) and SEM image of the PTFE film after 600 s of plasma etching (b). Each needle is covered by a covalently grafted mixed brush that consists of hydrophobic and hydrophilic polymers (second level) depicted schematically in panels c–e. Its morphology results from an interplay between lateral and vertical phase segregation of the polymers, which switches the morphology and surface properties upon exposure to different solvents. In selective solvents, the preferred polymers preferentially occupies the top of the surface (c and e), while in non-selective solvents, both polymers are present in the top layer (d). The lower panels (f and g) show AFM images (model smooth substrate) of the different morphologies after exposure to different solvents. Reprinted with permission from Ref. [215] (*J Am Chem Soc* 2003;125:3896, Copyright (2003) American Chemical Society).

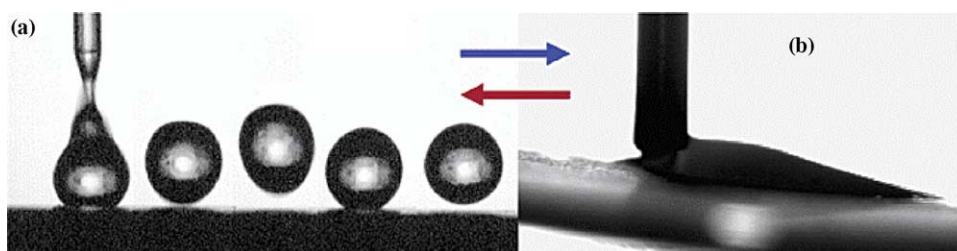


Fig. 59. Photograph of a water drop deposited onto the SAS: the stroboscopic image shows that a water drop jumps and rolls on the ultrahydrophobic surface obtained after exposure of the sample to toluene (a). In contrast, exposure to acidic water switches the sample to a hydrophilic state and the water drop spreads on the substrate (b). Reprinted with permission from Ref. [215] (J Am Chem Soc 2003;125:3896, Copyright (2003) American Chemical Society).

that the lateral structures in dry film and under solvent are similar, with the sizes in the swollen state somewhat larger, that is quite reasonable for a good solvent; (4) the surface structures observed for dry mixed brushes are in good agreement with theoretical predictions made for the brushes in solvent. Based on that, the brush morphology was studied for the dry mixed brushes of different compositions with AFM and XPEEM considered to be relevant to the actual morphology of brushes in different solvents [186,189,191,194,199,201,204–206,210,213]. The integral chemical composition of the top layer of the mixed brushes is evaluated with contact angle, nanomechanical probing, ζ -potential, and XPS methods. Adsorption of colloidal particles and adhesion testing were used to probe the surface composition of mixed brushes.

7. Prospective applications of responsive brushes

The field of synthesis and probing of mixed brushes is very new. The first publication on the synthesis and experimental study was published in 1999 [190] in earlier theoretical analysis and experiments, the promising unique behavior of the mixed brushes for tuning and regulating the interfacial interactions in colloidal and biological systems were highlighted [164,165,167,177,214]. As remarkable representative of the class of responsive materials, mixed brushes may find diverse applications for the development of smart materials, devices, sensors, imaging technologies, changeable biomaterials, molecular lubricants, means for regulations of stability and rheology in colloidal dispersions, separation,

and chromatography. Here, we present several recent examples.

Reversible tuning of the surface wetting behavior can be performed with mixed brushes in a broad range of contact angle values. Surface texture may strongly

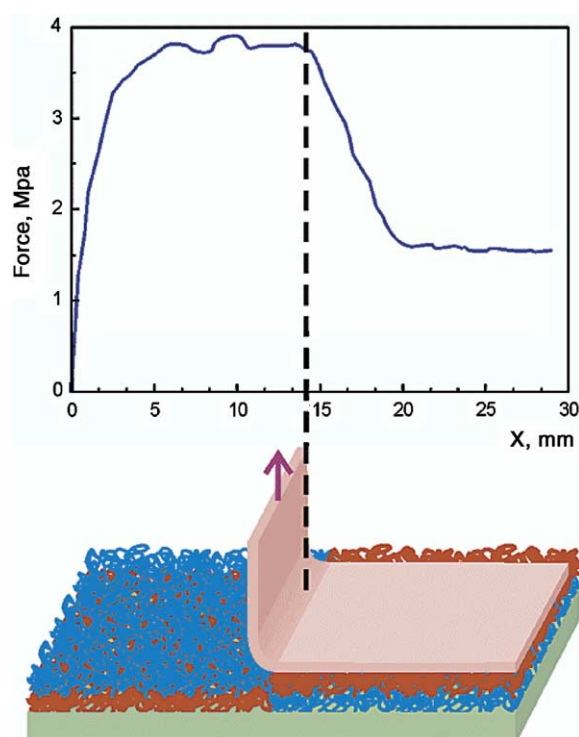


Fig. 60. Switching adhesion with SAS: the plot presents the change of the force applied to the Tesa band defoliated from SAS versus distance (X) from the starting point. The dashed line marks the border between ultrahydrophobic (orange) and hydrophilic (blue) areas on SAS. Reprinted with permission from Ref. [215] (J Am Chem Soc 2003;125:3896, Copyright (2003) American Chemical Society).

amplify the switching effect between wetting and non-wetting states. For example, the PS/P2VP mixed brush was grafted onto a pre-treated surface with needle like topography (Fig. 58) [215]. The size of the vertical needles was at a micron scale. If the brush was switched to the hydrophobic state upon exposure to toluene or heating above T_g , the layer has shown a unique ultrahydrophobic behavior (complete non-wetting) with the contact angle reaching values of 160° . The state corresponds to the Cassie regime, where the water drops hang on the peaks of needles so that the largest fraction of the drop surface is in contact with air. If the mixed brush was switched into the hydrophilic state upon exposure to acidic water, the surface became completely wetted due to the capillary forces in the pores formed by the needle-like structure (wicking regime). Thus, the surface can be either highly wettable or completely non-wettable with self-cleaning properties (Fig. 59). Motornov et al. have shown that this effect can be obtained with the mixed brush grafted on the surface of polyamide textile as well [204].

Adhesion is complimentary to wetting and, thus, can also be tuned by switching of the mixed brush so that the surface switches from sticky to non-sticky behavior. Hence, by employing that interplay between adhesive and repellent properties, one may develop a diverse range of smart tribological materials. For example, the surface of a material coated with

the mixed brush switched into the ultrahydrophobic state is not sticky (Fig. 60), possesses self-cleaning behavior, and is resistant to external contaminations brought by the adsorption of molecules, impurities or microbes. However, when the contact with the other surface wetted with a drop of water or heated up, it switches to a sticky state and can form a stronger joint [204]. The contrast in adhesive and sticky behavior can be used to regulate *adsorption*, which then can be used for analysis, imprinting, separation, etc.

The phase segregation in mixed brushes can be used for *patterning* of the surfaces on a nanoscale either by employing self-assembly into nanoscopic dimple or ripple structures or using a lithography approach to switch the brush locally. This approach can be realized with microcontact printing technology. For example, the PDMS stamp was used to create chemical patterning on the surface of PS/P2VP mixed brush [194]. Initially, a hydrophilized PDMS stamp (Fig. 61a), which is profiled with shallow square holes (30 nm deep and $5\ \mu\text{m}$ wide), was fabricated. Holes formed a square lattice with a spacing of $10\ \mu\text{m}$ and occupied approximately 20% of the stamp surface. Because the length scale of the surface pattern is much larger than the length scale of lateral microphase separation in the brush, which is of the order of the molecules' extension, holes played the role of homogeneous substrates. The local

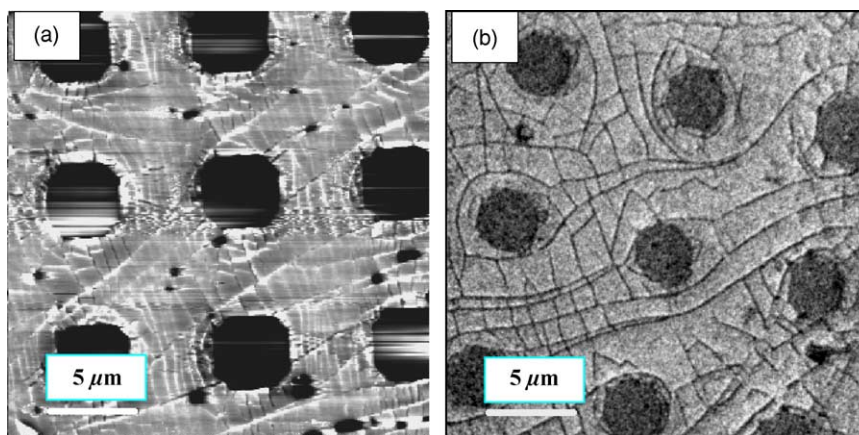


Fig. 61. (a) AFM image of the oxidized surface of PDMS stamp. (b) XPEEM-image of the binary brush after the contact with the oxidized stamp. Dark patterns correspond to higher fraction of PS, light patterns indicate the higher fraction of P2VP. The square-ordered holes on the surface of the stamp are transferred onto the PS-rich pattern of the brush (chemical contrast). Cracks on the oxidized surface of the stamp are also imprinted to the brush's top composition. Reprinted with permission from Ref. [194] (Polym Preprints 2003;44(1):478, Copyright (2003) American Chemical Society).

chemical composition of the top layer was measured by XPEEM with an example of the XPEEM image of the patterned brush surface presented in Fig. 61b.

As was observed, the P2VP fraction of the surface area corresponding to the holes on the stamp was lower (darker shading) than in the rest of the patterned surface area. The calculated ratio between the P2VP fraction in white and dark regions was 0.62. Thus, the hydrophilized stamp attracted P2VP and repelled PS. In the areas of stronger contact between stamp and brush, P2VP was enriched at the surface, while PS dominated the surface composition in the areas of weaker contact (holes). The network of ‘cracks’ seen

on the XPEEM image of the brush (Fig. 61b) reproduced the similar network on the stamp’s surface. The crack width was about 100 nm that gives an estimate for the resolution of the pattern transfer.

The particular physical state and surface morphology of the mixed brush can be controlled and fixed via chemical cross-linking from UV- or X-ray irradiation. Thus, by using photolithography, one can record the information on the mixed brush film. In illuminated areas, the brush loses the switching behavior and it is fixed either in a hydrophilic or hydrophobic state, while in non-illuminated areas, the brush retains the ability to switch (Fig. 62). The recorded information

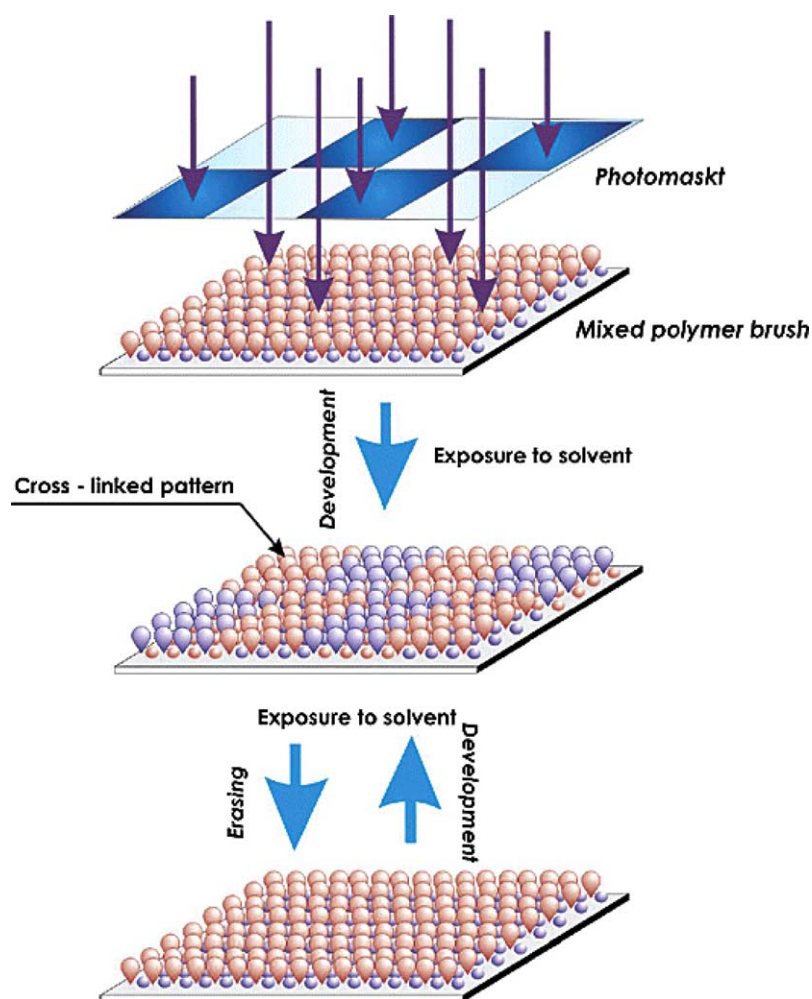


Fig. 62. Scheme of photolithography on mixed polymer brushes. Reprinted with permission from Ref. [216] (J Am Chem Soc 2003;25:8302, Copyright (2003) American Chemical Society).

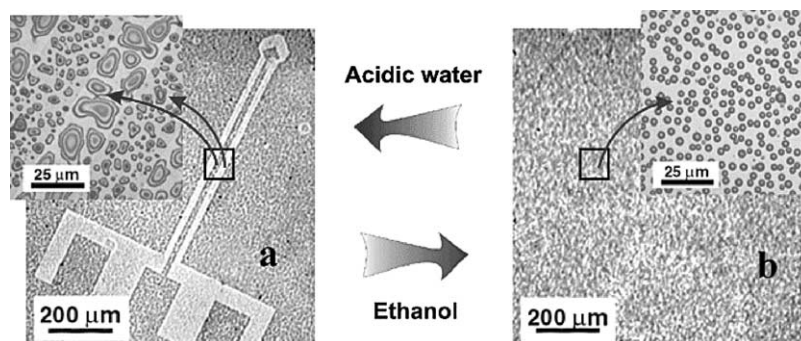


Fig. 63. Adsorption of water drops (optical microscopy) on the polymer brush with developed (a) and erased (b) patterns. Insets demonstrate zoomed in details: hydrophilic and hydrophobic regions are artificially colored in blue and red, respectively. Reprinted with permission from Ref. [216] (J Am Chem Soc 2003;25:8302, Copyright (2003) American Chemical Society).

can be reversibly developed or erased upon the exposure of the brush to different environments when the contrast between illuminated and non-illuminated areas appears or disappears depending on solvent quality. This new type of environment responsive lithography [216] could be used for imaging technologies (Fig. 63), the fabrication of the smart sensors—directly visualizing the result of the test.

For example, if the surface pattern is visualized at a particular pH, the smart surface can directly display the value of pH as an image (Fig. 64), or act as switchable channels for microfluidic technologies (Fig. 65). This example demonstrates the fabrication of switchable microchannels causing a valve to reversibly open or close the channel upon external stimuli. In this design, the mixed brush (1) was grafted

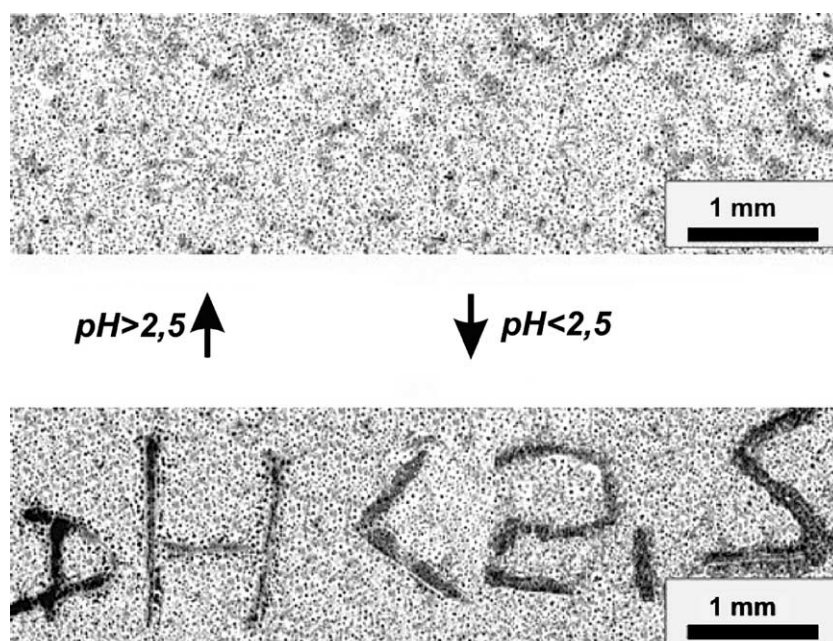


Fig. 64. Example of a smart sensor from the mixed brush grafted to Si wafer which displays the result of the analysis of acidic aqueous solution: the wafer was exposed to neutral water (top) and to water with pH 2.3 (bottom). The image appeared upon exposure to water vapor *only* if the sample had been treated with acidic water solution of pH < 2.5. Reprinted with permission from Ref. [216] (J Am Chem Soc 2003;25:8302, Copyright (2003) American Chemical Society).

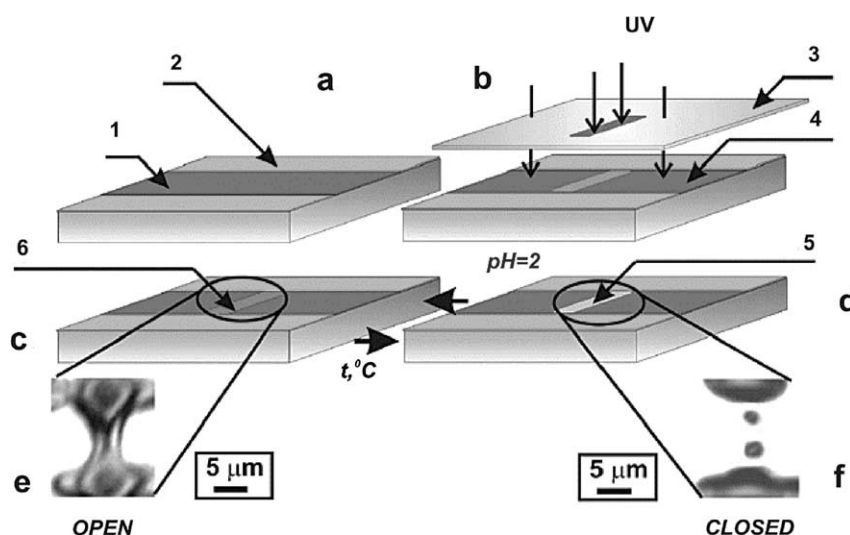


Fig. 65. Fabrication of a switchable channel employing environment responsive lithography (for explanation see the text of the paper). The images e and f show open and closed states of the switchable channel, respectively, as they appear in optical microscopy. Reprinted with permission from Ref. [216] (J Am Chem Soc 2003;25:8302, Copyright (2003) American Chemical Society).

between two hydrophilic channels (2) on a solid substrate (Fig. 65a). The switchable channel was fabricated (Fig. 65b) by photo-cross-linking of the brush through the photomask (3) resulting in the irradiated areas (4) losing the switching properties and serving as walls of the microchannel. The bottom of the microchannel (6) is hydrophilic upon exposure to acidic solution and, thus, water can flow through the microchannel (Fig. 65c and e). Upon heating above 80 °C or by changing the pH (Fig. 65d and f), the bottom surface of the channel switches into a hydrophobic state, resulting in closing the channel (5).

8. Conclusions

In conclusion, we have briefly presented a series of recent results related to reversible changes in structural organization and surface morphology of a variety of polymeric systems composed of block copolymers, random copolymers, polymer mixtures, mixed polyelectrolytes, and grafted polymer brushes of different types. We demonstrated how the reorganization of structural organization results in dramatic changes of surface properties of these materials, thus, creating switchable materials with controlled

surface wettability, mechanical response, heterogeneity, charge, adhesion, and chemical functionality. These properties can be controlled by direct manipulation of the chemical structure of a polymer nature, structural and morphological factors, and external stimuli and, therefore, these surfaces can be used as both sensing elements and active element responsive to environmental conditions.

Acknowledgements

The research of the authors in the field of polymer surfaces is supported by the National Science Foundation CMS-0099868 and DMR-0308982 Grants, ERC Program of National Science Foundation under Award Number EEC-9731680, and Grant M01-CL03 from Department of Commerce through National Textile Center. We also acknowledge the support of the Institute for Polymer Research Dresden (Germany), NSF Center for Advanced Engineering Fibers and Films (Clemson University), and the Center for Advanced Materials Processing (Clarkson University). Authors thank to M.C. Lemieux for reading the manuscript and making important suggestions.

References

- [1] Tsukruk VV. Assembly of supramolecular polymers in ultrathin films. *Prog Polym Sci* 1997;22:247.
- [2] Bhushan B, editor. *Tribology issues and opportunities in MEMS*. Dordrecht: Kluwer Academic Publishers; 1998.
- [3] Bhushan B, editor. *Micro/nanotribology and its applications*. Dordrecht: Kluwer Academic Publishers; 1997.
- [4] Pokius AV. *Adhesion and adhesion technology*. Munich: Hansen Gardner; 2002.
- [5] Graighead HG. Nanoelectromechanical systems. *Science* 2000;290:1532.
- [6] Tsukruk VV. Molecular lubricants and glues for micro- and nanodevices. *Adv Mater* 2001;13:95.
- [7] Lafuma A, Quere D. Superhydrophobic states. *Nat Mater* 2003;2:457.
- [8] Russel TP. Surface-responsive materials. *Science* 2002;297:964.
- [9] Creton C. Pressure-sensitive adhesives: an introductory course. *MRS Bull* 2003;28:434.
- [10] Tsukruk VV, Wahl K, editors. *Microstructure and microtribology of polymer surfaces*, vol. 741. Washington: ACS Symposium Series; 2000.
- [11] Tsukruk VV, Bliznyuk VN. Adhesive and friction forces between chemically modified silicon and silicon nitride surfaces. *Langmuir* 1998;14:446.
- [12] Sanchez I, editor. *Physics of polymer surfaces and interfaces*. New York: Manning; 1993.
- [13] Birshtein TM, Amoskov VM. Homeotropic and planar structures in liquid-crystalline polymer brushes. *Comput Theor Polym Sci* 2000;10(1/2):159.
- [14] Bliznyuk VN, Everson MP, Tsukruk VV. Nanotribological properties of organic boundary lubricants: Langmuir films versus self-assembled monolayers. *J Tribol* 1998;120:489.
- [15] Lukaš J, Sodhi RNS, Sefton MV. An XPS study of the surface reorientation of statistical methacrylate copolymers. *J Colloid Interface Sci* 1995;174:421.
- [16] Jalbert C, Koberstein JT, Hariharan A, Kumar SK. End group effects on surface properties of polymers: semiempirical calculations and comparison to experimental surface tensions for α,ω -functional poly(dimethylsiloxanes). *Macromolecules* 1997;30:4481.
- [17] Theodorou DN. Microscopic structure and thermodynamic properties of bulk copolymers and surface-active polymers at interfaces. 1. Theory. *Macromolecules* 1988;21:1411.
- [18] Theodorou DN. Microscopic structure and thermodynamic properties of bulk copolymers and surface-active polymers at interfaces. 2. Results for some representative chain architectures. *Macromolecules* 1988;21:1422.
- [19] Holly FJ, Refojo MF. Wettability of hydrogels. I. Poly(2-hydroxyethyl methacrylate). *J Biomed Mater Res* 1975;9:315.
- [20] Ruckenstein E, Lee SH. Estimation of the equilibrium surface free-energy components of restructuring solid-surfaces. *J Colloid Interface Sci* 1987;120:153.
- [21] Lee SH, Ruckenstein E. Surface restructuring of polymers. *J Colloid Interface Sci* 1987;120:529.
- [22] Lee SH, Ruckenstein E. Stability of polymeric surfaces subjected to ultraviolet-irradiation. *J Colloid Interface Sci* 1987;117:172.
- [23] Mason R, Jalbert CA, O'Rourke Muisener PAV, Koberstein JT, Elman JF, Long TE, Gunesin BZ. Surface energy and surface composition of end-fluorinated polystyrene. *Adv Colloid Interface* 2001;94:1.
- [24] Jalbert CJ, Koberstein JT, Balaji R, Bhatia Q, Salvati Jr. L, Yilgor I. Surface depletion of end groups in amine-terminated poly(dimethylsiloxane). *Macromolecules* 1994;27:2409.
- [25] Jerome R, Teyssie P, Pireaux JJ, Verbist J. Surface-analysis of polymers end-capped with metal carboxylates using X-ray photoelectron-spectroscopy. *Appl Surf Sci* 1986;27:93.
- [26] Elman JF, Johns BD, Long TE, Koberstein JT. A neutron reflectivity investigation of surface and interface segregation of polymer functional end groups. *Macromolecules* 1994;27:5341.
- [27] Jalbert C, Koberstein JT, Hariharan A, Kumar SK. End group effects on surface properties of polymers: semiempirical calculations and comparison to experimental surface tensions for α,ω -functional poly(dimethylsiloxanes). *Macromolecules* 1997;30:4481.
- [28] Hunt Jr. MO, Belu AM, Linton RW, DeSimone JM. End-functionalized polymers. 1. Synthesis and characterization of perfluoroalkyl-terminated polymers via chlorosilane derivatives. *Macromolecules* 1993;26:4854.
- [29] Wong D, Jalbert C, Koberstein JT. Surface reorganization kinetics of a model end-functionalized polymer system. *Polym Preprints* 1998;39(2):901.
- [30] O'Rourke-Muisener PA, Koberstein JT, Kumar S. Optimal chain architectures for the molecular design of functional polymer surfaces. *Macromolecules* 2003;36:771.
- [31] Höpken J, Möller M. Low-surface-energy polystyrene. *Macromolecules* 1992;25:1461.
- [32] Falsafi A, Tirrell M, Pocius AV. Compositional effects on the adhesion of acrylic pressure sensitive adhesives. *Langmuir* 2000;16:1816.
- [33] Johnson KL. *Contact mechanics*. Cambridge: Cambridge University Press; 1985.
- [34] Aymonier A, Papon E. Designing soft reactive adhesives by controlling polymer chemistry. *MRS Bull* 2003;28:424.
- [35] Paul CW. Hot-melt adhesives. *MRS Bull* 2003;28:440.
- [36] Murray CT, Rudman RL, Sabade MB, Pocius AV. Conductive adhesives for electronic assemblies. *MRS Bull* 2003;28:449.
- [37] Vaidya A, Chaudhury MK. Synthesis and surface properties of environmentally responsive segmented polyurethanes. *J Colloid Interface Sci* 2002;249:235.
- [38] Takahara A, Okkema AZ, Cooper SL, Coury A. Effect of surface hydrophilicity on ex vivo blood compatibility of segmented polyurethanes. *Biomaterials* 1991;12:324.
- [39] Okkema AZ, Fabrizio DJ, Grasel TG, Cooper SL, Zdrahala RJ. Bulk, surface and blood-contacting properties of polyether polyurethanes modified with polydimethylsiloxane macroglycols. *Biomaterials* 1989;10:23.

- [40] Deng Zh, Schreiber HP. Orientation phenomena at polyurethane surfaces. *J Adhesion* 1991;36:71.
- [41] Pike JK, Ho T, Wynne K. Water-induced surface rearrangements of poly(dimethylsiloxane-urea-urethane) segmented block copolymers. *Chem Mater* 1996;8:856.
- [42] Takahara A, Jo N, Kajiyama T. Surface molecular mobility and platelet reactivity of segmented poly(etherurethaneureas) with hydrophilic and hydrophobic soft segment components. *J Biomater Sci, Polym Ed* 1989;1:17.
- [43] Takahara A, Takahashi K, Kajiyama T. Effect of polyurethane surface-chemistry on its lipid sorption behavior. *J Biomater Sci, Polym Ed* 1993;5:183.
- [44] Zhang D, Ward RS, Shen YR, Somorjai GA. Environment-induced surface structural changes of a polymer: an in situ IR + visible sum-frequency spectroscopic study. *J Phys Chem B* 1997;101:9060.
- [45] Schmidt RL, Gardella JA, Magill JH, Salvati L, Chin RL. Study of surface composition and morphology of block copolymers of bisphenol A polycarbonate and poly(dimethylsiloxane) by X-ray photoelectron spectroscopy and ion scattering spectroscopy. *Macromolecules* 1985;18:2675.
- [46] Russell TP, Menelle A, Anastasiadis SH, Satija SK, Majkrzak CF. Unconventional morphologies of symmetric, diblock copolymers due to film thickness constraints. *Macromolecules* 1991;24:6263.
- [47] Iyengar DR, Perutz SM, Dai C-A, Ober CK, Kramer EJ. Surface segregation studies of fluorine-containing diblock copolymers. *Macromolecules* 1996;29:1229.
- [48] Huang E, Russell TP, Harrison C, Chaikin PM, Register RA, Hawker CJ, Mays J. Using surface active random copolymers to control the domain orientation in diblock copolymer thin films. *Macromolecules* 1998;31:7641.
- [49] Mansky P, Russell TP, Hawker CJ, Pitsikalis M, Mays J. Ordered diblock copolymer films on random copolymer brushes. *Macromolecules* 1997;30:6810.
- [50] Kellogg GJ, Walton DG, Mayes AM, Lambooy P, Russell TP, Gallagher PD, Satija SK. Observed surface energy effects in confined diblock copolymers. *Phys Rev Lett* 1996;76:2503.
- [51] Konrad M, Knoll A, Krausch G, Magerle R. Volume imaging of an ultrathin SBS triblock copolymer film. *Macromolecules* 2000;33:5518.
- [52] Toselli M, Messori M, Bongiovanni R, Malucelli G, Priola A, Pilati F, Tonelli C. Poly(epsilon-caprolactone)-poly(fluoroalkylene oxide)-poly(epsilon-caprolactone) block copolymers. 2. Thermal and surface properties. *Polymer* 2001;42:1771.
- [53] Lewis KB, Ratner BD. Observation of surface rearrangement of polymers using ESCA. *J Colloid Interface Sci* 1993;159:77.
- [54] Senshu K, Yamashita Sh, Mori H, Ito M, Hirao A, Nakahama S. Time-resolved surface rearrangements of poly(2-hydroxyethyl methacrylate-*block*-isoprene) in response to environmental changes. *Langmuir* 1999;15:1754.
- [55] Mori H, Hirao A, Nakahama S, Senshu K. Synthesis and surface characterization of hydrophilic-hydrophobic block copolymers containing poly(2,3-dihydroxypropyl methacrylate). *Macromolecules* 1994;27:4093.
- [56] Castner DG, Ratner BD, Grainger DW, Kim SW, Okano T, Suzuki K, Briggs D, Nakahama S. Surface characterization of 2-hydroxyethyl methacrylate/styrene copolymers by angle-dependent X-ray photoelectron spectroscopy and static secondary ion mass spectrometry. *J Biomater Sci, Polym Ed* 1992;3:463.
- [57] Senshu K, Yamashita Sh, Ito M, Hirao A, Nakahama S. Surface characterization of 2-hydroxyethyl methacrylate/styrene block copolymers by transmission electron microscopy observation and contact angle measurement. *Langmuir* 1995;11:2293.
- [58] Pientka Zb, Oike H, Tezuka Y. Atomic force microscopy study of environmental responses on poly(vinyl alcohol)-graft-polystyrene surfaces. *Langmuir* 1999;15:3197.
- [59] Tezuka Y, Okabayashi A, Imai K. Environmental responses on the surface of poly(vinyl alcohol) poly(tetrahydrofuran) graft-copolymers. *J Colloid Interface Sci* 1991;141:586.
- [60] Tezuka Y, Araki A. Temperature-modulated environmental responses on the surface of poly(vinyl alcohol)-polystyrene graft copolymers. *Langmuir* 1994;10:1865.
- [61] Tezuka Y, Nobe S, Shiomi T. Synthesis and surface formation of three-component copolymers having polystyrene-*block*-poly(dimethylsiloxane) graft segments. *Macromolecules* 1995;28:8251.
- [62] Tezuka Y, Ono T, Imai K. Environmentally induced macromolecular rearrangement on the surface of polyurethane-polysiloxane graft-copolymers. *J Colloid Interface Sci* 1990;136:408.
- [63] Tezuka Y, Yoshino M, Imai K. Environmental responses on the surface of polyurethane-based graft copolymers having uniform size polyether and polyamine segments. *Langmuir* 1991;7:2860.
- [64] Tezuka Y, Araki A, Shiomi T. Surface formation and environmental responses on polyurethane-polystyrene graft copolymers. *High Perform Polym* 1995;7:283.
- [65] De Crevoisier G, Fabre P, Corpart J-M, Leibler L. Switchable tackiness and wettability of a liquid crystalline polymer. *Science* 1999;285:1246.
- [66] O'Rourke Muisener PAV, Jalbert CA, Yuan C, Baetzold J, Mason R, Wong D, Kim YJ, Koberstein JT, Gunesin B. Measurement and modeling of end group concentration depth profiles for ω -fluorosilane polystyrene and its blends. *Macromolecules* 2003;36:2956.
- [67] Walton DG, Soo PP, Mayes AM, Allgor SJ, Fujii JT, Griffith LG, Ankner JF, Kaiser H, Johansson J, Smith GD, Barker JG, Satija SK. Creation of stable poly(ethylene oxide) surfaces on poly(methyl methacrylate) using blends of branched and linear polymers. *Macromolecules* 1997;30:6947.
- [68] Jones RAL, Richards RW. *Polymer at surfaces and interfaces*. Cambridge: Cambridge University Press; 1999.
- [69] Forrey C, Koberstein JT, Pan DH. Surface segregation in miscible blends of polystyrene and poly(vinyl methyl ether): comparison of theory and experiment. *Interface Sci* 2003;11:211.

- [70] Koberstein JT. Tailoring polymer interfacial properties by end group modification. In: Karim A, Kumar S, editors. *Polymer surfaces, interfaces and thin films*. New York: World Scientific; 2000. p. 115.
- [71] Hopkinson I, Kiff FT, Richards RW, Affrossman S, Hartshorne M, Pethrick RA, Munro H, Webster JRP. Investigation of surface enrichment in isotopic mixtures of poly(methyl methacrylate). *Macromolecules* 1995;28:627.
- [72] Koberstein JT. Polymer surface properties. In: *Encyclopedia of polymer science and technology*. New York: Wiley; 2001.
- [73] Pan DH, Prest WM. Surfaces of polymer blends—X-ray photoelectron-spectroscopy studies of polystyrene/poly(vinyl methyl-ether) blends. *J Appl Phys* 1985;58:286.
- [74] Bhatia QS, Pan DH, Koberstein JT. Preferential surface adsorption in miscible blends of polystyrene and poly(vinyl methyl ether). *Macromolecules* 1988;21:2166.
- [75] Jones RAL, Kramer EJ, Rafailovich MH, Sokolov J, Schwarz SA. Surface enrichment in an isotopic polymer blend. *Phys Rev Lett* 1989;62:280.
- [76] Jones RAL, Norton LJ, Kramer EJ, Composto RJ, Stein RS, Russell TP, Mansour A, Karim A, Felcher GP, Rafailovich MH, Sokolov J, Zhao H, Schwarz SS. The form of the enriched surface-layer in polymer blends. *Europhys Lett* 1990;12:41.
- [77] Bhatia QS, Burrell MC. Static SIMS study of miscible blends of polystyrene and poly(vinyl methyl-ether). *Surf Interface Anal* 1990;15:388.
- [78] Nakanishi H, Pincus PJ. Surface spinodals and extended wetting in fluids and polymer solutions. *J Chem Phys* 1983;79:997.
- [79] Schmidt I, Binder K. Model-calculations for wetting transitions in polymer mixtures. *J Phys-Paris* 1985;46:1631.
- [80] Hariharan A, Kumar SK, Russell TP. Surface segregation in binary polymer mixtures: a lattice model. *Macromolecules* 1991;24:4909.
- [81] Hariharan A, Kumar SK, Russell TP. Reversal of the isotopic effect in the surface behavior of binary polymer blends. *J Chem Phys* 1993;98:4163.
- [82] Schaub TF, Kellogg GJ, Mayes AM, Kulasekera R, Ankner JF, Kaiser H. Surface modification via chain end segregation in polymer blends. *Macromolecules* 1996;29:3982.
- [83] Hester JF, Banerjee P, Mayes AM. Preparation of protein-resistant surfaces on poly(vinylidene fluoride) membranes via surface segregation. *Macromolecules* 1999;32:1643.
- [84] Ohgaki A, Ohsugi H, Tanabe H. Surface properties of polymer films including multiblock copolymer. *Prog Org Coat* 1996;29:167.
- [85] Bergbreiter DE, Ponder BC, Aguilar G, Srinivas B. Temperature-responsive surface-functionalized polyethylene films. *Chem Mater* 1997;9:472.
- [86] Koberstein JT, Hu W, Duch D, Bhatia R, Lenk T, Smith DA, Brown HR, Lingelser JP, Gallot Y. Molecular design concepts for creating smart polymer surfaces. *Proc Annual Meet Adhesion Soc* 1997;20:283.
- [87] Koberstein JT, Duch D, Hu W, Lenk T, Bhatia R, Smith DA, Brown HR, Lingelser JP, Gallot Y. Creating smart polymer surfaces with selective adhesion properties. *J Adhesion* 1998;66:229.
- [88] Chen J, Fu Q, Smith DA, Koberstein JT. Creating functional groups on polymer surfaces with ω -functional surface-active block copolymers. *Polym Preprints* 2000;41(2):1651.
- [89] Thanawala SK, Chaudhury MK. Surface modification of silicone elastomer using perfluorinated ether. *Langmuir* 2000;16:1256.
- [90] Chan C-M. *Polymer surface modification and characterization*. Munich, Vienna, New York: Hanser; 1993.
- [91] Bergbreiter DE. Polyethylene surface-chemistry. *Prog Polym Sci* 1994;19:529.
- [92] Bergbreiter DE, Walchuk B, Holtzman B, Gray HN. Polypropylene surface modification by entrapment functionalization. *Macromolecules* 1998;31:3417.
- [93] Randall Holmes-Farley S, Reamey RH, Nuzzo R, McCarthy TJ, Whitesides GM. Reconstruction of the interface of oxidatively functionalized polyethylene and derivatives on heating. *Langmuir* 1987;3:799.
- [94] Whitesides GM, Laibinis PE. Wet chemical approaches to the characterization of organic surfaces: self-assembled monolayers, wetting, and the physical-organic chemistry of the solid-liquid interface. *Langmuir* 1990;6:87.
- [95] Randall Holmes-Farley S, Bain CD, Whitesides GM. Wetting of functionalized polyethylene film having ionizable organic acids and bases at the polymer-water interface: relations between functional group polarity, extent of ionization, and contact angle with water. *Langmuir* 1988;4:921.
- [96] Wilson MD, Whitesides GM. The anthranilate amide of 'polyethylene carboxylic acid' shows an exceptionally large change with pH in its wettability by water. *J Am Chem Soc* 1988;110:8718.
- [97] Bergbreiter DE, Kabza K. Annealing and reorganization of sulfonated polyethylene films to produce surface-modified films of varying hydrophilicity. *J Am Chem Soc* 1991;113:1447.
- [98] Carey DH, Ferguson GS. A smart surface: entropic control of composition at a polymer/water interface. *J Am Chem Soc* 1996;118:9780.
- [99] Carey DH, Grunzinger SJ, Ferguson GS. Entropically influenced reconstruction at the PBD-OX/water interface: the role of physical cross-linking and rubber elasticity. *Macromolecules* 2000;33:8802.
- [100] Khongtong S, Ferguson GS. Integration of bulk and interfacial properties in a polymeric system: rubber elasticity at a polybutadiene/water interface. *J Am Chem Soc* 2001;123:3588.
- [101] Khongtong S, Ferguson GS. A smart adhesive joint: entropic control of adhesion at a polymer/metal interface. *J Am Chem Soc* 2002;124:7254.
- [102] Genzer J, Efimenko K. Creating long-lived superhydrophobic polymer surfaces through mechanically assembled monolayers. *Science* 2000;290:2130.
- [103] Lampitt RA, Crowther JM, Badyal JPS. Switching liquid repellent surfaces. *J Phys Chem B* 2000;104:10329.

- [104] Israëls R, Leermakers FAM, Fleer GJ, Zhulina EB. Charged polymeric brushes: structure and scaling relations. *Macromolecules* 1994;27:3249.
- [105] Takei YG, Aoki T, Sanui K, Ogata N, Sakurai Y, Okanao T. Dynamic contact angle measurement of temperature-responsive surface properties for poly(*n*-isopropylacrylamide) grafted surfaces. *Macromolecules* 1994;27:6163.
- [106] Auroy P, Auvray L, Leger L. Characterization of the brush regime for grafted polymer layers at the solid–liquid interface. *Phys Rev Lett* 1991;66:719.
- [107] Raviv U, Tadmor R, Klein J. Shear and frictional interactions between adsorbed polymer layers in a good solvent. *J Phys Chem B* 2001;105:8125.
- [108] Grest GS, Murat M. Structure of grafted polymeric brushes in solvents of varying quality: a molecular dynamics study. *Macromolecules* 1993;26:3108.
- [109] Pincus P. Colloid stabilization with grafted polyelectrolytes. *Macromolecules* 1991;24:2912.
- [110] Galaev I, Mattiasson B. ‘Smart’ polymers and what they could do in biotechnology and medicine. *Trends Biotechnol* 1999;17:335.
- [111] Aksay A, Trau M, Manne S, Honma I, Yao N, Zhou L, Fenter F, Eisenberger PM, Gruner SM. Biomimetic pathways for assembling inorganic thin films. *Science* 1996;273:892.
- [112] Ito Y, Ochiai Y, Park YS, Imanishi Y. PH-sensitive gating by conformational change of a polypeptide brush grafted onto a porous polymer membrane. *J Am Chem Soc* 1997;119:1619.
- [113] Leger L, Raphaël E, Hervert H. Surface-anchored polymer chains: their role in adhesion and friction. *Adv Polym Sci* 1999;138:185.
- [114] Ruths M, Johannsmann D, Rühle J, Knoll W. Repulsive forces and relaxation on compression of entangled, polydisperse polystyrene brushes. *Macromolecules* 2000;33:3860.
- [115] Minsky P, Liu Y, Huang E, Russell TP, Hawker CJ. Controlling polymer–surface interactions with random copolymer brushes. *Science* 1997;275:1458.
- [116] Blossley R. Self-cleaning surfaces—virtual realities. *Nat Mater* 2003;2:301.
- [117] Lafuma A, Quere D. Superhydrophobic states. *Nat Mater* 2003;2:457.
- [118] Alexander S. Adsorption of chain molecules with a polar head a scaling description. *J Phys-Paris* 1977;38:983.
- [119] de Gennes P-G. Conformations of polymers attached to an interface. *Macromolecules* 1980;13:1069.
- [120] Brown CH. Photochromism. New York: Wiley; 1971.
- [121] Irie M. Photoresponsive polymers. *Adv Polym Sci* 1990;94:27.
- [122] Ulman A. An introduction to ultrathin organic films. San Diego: Academic Press; 1991.
- [123] Tsukruk VV, Bližnyuk VN. Side chain liquid crystalline polymers at interfaces. *Prog Polym Sci* 1997;22:1089.
- [124] Seki T, Skuragi M, Kawanishi Y, Suzuki Y, Tamaki T, Fukuda T, Ishimura K. Command surfaces of Langmuir–Blodgett films—photoregulations of liquid-crystal alignment by molecularly tailored surface azobenzene layers. *Langmuir* 1993;9:211.
- [125] Sekkat Z, Wood J, Geerts Y, Knoll W. A smart ultrathin photochromic layer. *Langmuir* 1995;11:2856.
- [126] Siewierski LM, Brittain WJ, Petrasch S, Foster MD. Photoresponsive monolayers containing in-chain azobenzene. *Langmuir* 1996;12:5838.
- [127] Seki T, Sekizawa H, Morino S-Y, Ichimura K. Inherent and cooperative photomechanical motions in monolayers of an azobenzene containing polymer at the air–water interface. *J Phys Chem B* 1998;102:5313.
- [128] Holland NB, Hugel T, Neuert G, Cattani-Scholze A, Renner C, Oesterhelt D, Moroder L, Seitz M, Gaub HE. Single molecule force spectroscopy of azobenzene polymers: switching elasticity of single photochromic macromolecules. *Macromolecules* 2003;36:2015.
- [129] Dante S, Advincula R, Frank CW, Stroeve P. Photoisomerization of polyionic layer-by-layer films containing azobenzene. *Langmuir* 1999;15:193.
- [130] Ichimura K, Oh S-K, Nakagawa M. Light-driven motion of liquids on a photoresponsive surface. *Science* 2000;288:1624.
- [131] Nath N, Chilkoti A. Creating smart surfaces using stimuli responsive polymers. *Adv Mater* 2002;14:1243.
- [132] Schild HG. Poly(*n*-isopropylacrylamide)—experiment, theory and application. *Prog Polym Sci* 1992;17:163.
- [133] Kato K, Uchida E, Kang E, Uyama Y, Ikada Y. Polymer surface with graft chains. *Prog Polym Sci* 2003;28:209.
- [134] Kikuchi A, Okuhara M, Karikusa F, Sakurai Y, Okano T. Two-dimensional manipulation of confluent cultured vascular endothelial cells using temperature-responsive poly(*n*-isopropylacrylamide)-grafted surfaces. *J Biomater Sci, Polym Ed* 1998;9:1331.
- [135] Ista LK, Perez-Luna VH, Lopez GP. Surface-grafted, environmentally sensitive polymers for biofilm release. *Appl Environ Microbiol* 1999;65:1603.
- [136] Ista LK, Mendez S, Perez-Luna VH, Lopez GP. Synthesis of poly(*n*-isopropylacrylamide) on initiator-modified self-assembled monolayers. *Langmuir* 2001;17:2552.
- [137] Kidoaki S, Ohya S, Nakayama Y, Masuda T. Thermoresponsive structural change of a poly(*n*-isopropylacrylamide) graft layer measured with an atomic force microscope. *Langmuir* 2001;17:2403.
- [138] Harmon ME, Kuckling D, Frank CW. Photo-cross-linkable PNIPAAm copolymers. 5. Mechanical properties of hydrogel layers. *Langmuir* 2003;19:10660.
- [139] Jones DM, Smith JR, Huck WT, Alexander C. Variable adhesion of micropatterned thermoresponsive polymer brushes: AFM investigations of poly(*n*-isopropylacrylamide) brushes prepared by surface-initiated polymerizations. *Adv Mater* 2002;14:1130.
- [140] Frechet JM. Functional polymers and dendrimers—reactivity, molecular architecture, and interfacial energy. *Science* 1994;263:1711. Tomalia DA. Starburst cascade dendrimers—fundamental building-blocks for a new nanoscopic chemistry set. *Adv Mater* 1994;6:529. Jansen JF, de Brabander-van den Berg EM, Meijer EW. Encapsulation of guest molecules into a dendritic box. *Science* 1994;266:1226.

- Percec V, Kawasumi M. Toward willowlike thermotropic dendrimers. *Macromolecules* 1994;27:4441.
- [141] Tsukruk VV. Dendritic macromolecules at interfaces. *Adv Mater* 1998;10:253.
- [142] Hashemzadeh M, McGrath DV. Toward photoresponsive dendritic self-assembly. *Polym Preprints* 1998;39(2):338.
- [143] Weener J, Maijer EW. Photoresponsive dendritic monolayers. *Adv Mater* 2000;12:741.
- [144] Larson K, Vaknin D, Villavicencio O, McGrath D, Tsukruk VV. Molecular packing of amphiphiles with crown polar heads at the air–water interface. *J Phys Chem B* 2002;106:7246.
- [145] Sidorenko A, Houphouet-Boigny C, Villavicencio O, McGrath DV, Tsukruk VV. Low generation photochromic monodendrons on a solid surface. *Thin Solid Films* 2002;410:147.
- [146] Genson K, Vaknin D, Villavicencio O, McGrath DV, Tsukruk VV. Microstructure of amphiphilic monodendrons at the air–water interface. *J Phys Chem B* 2002;106:11277.
- [147] Peleshanko S, Sidorenko A, Larson K, Villavicencio O, Ornatka M, McGrath DV, Tsukruk VV. Langmuir–Blodgett monolayers from lower generation amphiphilic monodendrons. *Thin Solid Films* 2002;406:233.
- [148] Sidorenko A, Houphouet-Boigny C, Villavicencio O, Hashemzadeh M, McGrath DV, Tsukruk VV. Photoresponsive Langmuir monolayers from azobenzene-containing dendrons. *Langmuir* 2000;16:10569.
- [149] Tsukruk VV, Luzinov I, Larson K, Li S, McGrath DV. Intralayer reorganization of photochromic molecular films. *J Mater Sci Lett* 2001;20:873.
- [150] Belge G, Beyerlein D, Betsch C, Eichhorn K, Gauglitz G, Grundkle K, Voit B. Suitability of hyperbranched polyester for sensoric applications—investigation with reflectometric interference spectroscopy. *Anal Bioanal Chem* 2002;374:403.
- [151] Fler GJ, Cohen Stuart MA, Scheutjens JM, Cosgrove T, Vincent B. *Polymers at interfaces*. London: Chapman&Hall; 1993.
- [152] Biesalski M, Ruehe J, Kuegler R, Knoll W. Polyelectrolytes at solid surfaces: multilayers and brushes. In: Tripathy SK, Kumar J, Nalwa HS, editors. *Handbook of polyelectrolytes and their applications*. Stevenson Ranch: American Scientific Publishers; 2002. p. 39.
- [153] Biesalski M, R  he J. Preparation and characterization of a polyelectrolyte monolayer covalently attached to a planar solid surface. *Macromolecules* 1999;32:2309.
- [154] Zhang H, Ito Y. Smart materials using signal responsive polyelectrolytes. In: Tripathy SK, Kumar J, Nalwa HS, editors. *Handbook of polyelectrolytes and their applications*. Stevenson Ranch: American Scientific Publishers; 2002. p. 183.
- [155] Kurihara K, Murase Y. Polyelectrolyte brushes. In: Tripathy SK, Kumar J, Nalwa SH, editors. *Handbook of polyelectrolytes and their applications*. Stevenson Ranch: American Scientific Publishers; 2002. p. 207.
- [156] Kokufuta E. Controlled permeation through membranes modified with smart polymers: smart polyelectrolytes that undergo configurational transition on hydrophobic membrane surfaces. In: Galaev IY, Mattiasson B, editors. *Smart polymers for bioseparation and bioprocessing*. London and New York: Taylor&Francis; 2002. p. 122.
- [157] Park YS, Ito Y, Imanishi Y. PH-controlled gating of a porous glass filter by surface grafting of polyelectrolyte brushes. *Chem Mater* 1997;9:2755.
- [158] Zhang H, Ito Y. PH control of transport through a porous membrane self-assembled with a poly(acrylic acid) loop brush. *Langmuir* 2001;17:8336.
- [159] Bergbreiter DE, Walchuk B, Holtzman B, Gray HN. Polypropylene surface modification by entrapment functionalization. *Macromolecules* 1998;31:3417.
- [160] Krausch G, Magerle R. Nanostructured thin films via self-assembly of block copolymers. *Adv Mater* 2002;14:1579.
- [161] Bates FS, Fredrickson GH. Block copolymer thermodynamics—theory and experiment. *Annu Rev Phys Chem* 1990;41:525.
- [162] Mansky P, Chaikin P, Thomas EL. Monolayer films of diblock copolymer microdomains for nanolithographic applications. *J Mater Sci* 1995;30:1987.
- [163] Park M, Harrison C, Chaikin PM, Register RA, Adamson DH. Block copolymer lithography: periodic arrays of ~ 1011 holes in 1 square centimeter. *Science* 1997;276:1401.
- [164] Zhulina EB, Singh C, Balazs AC. Forming patterned films with tethered diblock copolymers. *Macromolecules* 1996;29:6338.
- [165] Zhulina EB, Singh C, Balazs AC. Self-assembly of tethered diblocks in selective solvents. *Macromolecules* 1996;29:8254.
- [166] Zhao B, Brittain WJ. Synthesis of tethered polystyrene-*block*-poly(methyl methacrylate) monolayer on a silicate substrate by sequential carbocationic polymerization and atom transfer radical polymerization. *J Am Chem Soc* 1999;121:3557.
- [167] Zhao B, Brittain WJ. Synthesis, characterization, and properties of tethered polystyrene-*b*-polyacrylate brushes on flat silicate substrates. *Macromolecules* 2000;33:8813.
- [168] Zhao B, Brittain WJ, Zhou W, Cheng SZD. Nanopattern formation from tethered PS-*b*-PMMA brushes upon treatment with selective solvents. *J Am Chem Soc* 2000;122:2407.
- [169] Zhao B, Brittain WJ, Zhou W, Cheng SZD. AFM study of tethered polystyrene-*b*-poly(methyl methacrylate) and polystyrene-*b*-poly(methyl acrylate) brushes on flat silicate substrates. *Macromolecules* 2000;33:8821.
- [170] Matyjaszewski K, Miller PJ, Shukla N, Immaraporn B, Gelman A, Luokala BB, Siclovian TM, Kickelbick G, Vallant T, Hoffmann H, Pakula T. Polymers at interfaces: using atom transfer radical polymerization in the controlled growth of homopolymers and block copolymers from silicon surfaces in the absence of untethered sacrificial initiator. *Macromolecules* 1999;32:8716.
- [171] Kim J-B, Huang W, Bruening ML, Baker GL. Synthesis of triblock copolymer brushes by surface-initiated atom transfer radical polymerization. *Macromolecules* 2002;35:5410.

- [172] Zhao H, Shipp DA. Preparation of poly(styrene-*block*-butylacrylate) block copolymer–silicate nanocomposites. *Chem Mater* 2003;15:2693.
- [173] Baum M, Brittain WJ. Synthesis of polymer brushes on silicate substrates via reversible addition fragmentation chain transfer technique. *Macromolecules* 2002;35:610.
- [174] Sumerlin BS, Lowe AB, Stroud PA, Zhang P, Urban MW, McCormick CL. Modification of gold surfaces with water-soluble (co)polymers prepared via aqueous reversible addition-fragmentation chain transfer (RAFT) polymerization. *Langmuir* 2003;19:5559.
- [175] Quirk RP, Mathers RT, Cregger T, Foster MD. Anionic synthesis of block copolymer brushes grafted from a 1,1-diphenylethylene monolayer. *Macromolecules* 2002;35:9964.
- [176] Advincula R, Zhou Q, Park M, Wang S, Mays J, Sakellariou G, Pispas S, Hadjichristidis N. Polymer brushes by living anionic surface initiated polymerization on flat silicon (SiO₂) and gold surfaces: homopolymers and block copolymers. *Langmuir* 2002;18:8672.
- [177] Zhulina EB, Balazs AC. Designing patterned surfaces by grafting Y-shaped copolymers. *Macromolecules* 1996;29:2667.
- [178] Julthongpipit D, Lin Y-H, Teng J, Zubarev ER, Tsukruk VV. Y-shaped polymer brushes: nanoscale switchable surfaces. *Langmuir* 2003;19:7832.
- [179] Marko JF, Witten TA. Phase separation in a grafted polymer layer. *Phys Rev Lett* 1991;66:1541.
- [180] Singh C, Pickett GT, Zhulina B, Balazs AC. Modeling the interactions between polymer-coated surfaces. *J Phys Chem B* 1997;101:10614.
- [181] Singh C, Pickett GT, Balazs AC. Interactions between polymer-coated surfaces in poor solvents. 1. Surfaces grafted with A and B homopolymers. *Macromolecules* 1996;29:7559.
- [182] Müller M. Phase diagram of a mixed polymer brush. *Phys Rev* 2002;E65:030802(R).
- [183] Soga KG, Zuckermann MJ, Guo H. Binary polymer brush in a solvent. *Macromolecules* 1996;29:1998.
- [184] Lai PY. Binary mixture of grafted polymer chains: a Monte Carlo simulation. *J Chem Phys* 1994;100:3351.
- [185] Matsen MW, Schick M. Stable and unstable phases of a diblock copolymer melt. *Phys Rev Lett* 1994;72:2660.
- [186] Minko S, Usov D, Goresnik E, Stamm M. Environment-adopting surfaces with reversibly switchable morphology. *Macromol Rapid Commun* 2001;22:206.
- [187] Müller M. Unpublished results; 2003.
- [188] Stamouli A, Pelletier E, Koutsos V, Vegte EVD, Hadziioannou G. An atomic force microscopy study on the transition from mushrooms to octopus surface ‘micelles’ by changing the solvent quality. *Langmuir* 1996;12:3221.
- [189] Minko S, Patil S, Datsyuk V, Simon F, Eichhorn K-J, Motornov M, Usov D, Tokarev I, Stamm M. Synthesis of adaptive polymer brushes via ‘grafting to’ approach from melt. *Langmuir* 2002;18:289.
- [190] Sidorenko A, Minko S, Schenk-Meuser K, Duschner H, Stamm M. Switching of polymer brushes. *Langmuir* 1999;15:8349.
- [191] Minko S, Müller M, Usov D, Scholl A, Froeck C, Stamm M. Lateral versus perpendicular segregation in mixed polymer brushes. *Phys Rev Lett* 2002;88:035502.
- [192] Lemieux M, Usov D, Minko S, Stamm M, Shulha H, Tsukruk VV. Reorganization of binary polymer brushes: reversible switching of surface microstructures and nanomechanical properties. *Macromolecules* 2003;36:7244.
- [193] Lemieux M, Minko S, Usov D, Stamm M, Tsukruk VV. Direct measurement of thermoelastic properties of glassy and rubbery polymer brush nanolayers grown by ‘grafting-from’ approach. *Langmuir* 2003;19:6126.
- [194] Minko S, Usov D, Luchnikov V, Müller M, Ionov L, Scholl A, Pfützte G, Stamm M. Responsive mixed polymer brushes for patterning of surfaces. *Polym Preprints* 2003;44(1):478.
- [195] Shusharina NP, Linse P. Oppositely charged polyelectrolytes grafted onto planar surface: mean-field lattice theory. *Eur Phys J E* 2001;6:147.
- [196] Shusharina NP, Linse P. Polyelectrolyte brushes with specific charge distribution: mean-field lattice theory. *Eur Phys J E* 2001;4:399.
- [197] Huobenov N, Minko S, Stamm M. Mixed polyelectrolyte brush from oppositely charged polymers for switching of surface charge and composition in aqueous environment. *Macromolecules* 2003;36:5897.
- [198] Tsukruk VV, Kogure A, Maruyama K, Sone Y, Shimomura M. Graft polymerization of vinyl monomers from inorganic ultrafine particles initiated by azo groups introduced onto the surface. *Polym J* 1990;22:827.
- [199] Minko S, Stamm M, Goresnik E, Usov D, Sidorenko A. Environmentally responsive polymer brush layers for switchable surface properties. *Polym Mater: Sci Engng* 2000;83:533.
- [200] Boven G, Oosterling MLCM, Challa G, Schouten A. Grafting kinetics of poly(methyl methacrylate) on microparticulate silica. *Polymer* 1990;31:2377.
- [201] Usov D, Stamm M, Minko S, Froeck C, Scholl A, Müller MI. Nanostructured polymer brushes with reversibly changing properties. *Proc Mater Res Soc* 2002;727:R25.
- [202] Tsukruk VV, Luzinov I, Julthongpipit D. Sticky molecular surfaces: epoxysilane self-assembled monolayers. *Langmuir* 1999;15:3029.
- [203] Luzinov I, Julthongpipit D, Liebmann-Vinson A, Cregger T, Foster MD, Tsukruk VV. Epoxy-terminated self-assembled monolayers: molecular glues for polymer layers. *Langmuir* 2000;16:504.
- [204] Motornov M, Minko S, Eichhorn K-J, Nitschke M, Simon F, Stamm M. Reversible tuning of wetting behavior of polymer surface with responsive polymer brushes. *Langmuir* 2003;19:8077.
- [205] Luzinov I, Swaminatha Iyer K, Klep V, Zdyrko B, Draper J, Liu Y. Macromolecular anchoring layer for synthesis of polymer brushes. *Polym Preprints* 2003;44:437.
- [206] Iyer SK, Zdyrko B, Malz H, Pionteck J, Luzinov I. Polystyrene layers grafted to macromolecular anchoring layer. *Macromolecules* 2003;36:6519.
- [207] Ejaz M, Ohno K, Tsujii Y, Fukuda T. Nanopatterned surface morphology of well-defined mixed homopolymer brushes fabricated by living radical polymerization. *Polym Preprints* 2003;44:532.

- [208] Zhao B. Synthesis of binary mixed homopolymer brushes by combining atom transfer radical polymerization and nitroxide-mediated radical polymerization. *Polymer* 2003;44:4079.
- [209] Julthongpiput D, LeMieux MC, Bergman KN, Tsukruk VV. Switching properties of glassy and rubbery polymer binary brushes grafted to functionalized silicon surface. *Polym Mater: Sci Engng* 2003;89:342.
- [210] Klep V, Minko S, Luzinov I. Mixed polymer layers by grafting to/grafting from combination. *Polym Mater: Sci Engng* 2003;89:248.
- [211] Lemieux MC, Usov D, Minko S, Stamm M, Tsukruk VV. Reorganization of binary polymer brushes: reversible switching of surface microstructures and nanomechanical properties. *Macromolecules* 2003;36:7244.
- [212] Lemieux MC, Minko S, Usov D, Stamm M, Tsukruk VV. Tunable microstructure and nanomechanical properties in a binary polymer brush. *Polym Mater: Sci Engng* 2003;89.
- [213] Julthongpiput D, Lin Y-H, Teng J, Zubarev ER, Tsukruk VV. Y-shaped amphiphilic brushes with switchable micellar nanoscale surface structures. *J Am Chem Soc* 2003;125:15912.
- [214] Chen C, Dan N, Dhoots S, Tirrell M, Mays J, Watanabe H. Effect of solvent quality on pure and mixed brushes. *Israel J Chem* 1995;35:41.
- [215] Minko S, Müller M, Motornov M, Nitschke M, Grundke K, Stamm M. Two-level structured self-adaptive surfaces with reversibly tunable properties. *J Am Chem Soc* 2003;125:3896.
- [216] Ionov L, Minko S, Stamm M, Gohy JF, Jérôme R, Scholl A. Reversible chemical patterning on stimuli-responsive polymer film: environment-responsive lithography. *J Am Chem Soc* 2003;125:8302.